10/7-30-96 JS (1)

LBL-37880
UC-406
CONF-9504205 – —

Lawrence Berkeley Laboratory
UNIVERSITY OF CALIFORNIA

Accelerator & Fusion
Research Division

Proceedings of the Workshop on Neutron Instrumentation for a Long-Pulse Spallation Source

Editors: J. Alonso, R. Pynn, T. Russell, and L. Schroeder

April 1995

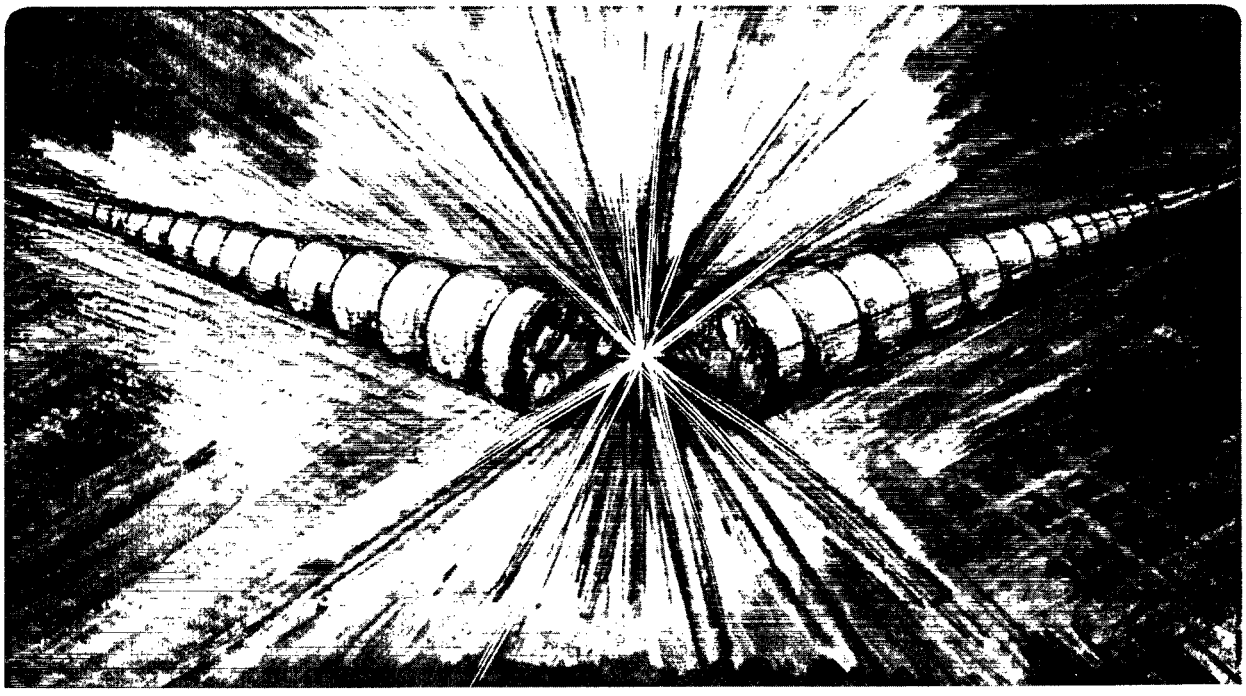

Prepared for the U.S. Department of Energy under Contract Number DE-AC03-76SF00098

LBL-37880
UC-406
CONF-9504205

Proceedings of the Workshop on Neutron Instrumentation for a Long-Pulse Spallation Source

April 18-21, 1995

Lawrence Berkeley National Laboratory
University of California
Berkeley, CA 94720

Editors: Jose Alonso†, Roger Pynn*,
Tom Russell‡, Lee Schroeder†

* Los Alamos National Laboratory
† Lawrence Berkeley National Laboratory
‡ IBM Almaden Research Center

This work was supported by the Director, Office of Energy Research, Office of Basic Energy Sciences of the U.S. Department of Energy under Contractr No. DE-AC03-76SF00098.

Workshop on Neutron Instrumentation for a Long-Pulse Spallation Source

Lawrence Berkeley National Laboratory
Berkeley, CA

April 18-21, 1995

PREFACE

This workshop was carried out under the auspices of the Lawrence Berkeley National Laboratory (LBNL) Pulsed Spallation Source activity and its Pulsed Spallation Source Committee (PSSC, chaired by Dr. Gabriel Aeppli). One of our activities has been the sponsorship of workshops related to neutron production by pulsed sources. This is the second such workshop held at LBNL, the first, entitled "Ion Source Issues Relevant to a Pulsed Spallation Neutron Source," was held in October of 1994. At the Crystal City PSSC meeting (December 5, 1994) a decision was made to hold a workshop on the instrumentation opportunities at a long-pulse spallation source (LPSS). The enclosed material represents the results of deliberations of the three working groups into which the participants were divided, covering elastic scattering, inelastic scattering and fundamental physics, as well as contributions from individual participants. We hope that the material in this report will be useful to the neutron scattering community as it develops a road-map for future neutron sources.

The workshop was held at LBNL in mid-April with about sixty very dedicated participants from the US and abroad. Roger Pynn, in his opening address, presented the charge for the workshop:

- Based on the bench mark source parameters provided by Gary Russell (III-33, these proceedings), determine how a suite of spectrometers in each of the three working group's area of expertise would perform at an LPSS and compare this performance with that of similar spectrometers at a continuous source or a short-pulse source.

- Identify and discuss modifications to these spectrometers that would enhance their performance at an LPSS.

- Identify any uncertainties in the analysis of spectrometer performance that require further research (examples might include the use of choppers in regimes beyond current experience, the effect of pulse "tails," etc.). Describe what R&D is needed to resolve these issues.

- Discuss how the performance of instruments would be affected by changes in source parameters such as repetition rate, proton pulse length, and the characteristic time of pulse tails. Identify beneficial changes that could become goals for target/moderator designers.

- Identify novel methods that might be applied at an LPSS.

On behalf of the workshop participants, I wish to extend specific thanks to the support staff that contributed so much to the excellent productivity of this workshop: Mollie Field, who handled all the conference-coordination issues; and Tina Aitkens, Martha Condon and Joan Thompson who took care of all the logistics of xeroxing, computer interfacing, meeting-room scheduling and coordination, and general assistance. Joan, who travelled from Los Alamos, is to be particularly commended for working so effectively in a new environment.

Lee S. Schroeder
PSS Study Director

EXECUTIVE SUMMARY

Roger Pynn, Tom Russell, Lee Schroeder

Workshop participants were asked to assess the performance of a one megawatt (1 MW) Long-Pulse Spallation Source (LPSS) for neutron scattering and fundamental physics (the specific charge is given in the Preface on the preceding page). Several recent reviews and workshops [1,2] have articulated the case for a broad range of instrumentation in each of these areas and this case was not reexamined at the workshop. Rather, by assessing the performance of many types of instruments, workshop participants defined the scientific areas in which a 1 MW LPSS would excel or provide capabilities not available elsewhere in the United States. The following bullets summarize the principal conclusions of the workshop.

Neutronic Performance of a 1 MW LPSS

- Participants were provided with a benchmark calculation of the performance for a one megawatt (1 MW) LPSS with 1 msec pulses. At 60 Hz, the benchmark calculation predicts an average **cold** neutron flux that is about 25% of that provided by the best cold source at the 60 MW research reactor at the Institut Laue Langevin (ILL) in Grenoble, France. The spectral distribution for cold sources at an LPSS and a reactor are also similar. The **thermal** neutron flux of the benchmark LPSS is similar to that obtained with a 10 MW reactor.

- The benchmark simulations include major engineering realities that affect performance, such as target and moderator coolants, the absence of reflector material in beam lines etc. However, more subtle engineering realities — such as piping for moderator fluids — are not included. These will result in performance degradation.

- The use of grooved moderators, different target/moderator geometries, and different combinations of reflector materials may increase the peak (and integrated) neutron flux in each pulse over that produced by the benchmark target. Such gains will tend to off-set the performance losses due to "engineering" effects described above.

- The benchmark calculations of the neutron fluxes, spectra, and pulse shapes were assessed by experts at the meeting as conservative estimates of achievable performance. Participants pointed out that the use of reflectors that are faster than those used in the benchmark will reduce both the rise time of the neutron pulses and the extent of pulse tails — both desirable features for neutron scattering spectrometers.

- A short-pulse spallation source (SPSS) with 1 MW of proton beam power incident on a single neutron-production target that is surrounded by coupled moderators can provide between two and three times the peak neutron intensity of a 1 MW LPSS that has the same repetition rate and 1 msec pulses. Both short and long-pulse sources give the same average neutron fluxes when similar moderators and reflectors are used. Comparisons of performance for the two types of sources for neutron scattering depend upon the details of particular instruments, and involve practical as well as theoretical considerations.

Performance of Neutron Scattering Spectrometers at a 1 MW LPSS

- Most neutron scattering spectrometers can benefit from the pulsed nature of the LPSS neutron beam and achieve a performance gain by using time-of-flight methods. In the best cases, this gain leads to performance at the benchmark 1 MW LPSS that is between 3 and 4 times that achievable at the ILL. Overall, performance appears to be comparable to that of the ILL for many applications.

- Of the LPSS spectrometers examined at the workshop, those which perform best are the ones which do not have a need for very high incident-wavelength resolution. Many of these spectrometers use cold neutrons. In this sense, a 1 MW LPSS complements traditional, present-generation, short-pulse spallation sources which produce the pulse lengths that are required for high resolution studies with thermal or epithermal neutrons.

- With the exception of the small-angle neutron scattering (SANS) spectrometer and the reflectometer, all instrument comparisons were based on analytic calculations performed at the workshop. Some of these could be in error by as much as a factor of two. More detailed analysis can be obtained from Monte Carlo simulations which have already been undertaken for SANS and reflectometry. Workshop participants recommended that simulations should be performed for other spectrometers to substantiate the conclusions reached at the workshop. Such calculations can also be used to optimize spectrometer design, which may result in further performance gains.

- The effect of the instantaneous fast neutron background that coincides with each proton pulse at an LPSS needs to be further investigated for cases where spectrometers are designed to measure during the proton pulses.

- Several of the spectrometers considered at the workshop require choppers to be placed close to the neutron source. The performance, reliability, and maintainability of these choppers needs to be considered and will require R&D.

Nuclear and Fundamental Physics at a 1 MW LPSS

- A 1 MW LPSS would provide a very effective source of ultracold neutrons (UCN) for nuclear physics research. If current ideas about solid deuterium sources prove correct, an ultracold neutron source at a 1 MW LPSS would be one to two orders of magnitude more intense than the UCN source at the ILL reactor.

- Although a solid-deuterium ultracold neutron source makes no use of the pulsed nature of the LPSS, it could be installed more easily at a spallation source than at an existing or refurbished nuclear reactor for both technical and regulatory reasons.

Other Uses of a 1 MW LPSS

- Several workshop participants pointed out that a 1 MW LPSS could be used effectively for various non-destructive evaluation techniques including: cold-neutron and high-neutron-energy radiography or tomography, prompt gamma ray analysis, gamma ray activation analysis, and neutron depth profiling. The production of neutron-rich isotopes and materials irradiation studies would also be possible. None of these uses were considered in detail at the workshop.

Conclusion

- Participants at the workshop evaluated a broad range of neutron instrumentation by comparing calculated performance at the benchmark 1 MW LPSS with calculated performances at existing reactors and short pulse spallation sources. A 1 MW LPSS appears to be equivalent to a high-flux beam reactor such as the ILL for many applications and to be superior for some experiments. Such a source will allow the development of new experimental techniques based on the time-of-flight method and offers a new way of making progress in the neutron scattering field.

References

[1] *Neutron Sources for America's Future*, Report of the Basic Energy Sciences Advisory Committee Panel on Neutron Sources (DOE/ER-0576P)

[2] *Technology and Science at a High-Power Spallation Source*, Proceedings of Workshop held at Argonne National Laboratory, May 13-16, 1993, Published by Argonne National Laboratory, Feb. 1994.

Workshop on Neutron Instrumentation for a Long-Pulse Spallation Source

Lawrence Berkeley National Laboratory Berkeley, CA

April 18-21, 1995

TABLE OF CONTENTS

LPSS Workshop, April 18-21, 1995, Berkeley CA

Workshop on Neutron Instrumentation for a Long-Pulse Spallation Source

Lawrence Berkeley National Laboratory Berkeley, CA

April 18-21, 1995

LIST OF PARTICIPANTS

Gabriel Aeppli
AT&T Bell Labs
Room 1D-364
600 Mountain Avenue
Murray Hill, NJ 07974

Berthold Alefeld
KFA Jülich, IFF
Postfach 1913
D-52425 Jülich
GERMANY

Jose Alonso
Lawrence Berkeley Laboratory
MS/71-259
1 Cyclotron Road
Berkeley, CA 94720

Bill R. Appleton
Oak Ridge National Laboratory
Bldg 4500N, MS 6240
P.O. Box 2008
Oak Ridge, TN 37831-6240

Masatoshi Arai
Department of Physics
Kobe University
1-1, Rokkodai, Nada
Kobe, 657 JAPAN

John D. Axe
Physics Department
Brookhaven National Laboratory
Bldg. 510A
P.O. Box 5000
Upton, NY 11973-5000

William A. Barletta
Lawrence Berkeley Laboratory
MS/50-149
1 Cyclotron Road
Berkeley, CA 94720

Guenter Bauer
Paul Scherrer Institute
CH-5232 Villigen
SWITZERLAND

Collin L. Broholm
Johns Hopkins University
Charles & 34th Streets
Baltimore, MD 21218

John Browne
Los Alamos National Laboratory
LANSCE, MS H845
Los Alamos, NM 87545

Colin J. Carlile
ISIS Facility
Rutherford-Appleton Laboratory
Chilton, Didcot OXON OX11 0QX
UNITED KINGDOM

Timothy Chupp
Physics Department
University of Michigan
2071 Randall Hall
Ann Arbor, MI 48109

Harald Conrad
KFA Jülich, IFF
Postfach 1913
D-52425 Jülich
GERMANY

R. Kent Crawford
IPNS Division
Argonne National Laboratory
Building 360
9700 South Cass Avenue
Argonne, IL 60439

Luke L. Daemen
Los Alamos National Laboratory
LANSCE, MS H805
Los Alamos, NM 87545

Workshop on Neutron Instrumentation for a Long-Pulse Spallation Source

Lawrence Berkeley National Laboratory
Berkeley, CA

April 18-21, 1995

LIST OF PARTICIPANTS

Gian P. Felcher
Argonne National Laboratory
Bldg. 223 - MSD
9700 South Cass Avenue
Argonne, IL 60439

Michael Fitzsimmons
Los Alamos National Laboratory
LANSCE, MS H805
Los Alamos, NM 87545

Stuart Freedman
Physics Department
Lawrence Berkeley Laboratory
366 LaConte Hall
Berkeley, CA 94720

Charles J. Glinka
Nat. Inst. of Science and Technology
Bldg. 235/E-151
Gaithersburg, MD 20899

Geoffrey L. Greene
Los Alamos National Laboratory
P-23
MS D449
Los Alamos, NM 87545

William A. Hamilton
Oak Ridge National Laboratory
Bldg 7962, MS 6393
P.O. Box 2008
Oak Ridge, TN 37831-6393

Rex P. Hjelm
Los Alamos National Laboratory
LANSCE, MS H805
Los Alamos, NM 87545

Michael Johnson
ISIS Facility
Rutherford-Appleton Laborabory
Chilton, Didcot OXON OX11 0QX
UNITED KINGDOM

Gordon Kearley
Physics Department
Institute Laue-Langevin
156X Centre de Tri
F-38042 Grenoble Cedex 9
FRANCE

Thomas E. Mason
Department of Physics
University of Toronto
Toronto, ONTARIO M5S 1A7
CANADA

Denis B. McWhan
National Synchrotron Light Source
Brookhaven National Laboratory
Bldg. 725B
P.O. Box 5000
Upton, NY 11973-5000

Ferenc Mezei
Hahn-Meitner Institut
BENSC
Glieneckerstrasse 100
D-14109 Berlin
GERMANY

Andre F. Michaudon
Los Alamos National Laboratory
LANSCE, MS H805
Los Alamos, NM 87545

David Moncton
Office of the Director
Argonne National Laboratory
Building 360
9700 South Cass Avenue
Argonne, IL 60439

Herb A. Mook
Oak Ridge National Laboratory
Solid State Div., Bldg 7962
P.O. Box 2008
Oak Ridge, TN 37831-6393

Workshop on Neutron Instrumentation for a Long-Pulse Spallation Source

Lawrence Berkeley National Laboratory
Berkeley, CA

April 18-21, 1995

LIST OF PARTICIPANTS

Hannu Mutka
Institute Laue-Langevin
156X Centre de Tri
F-38042 Grenoble Cedex 9
FRANCE

Glenn A. Olah
Los Alamos National Laboratory
MS J586
Los Alamos, NM 87545

Raymond Osborn
Argonne National Laboratory
Bldg. 223 - MSD
9700 South Cass Avenue
Argonne, IL 60439

Laurence Passell
Brookhaven National Laboratory
Bldg. 510B
P.O. Box 5000
Upton, NY 11973-5000

Geoffrey Penfold
Neutron Division
Rutherford-Appleton Laboratory
Chilton, Didcot OXON OX11 0QX
UNITED KINGDOM

Eric J. Pitcher
Los Alamos National Laboratory
LANSCE, MS H805
Los Alamos NM 87545

Roger Pynn
Los Alamos National Laboratory
LANSCE, MS H805
Los Alamos, NM 87545

James W. Richardson, Jr.
IPNS Division
Argonne National Laboratory
Building 360
9700 South Cass Avenue
Argonne, IL 60439

Robert A. Robinson
Los Alamos National Laboratory
LANSCE, MS H805
Los Alamos, NM 87545

Gary J. Russell
Los Alamos National Laboratory
LANSCE, MS H805
Los Alamos, NM 87545

Thomas Russell
IBM-Almaden Research Laboratory
MS K93/802
650 Harry Road
San Jose, CA 95120

Benno P. Schoenborn
Los Alamos National Laboratory
LANSCE, MS H880
Los Alamos, NM 87545

Lee Schroeder
Lawrence Berkeley Laboratory
MS 50D-106
1 Cyclotron Road
Berkeley, CA 94720

Phillip Seeger
Sumner Associates
239 Loma Escolar
Los Alamos, NM 87544

Stephen M. Shapiro
Department of Physics
Brookhaven National Laboratory
Bldg. 510B
P.O. Box 5000
Upton, NY 11973-5000

Workshop on Neutron Instrumentation for a Long-Pulse Spallation Source

Lawrence Berkeley National Laboratory
Berkeley, CA

April 18-21, 1995

LIST OF PARTICIPANTS

Sunil Sinha
Argonne National Laboratory
9700 South Cass Avenue
Argonne, IL 60439

Greg Smith
Los Alamos National Laboratory
LANSCE, MS H805
Los Alamos, NM 87545

Uschi Steigenberger
ISIS Facility
Rutherford-Appleton Laboratory
Chilton, Didcot OXON OX11 0QX
UNITED KINGDOM

Andrew Taylor
ISIS Facility
Rutherford-Appleton Laboratory
Chilton, Didcot OXON OX11 0QX
UNITED KINGDOM

Pappannan Thiyagarajan
IPNS Division, JA 105, Bldg 200
Argonne National Laboratory
9700 South Cass Avenue
Argonne, IL 60439

Iran L. Thomas
U.S. Department of Energy
ER-13, Room J-304, GTN
19901 Germantown Road
Germantown, MD 20874-1290

Frans Trouw
IPNS, Bldg 360
Argonne National Laboratory
9700 South Cass Avenue
Argonne, IL 69439

George D. Wignall
Oak Ridge National Laboratory
Solid State Div., Bldg 7962
P.O. Box 2008
Oak Ridge, TN 37831-6393

Working Group Reports

Spectrometer Type	Typical Science	Equiv ILL Instr.	Equiv ISIS Instr.	Neutron Energy	1 MW LPSS Performance*	Comments
Small Angle Scattering	structure of macromolecular assemblies					
– 20 m flight path; 10 Å wavelength		D22	LOQ	cold	0.6 x ILL	
– 20 m flight path; 6 Å wavelength		D22	LOQ	cold	1 x ILL	
Reflectometer	density profiles of layered structures	D17	CRISP	cold	3 - 5 x ILL	
Powder Diffraction	atomic structures of polycrystalline materials					
Low Resolution Powder Diffraction		D7		cold	0.5 - 1 x ILL	For powder diffraction, gains over ILL
Medium Resolution Powder Diffraction		D16		cold	6 x ILL	performance are already available at
High Resolution Powder Diffraction		D2B	HRPD	thermal	3 - 4 x ILL	existing short-pulse spallation sources
Amorphous Material Diffraction	atomic coordination in glasses	D4	LAD	hot	0.6 x ILL	for thermal and hot neutrons.
Single Crystal Diffraction						
Laue Diffraction	protein crystallography			thermal	1 x ILL	*comparison is with Laue instr. at ILL. Gains*
4-circle (small unit cells)	crystal structures for small unit cells	D8	SXD	thermal	1 x ILL	relative to traditional instr. are higher
Diffuse Scattering	lattice distortions, defects	D7		cold	3 - 4 x ILL	
Crystal Analyser Spectrometer	high energy molecular spectroscopy	IN1B	TFXA	hot	not feasible	Use conventional SPSS
High Energy Spectroscopy	high energy collective excitations	IN1	HET, MARI	hot	not feasible	Use conventional SPSS
High Resolution Inelastic Scattering	diffusion, tunnelling, magnetic excitations, 3-He					
– multi-chopper spectrometer		IN5		cold	2 - 4 x ILL	gain depends on useful dynamic range
– time focussed TOF spectrometer		IN6		cold	1.6 x ILL	
– backscattering (1 μeV resolution)		IN10		cold	0.25 - 4 x ILL	gain depends on useful dynamic range
– backscattering (10 μeV resolution)			IRIS	cold	2.6 x ISIS	
– backscattering with MUSICAL mono.				cold	2.5 - 4 x ILL	
Neutron Spin Echo	diffusion; polymer & spin glass dynamics	IN15		cold	1 x ILL	better dynamic range & Q resoln. for LPSS
S(Q,E) Spectroscopy	magnetic excitations; glassy dynamics	IN4C	HET	thermal	0.4 - 5 x ILL	gain depends on resolution required
Conventional Three Axis Machines	limited scans of collective excitations					
Cold Neutron TAS		IN14		cold	0.4 x ILL	Detector gating reduces background and
Thermal Neutron TAS		IN8		thermal	0.2 x ILL	increases performance at an LPSS by a
Hot Neutron TAS		IN1		hot	0.2 x ILL	further factor of 1 to 7 for all TAS.
Augmented Three Axis Machines	extended scans of collective excitations					
Multi-Analyser TAS (RITA)			PRISMA	cold	0.7 - 5 x ILL	gain depends on resolution required

* Compares count rates for "optimal" spectrometers at existing sources and the benchmark 1 MW LPSS for equal resolution in the important dimensions of (Q,E) space

ELASTIC SCATTERING RESEARCH AT A 1 MW LONG PULSE SPALLATION NEUTRON SOURCE

Elastic Scattering Working Group Report

R. Kent Crawford (ANL), Chairman

Introduction

The elastic scattering working group investigated instrumentation for powder diffraction, single-crystal diffraction, small-angle diffraction, and reflectometry. For this purpose, three subgroups were formed; one for powder diffraction and single-crystal diffraction, one for small-angle diffraction, and one for reflectometry. For the most part these subgroups worked separately, but for part of the time the reflectometry and small-angle diffraction subgroups met together to discuss areas of common interest. Contributors in each of these subgroups are indicated below along with the discussion of these subgroup deliberations.

Time-Averaged Intensity Comparisons

Unless specified otherwise, results from each of the subgroups were based on the assumption that the long-pulse spallation source (LPSS) has a 1-ms proton pulse width and operates at 60 Hz. In many cases the LPSS instrumentation is compared with both reactor and short-pulse spallation source (SPSS) instrumentation. The time-structures assumed for the SPSS are specified as necessary, since different time-structures are assumed in the different cases. For the LPSS the moderators are always coupled and unpoisoned, but for the SPSS the moderators can be either coupled or decoupled and poisoned or unpoisoned, as the case requires. In either case the output from any one moderator depends on the details of the source geometry and materials, including the contents, sizes and locations of all the other moderators, the presence or absence of decoupling materials, and the size and material of the reflector. Throughout this report it has been assumed that a 1-MW pulsed spallation source (long or short pulse) with coupled moderators produces a time-averaged flux equivalent to that of a 10-MW reactor for thermal neutrons (1/6 of the flux of the 60-MW ILL reactor) and equivalent to a 15-MW reactor for cold neutrons (1/4 of the flux of best ILL cold source), both of which are based on the benchmark calculations of Russell[1] and apply to the specific source configuration considered in those calculations. For the pulsed sources the moderators are assumed to be ambient temperature water for thermal neutrons and liquid hydrogen at ~20 K for cold neutrons. Grooved moderators, which might provide some intensity increase, have not been assumed.

The pulses from the coupled moderators have long tails, with as much as 20-30% of the total flux falling outside the nominal 1-ms pulse at the LPSS. For some of the types of time-of-flight (TOF) measurements at the LPSS or at coupled moderators on the SPSS these tails do not contribute to the useful flux, and in these cases the time-averaged flux must be discounted by a factor of ~0.8.

Basic TOF Equations, and Gain from Source Time Structure

The basic equations governing the elastic instruments are:

$$\lambda \cong 4000 \frac{t}{L} \tag{1}$$

$$\delta\lambda \cong 4000 \frac{\delta t}{L} \quad \text{or} \quad \delta\lambda \cong 4000 \frac{\delta t_c}{L} \tag{2}$$

$$\Delta\lambda_f \cong 4000 \frac{\Delta t}{L} \tag{3}$$

Here λ is the wavelength, $\delta\lambda$ the wavelength resolution, and $\Delta\lambda_f$ the wavelength bandwidth permitted by frame overlap, all in Å; t is the time-of-flight, δt is the width of the neutron pulse from the moderator, δt_c is the chopper pulse width when a chopper is used to shorten the pulse, and Δt is the portion of the period between source pulses which is useful for counting, all in s; and L is the source-sample-detector path length in m. (Throughout this report, unless specified otherwise, widths signified with the symbol δ are taken to be FWHM.) For a 1-ms 60-Hz LPSS, $\Delta t \sim 15$ ms since the rest of the 16.7 ms pulsing period is taken up by the fast background from the source prompt pulse and by chopper "penumbra" effects. The source time structure results in an intensity gain G_t of an LPSS or SPSS instrument relative to a similar TOF instrument at a reactor having the same time-averaged flux.

$$G_t \approx \frac{\Delta t}{\delta t} \quad \text{or} \quad G_t \approx \frac{\Delta\lambda}{\delta\lambda} \tag{4}$$

where the first version, giving the gain as the reciprocal of the effective source duty factor, holds if the full bandwidth $\Delta\lambda_f$ is useful for the science. If the pulse width δt results in a wavelength resolution $\delta\lambda$ better than that required by the science, the gain factors of Eq. 4 must be reduced to correspond to the required resolution rather than that actually attained.

Use of Choppers

A pulse-definition chopper can be placed at a relatively short distance L_c from the moderator to provide shorter pulses than those produced by the source. The same resolution can then be achieved with a shorter path length. If the chopper pulse width is $\delta t_c < \delta t$, then this chopper becomes a new effective source with intensity reduced by the factor $\delta t_c/\delta t$. The shorter path length results in a larger bandwidth, and if this bandwidth is all useful the time-of-flight gain, referenced to the unchopped source flux, then becomes

$$G_t \approx \frac{\delta t_c}{\delta t} \frac{\Delta t}{\delta t_c} = \frac{\Delta t}{\delta t} . \tag{5}$$

Thus, so long as the resulting bandwidth and resolution are useful, the addition of a pulse-definition chopper does not change the time-structure gain.

If a pulse-definition chopper at a distance L_c from the moderator is used to produce a pulse with width $\delta t_c << \delta t$, then the bandwidth passed by this chopper will be $\Delta\lambda_c$ given by

$$\Delta\lambda_c \cong 4000 \frac{\delta t}{L_c} \tag{6}$$

independent of the rest of the instrument. If the rest of the instrument is designed to use a bandwidth smaller than $\Delta\lambda_c$, then this bandwidth limitation due to the pulse-definition chopper becomes irrelevant. However, if the rest of the instrument is designed for a larger bandwidth, the pulse-definition chopper becomes the bandwidth-limiting element.

Such a pulse-definition chopper will also distort the wavelength spectrum it transmits, since it will select the shorter-wavelength transmitted neutrons from the end of the source pulse, and the longer-wavelength transmitted neutrons from the beginning of the source pulse where the wavelength distribution is somewhat different, as shown in Figure 1. The magnitude of this effect will depend on details of the reflector and moderator and on the wavelengths involved, and is best treated with Monte Carlo simulations. This sampling of different parts of the source pulse at different wavelengths also implies that the use of choppers to trim the tails off the source pulses will not produce satisfactory results, since different amounts of the tail will be transmitted at each wavelength. In many cases this wavelength dependence may not be important.

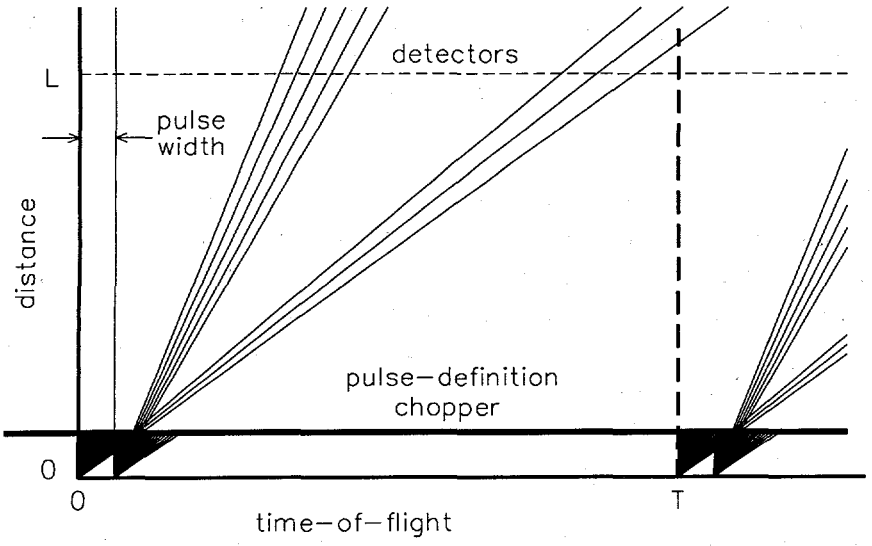

Fig. 1. Time-distance diagram for a pulse-definition chopper at an LPSS. This diagram illustrates how such a chopper limits the bandwidth reaching the detectors, and how the leading and trailing edges of the source pulse provide quite different wavelengths to the sample.

For pulse definition we want fast choppers which can transmit a relatively large bandwidth. This rules out Fermi choppers, making disk choppers the preferred technology. Disk choppers are operated on several existing instruments at reactors. Standard technology involves 50 cm diameter aluminum choppers rotating at speeds up to 20,000 rpm (333 Hz) and covered with gadolinium-oxide paint. Since the chopper must be operated at a multiple of the source

frequency, this implies a maximum chopper frequency of 300 Hz. The peripheral velocity of such a chopper is ~470 m/s, so if the chopper slit width is equal to the beam width W, the chopper pulse will be triangular in shape and the shortest possible chopper pulse width will be δt_c = W/470 (FWHM), for W in m. Typical beam widths close to the moderator are ~10 cm, giving δt_c = 212 μs. Using identical counter-rotating choppers results in a triangular pulse with half this width, or δt_c = 106 μs. Shorter pulses can be obtained if narrower moderators are used, but this will cost intensity.

For the glass and liquids diffractometer, the chopper must work for wavelengths down to 0.2 Å. Since gadolinium-oxide paint becomes transparent to neutrons at wavelengths below ~0.5 Å, additional R&D would be required to develop other suitable absorbers (presumably boron-based) for a chopper for this instrument.

To obtain still shorter pulses, it is necessary to develop the technology to spin the choppers faster, or else to chop a narrower beam. Converging and diverging supermirror guide sections have been used to narrow the beam at a chopper and then expand it again to fill the guide. It may be possible to utilize this technology to meet all the requirements for pulse-limiting choppers for elastic instruments set forth below. However, there are a number of difficulties. For the 20 μs pulses required for some of the instruments, the beam would have to be reduced from the moderator size (~13 cm) down to ~2 cm, and then expanded again to fill the guide. This would have to be done for relatively short wavelength neutrons, and moreover, would have to be done relatively close to the moderator (Eqs. 3 and 6 give $L_c \sim L/15$) where radiation fields are high. Thus, if any of these instruments are seriously contemplated for inclusion at an LPSS, an adequately-funded R&D program must be undertaken to develop the necessary chopper and guide technology.

In addition to the possible use of pulse-definition choppers to shorten the pulse, each instrument will require a t_0 chopper to eliminate most of the fast neutron background from the prompt pulse, and one or more bandwidth-limiting choppers to prevent interference from frame-overlap neutrons. All of the TOF instruments for elastic scattering will appear schematically as shown in Figure 2. The inset to Figure 2 shows schematically the timing diagram associated with the different choppers on such instruments.

Other Factors in the Instrument Comparisons

The time-structure gain G_t discussed above is based on comparing TOF instruments at the pulsed sources with TOF instruments at a reactor. These comparisons are straightforward and are not subject to much uncertainty. However, the TOF technique is seldom used for elastic scattering measurements at a reactor, so the more appropriate comparisons would be with crystal-monochromator instruments (or velocity-selectors in the case of small-angle scattering) at the reactor. The comparison with crystal-monochromator instruments is much less straightforward, and even for optimized instruments it will vary depending on the desired resolution. These comparisons will be considered further in sections for the specific types of instruments.

Another important difference arises because the crystal-monochromator measures at a single wavelength, which is usually set at the most intense portion of the Maxwellian spectrum from the

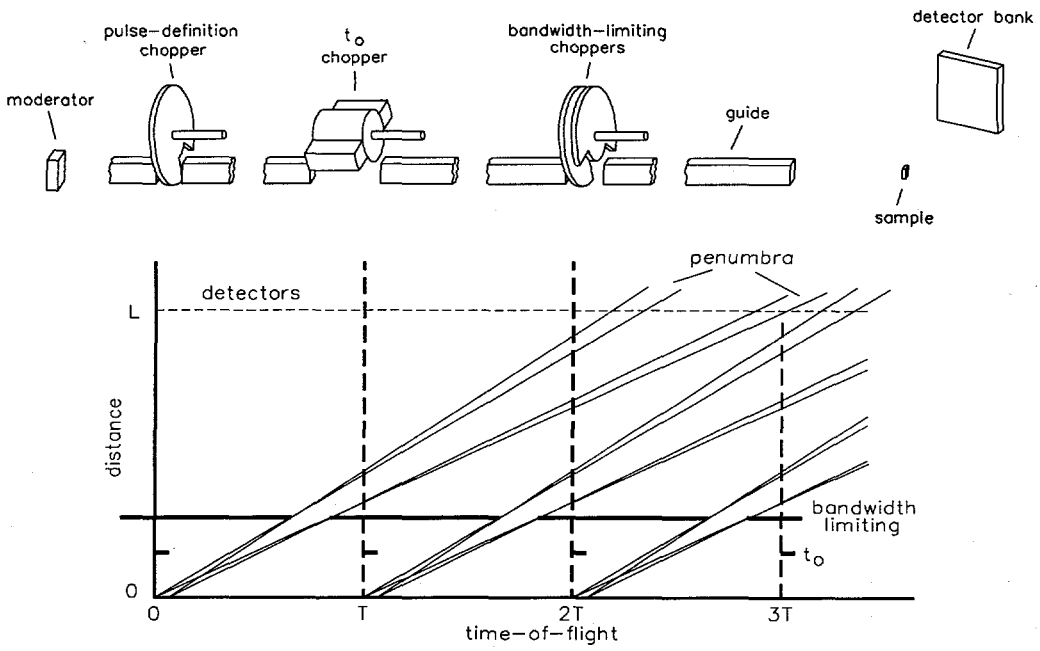

Fig. 2. Schematic representation of the major components of TOF instruments for elastic scattering at an LPSS. All instruments probably need t_0 and bandwidth-limiting choppers. Only some of the instruments will use guides, and many will not need pulse-definition choppers. The lower part of the figure shows the timing diagram for the t_0 and bandwidth-limiting choppers.

moderator. The TOF instruments, on the other hand, measure over a band of wavelengths, and some of these wavelengths may come from less intense portions of the spectrum. Where appropriate, the instrument gain has been discounted to account for this.

One other difference between TOF and crystal-monochromator instruments has significant practical consequences. The use of crystal monochromators frequently makes it possible to "multiplex" several different instruments on a guide, with the monochromator for each instrument reflecting out only the very narrow band of wavelengths needed for that instrument. Multiplexing of TOF instruments may be possible in a few cases by using mirrors to reflect out the wavelength band needed by a particular instrument. However, since the TOF instruments achieve their gain by using relatively broad wavelength bands, such multiplexing of TOF instruments cannot be carried out to the same extent. Thus the exclusive use of TOF may impose a practical limit on the number of instruments that can be included around one target station.

Simulations

Simulations of specific instruments for protein crystallography, small-angle diffraction, and reflectometry at an LPSS were carried out prior to the workshop by Benno Schoenborn,[2] Phil Seeger and Glen Olah,[3] and Mike Fitzsimmons[4] and Greg Smith[5] respectively. The results were presented in the plenary session on the first day of the workshop. These simulations confirmed that the simple expressions given above for the instrument resolution, bandwidth, and

time-structure gain produced reasonable quantitative results. The specific instrument configurations used in these simulations provided a focus for discussion in each of the respective subgroups, where some of the implications were further explored. The Monte Carlo routines used in some of these simulations can be readily adapted to investigate other instrument configurations and issues as seems appropriate. Several such additional investigations were suggested by the various elastic scattering subgroups.

Powder Diffraction

Contributors: Kent Crawford, ANL; Mike Fitzsimmons, LANL; Mike Johnson, ISIS; Roger Pynn, LANL; Jim Richardson, ANL; Rob Robinson, LANL; Phil Seeger, LANL.

The powder-diffraction subgroup felt that general-purpose powder diffractometers with at least three different resolutions would be required to cover the full range of science. These would be a high-intensity instrument with nominal resolution of $\delta d/d \sim 0.01$-0.02, a medium-resolution instrument with $\delta d/d \sim 0.002$-0.005, and a high-resolution instrument with $\delta d/d \sim 0.0005$. In addition, a different instrument would be required for optimized diffraction studies of glasses and liquids. Tables 1 and 2 show parameters for such instruments at an LPSS and an SPSS respectively. These parameters are discussed in the following sections.

High-Intensity/Medium-Resolution Powder Diffractometers at the LPSS

For the high-intensity instrument a minimum wavelength of $\lambda_{min} = 2$ Å permits the study of d-spacings down to 1 Å in backscattering, and this is adequate for most low-resolution applications. If the full pulse width is utilized, then Eq. 2 shows that a path length of L = 100 m is required to achieve $\delta d/d = 0.02$ in backscattering at λ_{min}. (In backscattering $\cot\theta$ goes to zero, so the geometrical contribution to the resolution vanishes and the resolution is just $\delta d/d = \delta\lambda/\lambda$.) However, as was noted in the introduction, use of a pulse-definition chopper will allow us to shorten this path and has the added advantage of producing a much more symmetrical pulse without the long tails.

The minimum source-chopper distance is $L_c \sim 2.5$ m, and at this distance Eq. 6 shows that the chopper will pass a bandwidth of $\Delta\lambda_c = 1.6$ Å. The shortest flight path that can utilize the full 1.6 Å bandwidth (i.e., $\Delta\lambda_c = \Delta\lambda_f$) in the ~15 ms available counting time is thus L = 40 m. The desired resolution $\delta\lambda = 0.04$ Å with the 37.5 m chopper-detector distance then requires a chopper pulse width of $\delta t_c = 375$ μs. The full 1.6 Å bandwidth is useful for most low-resolution experiments. This set of instrument parameters is indicated as High-intensity-B in Table 1. If the chopper is removed so that the full pulse width is used, the backscattering resolution becomes $\delta\lambda = 0.1$ Å, giving 5% resolution. These conditions are indicated as High-intensity-A in Table 1. This resolution is adequate to separate peaks at large d-spacings. In this mode the pulse tail will make it difficult to measure the background accurately, but the higher intensity may be important for some experiments. For the medium-resolution instrument, a minimum wavelength of $\lambda_{min} =$ 1 Å is required to study d-spacings down to 0.5 Å. A wavelength resolution of $\delta\lambda = 0.002$ Å with a flight path of 40 m requires that the chopper at $L_c = 2.5$ m produce a pulse of $\delta t_c = 19$ μs. These conditions are indicated as Med.-resolution in Table 1. This pulse width may be possible with suitable choppers and converging/diverging guides. If it is, then all of these high-intensity

and medium resolution applications, requiring resolutions from 0.2% to 5% can be satisfied by a single instrument, just by changing the chopping pulse width. Even if the minimum achievable pulse width is only 50 μs, the instrument can still span the range of resolutions from 0.5% to 5%. If desired, the chopping requirements can be relaxed somewhat by making the instrument flight path longer, but this will be at the expense of a reduced wavelength bandwidth.

The geometrical resolution becomes important at the smaller values of 2θ so d-spacings are measured with poorer resolution in the lower angle detectors. However, for large d-spacings the peaks are less dense and so a poorer resolution there is adequate in many cases. If data from 30°-150° can be used, then the full range of d-spacings required for most experiments can be collected with a single instrument setting. Otherwise several different measurements must be made with the choppers set to pass a different wavelength band in each case.

Since the full bandwidth is used in all cases, the time-structure gain is $G_t = 15$ for each of these modes. Either a thermal or a cold moderator can be used for this instrument, depending on which wavelengths are to be emphasized. For present purposes, we assume the instrument will view a cold moderator with time-averaged flux 1/4 that at ILL (Φ_{th}). For the High-intensity-B and the Medium-resolution modes, the intensity should be discounted by the factor of 0.8 (G_{pt}), since no use is made of the pulse tails. For the two low-resolution modes, all detector angles will probably be used, so there will be no particular detector-solid-angle difference between the TOF instrument at the LPSS and a crystal-monochromator instrument at the reactor, but for the medium-resolution version we assume the backscattering gain factor of 10 (G_{bs}) indicated by Mezei.[8] In all three modes we assume a factor of 5 ($1/G_{cmf}$) advantage for the focusing capabilities of the crystal-monochromator. This is a rough number based on the fact that practical focusing crystal monochromators can produce a maximum vertical acceptance angle of about 5° at the sample, while a supermirror guide can produce at most about 1° at 2 Å. The guide-tube losses for the TOF instrument are ~0.7 (G_{gtl}), and the monochromator reflectivity at the reactor is ~0.5-0.7 ($1/G_{mr}$).

The "Reactor Equiv" column in Table 1 attempts to compare the LPSS TOF instruments with their crystal-monochromator counterparts at a reactor. The comparison factor is just given by the product of the time-averaged flux and the various gain factors G_i indicated here, with the values for the factors given in the table footnotes.

$$\text{Reactor equiv} = \Phi_{th} \prod G_i \qquad (7)$$

It should be emphasized that this column is intended to provide only rough performance indications, and because of the many approximations the values given can easily be off by a factor of two or more in either direction.

High-Resolution Powder Diffractometers at an LPSS

Finally, for the high-resolution instrument with $\delta d/d \sim 0.0005$, a pulse width of 5 μs would be required for a 40 m flight path. This is not practical. In order to get the required pulse width up to ~20 μs, a flight path of L = 160 m is required. In many cases it will be desirable to cover the full d-spacing range using only the backscattering bank, where the resolution is highest. To do

Table 1 -- Parameters for Powder Diffractometers at a 1-MW 60-Hz 1-ms LPSS*

	λ_{min} (Å)	$\delta\lambda/\lambda_{min}$	L[a] (m)	δt_c (μs)	$\Delta\lambda$ (Å)	2θ=150° d_{min}	2θ=150° d_{max}	2θ=90° d_{min}	2θ=90° d_{max}	2θ=30° d_{min}	2θ=30° d_{max}	Mod[b]	Reactor Equiv[c]
High-intensity-A	2.0	0.05	40	-	1.6	1.0	1.9	1.4	2.5	3.8	6.9	C	0.75×ILL[d]
High-intensity-B	2.0	0.02	40	94	1.6	1.0	1.9	1.4	2.5	3.8	6.9	C	0.6×ILL[e]
Med.-resolution	1.0	0.002	40	19	1.6	0.5	1.3	0.7	1.8	1.9	5.0	C	6.0×ILL[f]
High-resolution	1.0	0.0005	160	20	0.4	0.5	0.7	0.7	1.0	1.9	2.7	Th	4.0×ILL[g]

						2θ=90° Q_{max}	2θ=90° Q_{min}	2θ=6° Q_{max}	2θ=6° Q_{min}			
Glass and liquid	0.2	0.01	40	19	1.6	44	4.9	3.3	0.4			0.6×ILL[h]

* Units for d are Å; units for Q are $Å^{-1}$.

a Flight path length is not optimized to place the desired wavelengths between t_0 pulses.

b Moderator: C = coupled liquid hydrogen; Th = coupled water.

c Data rate of TOF instrument at 1-MW LPSS relative to crystal-monochromator instrument at ILL. These relative rate estimates may be off by as much as a factor of two in either direction. See text.

d Eq. 7 with Φ_{th} = (1/4) ILL, $G_t = 15$, $G_{cmf} = 1/5$, $G_{gl} = 0.7$, $G_{mr} = 1/0.7$; all other $G_i = 1$.

e Eq. 7 with Φ_{th} = (1/4) ILL, $G_t = 15$, $G_{pt} = 0.8$, $G_{cmf} = 1/5$, $G_{gtl} = 0.7$, $G_{mr} = 1/0.7$; all other $G_i = 1$.

f Eq. 7 with Φ_{th} = (1/4) ILL, $G_t = 15$, $G_{pt} = 0.8$, $G_{bs} = 10$, $G_{cmf} = 1/5$, $G_{gtl} = 0.7$, $G_{mr} = 1/0.7$; all other $G_i = 1$.

g Eq. 7 with Φ_{th} = (1/6) ILL, $G_t = 15$, $G_{pt} = 0.8$, $G_{bs} = 10$, $G_{cmf} = 1/5$, $G_{gtl} = 0.7$, $G_{mr} = 1/0.7$; all other $G_i = 1$.

h Eq. 7 with Φ_{th} = (1/6) ILL, $G_t = 15$, $G_{pt} = 0.8$, $G_{cmf} = 1/5$, $G_{gtl} = 0.7$, $G_{mr} = 1/0.5$; all other $G_i = 1$.

Table 2 -- Parameters for Powder Diffractometers at a 1-MW 60-Hz SPSS*

	λ_{min} (Å)	$\delta\lambda/\lambda_{min}$	L[a] (m)	δt^b (μs)	$\Delta\lambda$ (Å)	2θ=150° d_{min}	2θ=150° d_{max}	2θ=90° d_{min}	2θ=90° d_{max}	2θ=30° d_{min}	2θ=30° d_{max}	Mod[c]	Reactor Equiv[d]
High-intensity	2.0	0.004[e]	12[e]	25	5.0	1.0	3.6	1.4	4.9	3.8	13.5	d-C	0.7×ILL[f]
Med.-resolution	1.0	0.002	20	10	3.0	0.5	2.1	0.7	2.8	1.9	7.7	d-Th	36×ILL[g]
High-resolution	1.0	0.0005	80	10	0.7	0.5	0.9	0.7	1.2	1.9	3.3	d-Th	50×ILL[h]

						2θ=90° Q_{max}	2θ=90° Q_{min}	2θ=6° Q_{max}	2θ=6° Q_{min}			
Glass and liquid	0.2	0.007[e]	12[e]	4	5.0	44	1.7	3.3	0.1			17×ILL[j]

* Units for d are Å; units for Q are $Å^{-1}$.

a Flight path length is not optimized to place the desired wavelengths between t_0 pulses.

b Source pulse widths based on calculations for a poisoned, decoupled water moderator[6] or on measurements for a decoupled liquid hydrogen moderator.[7]

c Moderator: d-C = decoupled liquid hydrogen; d-Th = decoupled water.

d Data rate of TOF instrument at 1-MW SPSS relative to crystal-monochromator instrument at ILL. These relative rate estimates may be off by as much as a factor of two in either direction. See text.

e Path length extended to 12 m to be realistic. This gives a wavelength resolution much better than required, but the geometrical resolution can be relaxed to match the desired resolution

f Eq. 7 with Φ_{th} = (1/4) ILL, $G_{dm} = 1/6$, $G_t = 600$, $G_{\delta\lambda} = 0.2$, $G_s = 1/3$, $G_{cmf} = 1/5$, $G_c = 1.4$, $G_{mr} = 1/0.7$; all other $G_i = 1$.

g Eq. 7 with Φ_{th} = (1/6) ILL, $G_{dm} = 1/10$, $G_t = 1500$, $G_s = 1/2$, $G_{bs} = 10$, $G_{cmf} = 1/5$, $G_{mr} = 1/0.7$; all other $G_i = 1$.

h Eq. 7 with Φ_{th} = (1/6) ILL, $G_{dm} = 1/10$, $G_t = 1500$, $G_{bs} = 10$, $G_{cmf} = 1/5$, $G_{gtl} = 0.7$, $G_{mr} = 1/0.7$; all other $G_i = 1$.

j Eq. 7 with Φ_{th} = (1/6) ILL, $G_{dm} = 1/10$, $G_t = 3750$, $G_{\delta\lambda} = 0.7$, $G_{cmf} = 1/5$, $G_{mr} = 1/0.5$; all other $G_i = 1$.

this, measurements must be made with several different settings of the chopper phase, each time using a different wavelength band. The reactor equivalent is again given by Eq. 7 with the gain factors indicated in Table 1. This instrument can probably be built, but a high-resolution powder diffractometer at an SPSS performs so much better (see Table 2) that this instrument is probably not worth building at an LPSS (unless no suitable SPSS is available).

Glasses and Liquids Diffractometer at an LPSS

For glasses and liquids it is important to be able to measure up to a Q of 40-50 $Å^{-1}$ using only scattering angles below 90°, as this minimizes the Placzek corrections. A wavelength resolution of $\delta\lambda/\lambda = 0.01$ is required. These conditions imply $\lambda_{min} = 0.2$ Å so $\delta\lambda = 0.002$ Å. These can be achieved with L = 40 m and $\delta t_c = 19$ μs. The bandwidth is $\Delta\lambda_f = 1.6$ Å, so with a minimum scattering angle of 6° the instrument can measure over the range $Q_{max} = 44$ $Å^{-1}$ down to $Q_{min} = 0.4$ $Å^{-1}$ with a single instrument setting. If smaller Q_{min} is required, additional measurements with different chopper phasing will be necessary. The reactor equivalent is again given by Eq. 7 with the gain factors indicated in Table 1. This instrument could be built, although backgrounds may be high at the shortest wavelengths. However, a glass and liquids diffractometer at an SPSS performs so much better (see Table 2) that it is probably not worth building a special instrument for this purpose at an LPSS unless no suitable SPSS is available. Parameters for this instrument are similar to those for the high-intensity/medium-resolution powder diffractometer, so that multi-purpose instrument might also be used for some glass and liquids diffraction measurements.

Powder Diffractometer at an SPSS

To see how the LPSS instruments compare with those at an SPSS, the parameters for "comparable" SPSS instruments are indicated in Table 2. The SPSS instruments in this table use the traditional poisoned, decoupled moderators. For low-resolution applications, an SPSS instrument with a coupled moderator might also be considered. In this case the gain would be a factor of ~3 over the LPSS instrument because of the higher peak flux at the SPSS moderator.

As shown in Table 2, a much shorter instrument flight path can be used to achieve comparable resolution at an SPSS with poisoned, decoupled moderators. The resulting increase in bandwidth is all (or nearly all) useful, since at the highest wavelength d-spacings of interest (up to ~5 Å) are still being measured in backscattering. In addition to the gain factors introduced above for the LPSS, some new gain factors enter into the SPSS performance. The use of decoupled moderators reduces the flux by a factor $(1/G_{dm})$ of 6 for liquid hydrogen[7] and 10 for water.[9] The use of a broad bandwidth means that portions of the data will be measured with fluxes far down from the maximum of the spectrum, reducing the effective intensity by another factor $(1/G_s)$ of ~2-3. On short flight paths, the natural collimation of the instrument allows greater angular acceptance than can be provided by a guide, and for a 10 cm wide moderator this results in a reduction of the crystal-monochromator focusing advantage by a factor $G_c \approx (0.1/0.00350\ L\ \lambda)^2$. In some cases the flight path cannot be made as short as resolution dictates, so the actual wavelength resolution is better than required. The factor $G_{\delta\lambda} = \delta\lambda_{actual}/\delta\lambda_{required}$ is used to account for this.

Residual Stress Measurements

Both the medium-resolution and the high-resolution powder diffractometers discussed here would work very well for residual stress measurements. For this purpose, the instruments should be equipped with suitable collimation in the incident and scattered beams to define the specific locations being probed within the sample. A large sample area and suitable sample-translation mechanisms would also be required. Several chopper settings would probably be needed to cover the required d-spacings at the angles demanded by the scattered beam collimators. Because of the restricted angular collimation used in residual stress measurements to probe small volumes within bulk samples, gains relative to crystal-monochromator instruments would not be the same as those in Tables 1 or 2.

Texture Measurements

The medium-resolution powder diffractometer discussed here could be used for texture measurements. To be even more useful for this purpose, the instrument could be equipped with 2D position-sensitive detectors in at least one of the detector banks. An appropriate computer-driven sample-orienting goniometer is also necessary.

Magnetic Structures

For magnetic-structure measurements, wavelengths of 2-10 Å are useful, and resolutions of ~1% are required. For measurements which follow a single peak while varying some external parameter, resolutions up to 10% can be tolerated. These conditions can be achieved on the high-intensity powder diffractometer discussed above. The small bandwidth of the LPSS instruments can be readily polarized at long wavelengths.

Fourier Diffractometer

A high-resolution Fourier diffractometer[10] has recently been successfully operated at the IBR-II pulsed reactor at Dubna. This instrument shows promise of producing resolution comparable to that of the HRPD diffractometer at ISIS, but the signal/background was significantly worse than at HRPD. IBR-II has a relatively long pulse (~300 μs), so this suggests that it would be useful to analyze the performance of a Fourier diffractometer for various applications at a LPSS. Unfortunately, the powder diffraction subgroup did not have time to attempt such an analysis, so this is left as a suggested future exercise.

Powder Diffraction Summary

The performance comparisons in Tables 1 and 2 are intended as only as a rough guide to relative performance of instruments at the different types of sources. There are uncertainties in each of the relative gain factors included here and other important factors may have been omitted entirely, so the comparisons with a reactor could easily be off by a factor of two or more in either direction. The picture is even more confusing, because the resolution of crystal-monochromator instruments has a considerably different dependence on d-spacing than does that of the LPSS

TOF instruments, and the variation in resolution with d-spacing is even different for LPSS and SPSS instruments. Thus making an objective comparison depends on subjective choices of what resolution is important for each d range. Because of this complexity, more accurate quantitative comparisons must be made on the basis of rather detailed instrument designs aimed at achieving certain specified resolution criteria, and will not be attempted here. Despite these caveats, the assessments made in Tables 1 and 2 are thought to be fairly realistic, and are reasonably consistent with similar comparisons that have been made in the past.[11] Powder diffractometers at existing lower-power SPSS facilities have demonstrated data rates as high or higher than the rates at comparable ILL instruments, which is again consistent with what would be expected from Table 2.

As a general conclusion, it appears that powder diffraction could probably be done somewhat more effectively at a 1-MW LPSS than at a 60-MW reactor. The estimates here indicate that data rates on a medium or high resolution LPSS instrument could be a factor of 4-6 higher than on optimized instruments at ILL. Gains are estimated to be somewhat lower for low resolution instruments and for the glasses and liquids diffractometer, because these tend to be operated in an angle-dispersive mode where detector solid angle coverage is roughly the same in both TOF and crystal-monochromator instruments It also is shown here that powder diffraction is even more effective at an SPSS than at an LPSS, except in a limited number of cases where part of the SPSS bandwidth is not useful (e.g., measurement of single peaks). Thus it does not appear to make much sense to invest heavily in powder diffraction at an LPSS unless no suitable SPSS is available. It may be useful to have at least one powder diffraction instrument at the LPSS as a support to the other scientific programs there. In this case, the most likely candidate would be the high-intensity/medium-resolution powder diffractometer discussed above, as this instrument appears to perform fairly well at the LPSS and is very versatile. The 40-m flight path considered here for this instrument is the shortest practical, because of the bandwidth-limitations of the pulse-definition chopper. However, the instrument could utilize a longer flight path to concentrate more flux in a narrower wavelength band, with essentially the same overall performance, if this seems better matched to the intended science. The possibility of including these diffraction capabilities on an instrument intended for inelastic measurements could also be investigated.

Because of the need for many choppers and the demanding requirements for some of these choppers, TOF powder diffractometers at an LPSS will usually be more complicated instruments than are their counterparts at an SPSS, and will be more costly to construct and maintain. Some of the reactor instruments with focusing monochromators and area-position-sensitive detectors are also complicated, so there the comparison of complexity with the LPSS instruments is less obvious.

If the choppers can be made to function as required, then they give the LPSS instruments an advantage in terms of flexibility and versatility. As was shown above, it might be possible to have the same LPSS instrument function as both a high-intensity and medium-resolution powder diffractometer as well as a diffractometer for glasses and liquids, and to be reasonably well optimized for each of these functions. The SPSS instruments are not this flexible, so that a separate instrument must be optimized for each of these functions. The crystal-monochromator instruments are less flexible as well.

All of the LPSS instruments discussed above, and most of the SPSS instruments, would benefit from having the source run at a lower repetition rate with the same power and pulse width. Operation at 30 Hz instead of 60 Hz under these conditions would lead to nearly a factor of 2 gain for most instruments.

Before any powder diffractometer is built at the LPSS, a number of issues warrant further exploration. Foremost among these is the design and development of fast disk choppers and the associated converging and diverging supermirror guides which will work reliably in the high radiation environment ~2.5 m from the moderator. These choppers and guides will become highly activated and must be designed to facilitate rapid replacement when problems occur. This should be the focus of an early R&D program, particularly since similar chopper requirements will be encountered for many of the other instruments at an LPSS. Other issues related to powder diffraction which should be explored include:

- Monte Carlo investigation of the spectrum distortion caused by a pulse-definition chopper due to the wavelength dispersion and the differing natures of the leading and trailing edges of the source pulse. Investigation of the resulting wavelength-dependent pulse shape is also needed.
- Detailed investigation, possibly by Monte Carlo techniques, of the relative merits of TOF and crystal-monochromator diffractometers at a reactor. Such information would help to further elucidate the relative merits of powder diffraction at an LPSS relative to that on a crystal-monochromator diffractometer at a reactor.
- Possible usefulness of a Fourier Diffractometer at a LPSS.
- Background issues associated with the occurrence of the prompt pulse during the time interval appropriate for counting the wavelength band of interest. (The instrument flight path length can be chosen so that one particular wavelength band arrives at times which are free from the prompt pulse, but if several different wavelength bands must be selected by rephasing the choppers, then it may no longer be possible to maintain an appropriate clear counting time in all cases.)
- Background issues associated with the fact that the disk choppers are relatively transparent to fast neutrons, and so may not perform pulse-definition or bandwidth-limiting tasks as cleanly as desired. The use of curved guides would alleviate most of these problems, but would also restrict the minimum wavelength that could be used.

Single-Crystal Diffraction

Contributors: John Axe, BNL; Kent Crawford, ANL; Mike Johnson, ISIS; Jim Richardson, ANL; Rob Robinson, LANL; Benno Schoenborn, LANL; Phil Seeger, LANL; Stephen White, Univ. of Calif., Irvine

Introduction

The methods that would be used for single-crystal crystallography at an LPSS or an SPSS are quite different from the methods that have traditionally been used for this purpose at reactors, and are much more closely related to the newer Laue methods being developed for this purpose

at the reactors. It is important to understand these distinctions in order to make a valid comparison of the performance of reactor instruments with those at an LPSS or SPSS.

Single-crystal crystallographic studies at reactors up to now have normally used a crystal monochromator to direct a nearly monochromatic beam of neutrons (with a small wavelength spread $\delta\lambda$) onto the sample. Only a few of the scattering planes in the sample crystal will be oriented to satisfy the Bragg conditions for this small wavelength range and a particular sample orientation, and of these Bragg reflections, only a small subset is observed in the detector or multidetector. To scan through these reflections and to observe additional reflections, the sample or the detector (or both) must be rotated. Figure 3a shows the range of reciprocal space covered with a single crystal and detector setting in this monochromatic-beam process, and Figure 3b indicates the volume covered as the crystal orientation is stepped through 90° about the axis normal to the page (ω-scan).

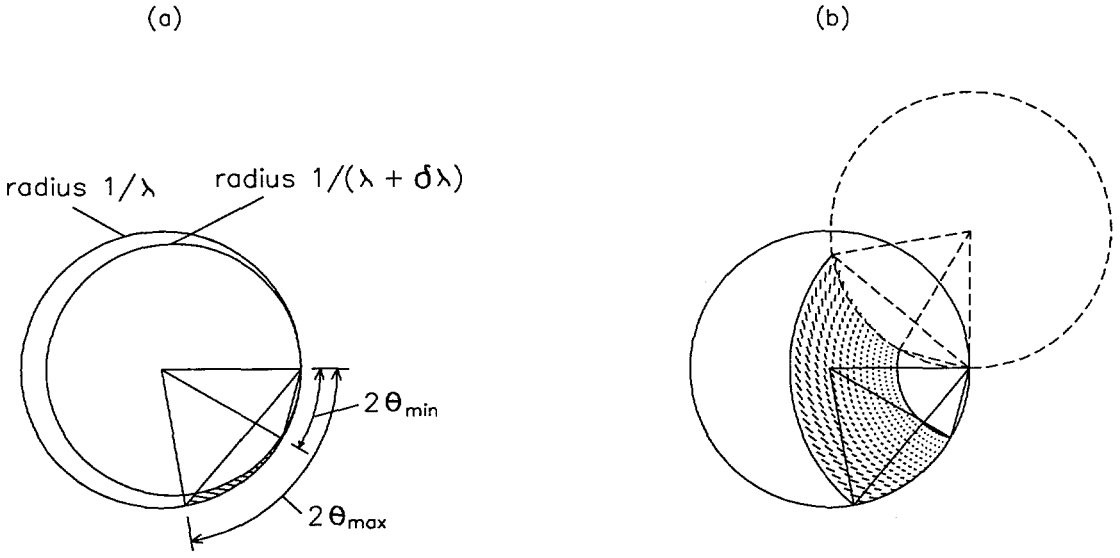

Fig. 3. Ewald-sphere construction for crystal-monochromator single-crystal diffraction instrument. A monochromatic beam with wavelengths spanning a narrow band of width $\delta\lambda$ at wavelength λ is incident on the sample. An area detector spans scattering angles from $2\theta_{min}$ to $2\theta_{max}$. (a) The hatched area shows the region of reciprocal space sampled for one crystal orientation. (b) The hatched area shows the region of reciprocal space covered when the crystal is rotated in small steps through 90° about the axis normal to the page.

In the standard Laue technique, a broad band of wavelengths (λ_{min} to λ_{max}) falls on the sample, and a position-sensitive detector (usually 2D) is used to observe all the reflections which diffract over a certain range of angles. This technique allows many (up to several thousand) reflections to be observed simultaneously, and so makes much more efficient use of the neutrons. However, since the data are collected in only a 2D data set (x and y positions on the detector) this technique can result in overlapping of many of the diffraction peaks, so that the peaks cannot be properly integrated. Furthermore, all of the wavelengths contribute to the background, while only a very

narrow wavelength range contributes to each Bragg reflection, so the signal/background is poor. Figure 4a shows the range of reciprocal space covered in the Laue process, using the same area detector spanning the same scattering angles as in Figure 3. In order to cover an even greater volume of reciprocal space, the crystal can again be rotated to a new orientation and the measurements repeated. However, this time the rotation can proceed in large steps, as shown in Figure 4b. The individually-sampled volumes may not pack very efficiently, so when the step size is chosen to provide the most efficient coverage, there is usually some overlap between the individual regions covered, as shown in the figure.

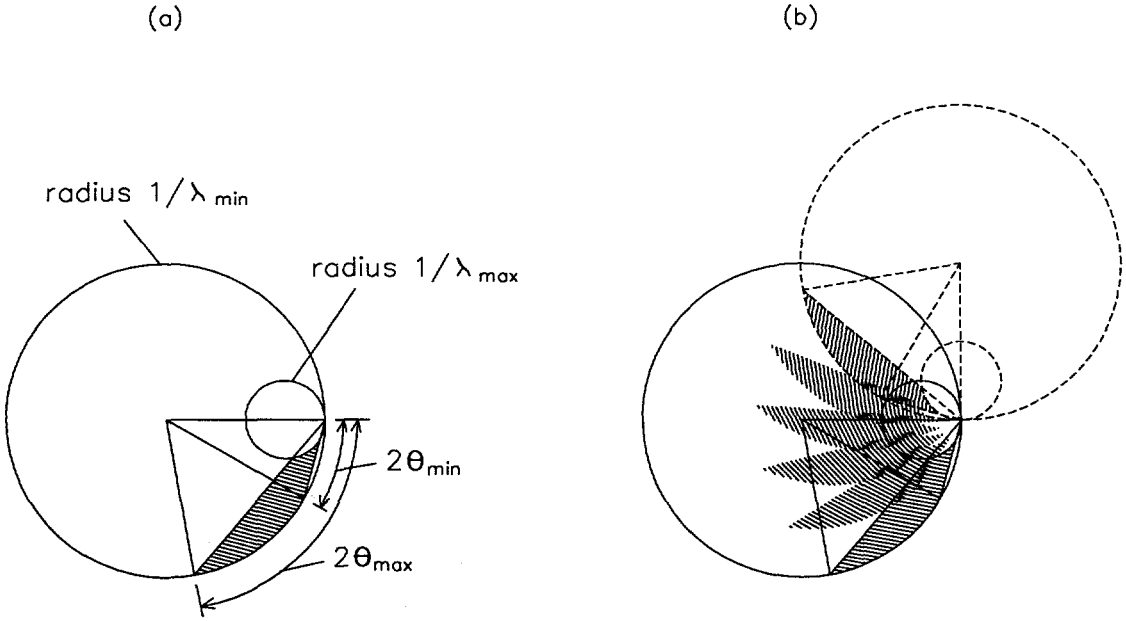

Fig. 4. Ewald-sphere construction for TOF Laue single-crystal diffraction instrument. Wavelengths spanning a wide band between λ_{min} and λ_{max} are incident on the sample. An area detector spans scattering angles from $2\theta_{min}$ to $2\theta_{max}$. (a) The hatched area shows the region of reciprocal space sampled for one crystal orientation. (b) The hatched area shows the region of reciprocal space covered when the crystal is rotated in several large steps through 90° about the axis normal to the page.

In the time-of-flight Laue (TOF Laue) technique, a broad band of wavelengths from a pulsed source (or from a chopper at a reactor) falls on the sample, and a position-sensitive detector is again used to observe the resulting reflections. If the wavelength range and the angular range are the same as for the standard Laue measurement, then the same large number of reflections will be measured with a single crystal orientation. The diagram of Figure 4a again applies. However, in this case all of the neutrons are sorted according to their arrival time as well as to the position on the detector. The inclusion of this TOF or wavelength dimension results in a 3D data set (detector x and y positions, and TOF), that allows complete separation of orders if the wavelength resolution and the detector spatial resolution are adequate. It also allows each peak to be individually integrated, and this integral will include only the background due to the

wavelengths that also contributed to the peak. Again, reciprocal space is spanned by repeating these measurements for different crystal orientations, as in Figure 4b.

In the quasi-Laue technique, this wavelength band is restricted to a much narrower range, say perhaps 10-20% of the wavelength. This wavelength range is still large enough to integrate a large number of reflections, although not as many as when the full wavelength range is used. However, by restricting wavelengths to this shorter range, the background is significantly reduced and the overlap of peaks is minimized. This technique is now being developed at several reactors.[12] In the instruments being developed, multilayer bandpass filters (coarse monochromators) are used to restrict the wavelength. Image-plate detectors are used to cover a large solid angle (>2π sr in some cases) with the high spatial resolution needed to minimize peak overlap. For a comparable-sized detector, this technique generates data equivalent to that measured in a single time-slice in the TOF Laue technique.

Background

For a steady-state source, the Laue technique with its overlaps, densely populated diffraction pattern, and increased background is not suitable for protein crystallography. In this case the reflection intensities are proportional to the acceptable wavelength band (~0.1 Å) for a reflection, but the sample background is proportional to all of the radiation hitting the crystal. This sample-dependent background is significant for protein crystals, because at least a third of the atoms are hydrogen atoms which have a large incoherent scattering. In some cases this incoherent scattering can be reduced by perdeuteration of the protein using recombinant genetic techniques. However, this method cannot presently be used with many of the proteins of known structure. Even in cases where this technique can be used, the cost may be prohibitive for the average university researcher.

Figure 5 shows the instantaneous differential flux per pulse on a sample viewing a water moderator on 60-Hz LPSS having a 500 μs proton pulse. For the TOF diffraction conditions described above we can say, for example, that a particular reflection "sees" all the radiation in Figure 5 within the horizontal band drawn at 1.2 Å with a width of 0.12 Å. The vertical lines show the range of nominal TOF values which must be integrated to accept most of the intensity from this reflection. However, integrating over this range of TOF includes all of the radiation between the vertical lines, and includes significant contributions from the long tails of the shorter-wavelength pulses. Background in protein crystallography is important because the majority of reflections have a poor peak-to-background ratio. Extending the source pulse width to 1 ms significantly increases this background. The background can be reduced by using a longer flight path, keeping the 500 μs proton pulse width (the curve in figure 5 will be less steep and the vertical band will include less radiation that does not contribute to the diffraction condition). The longer flight path will also provide better detector operation by spreading all the counts over most of the available time of 16.7 ms for a 60-Hz machine. Further improvement in the background without degrading the integrated intensity can be achieved by reducing the proton pulse length down to about 100 μs, or by decreasing the fraction of the intensity that is in the tails. However, this is only desirable if the integrated flux (beam power) is not appreciably reduced.

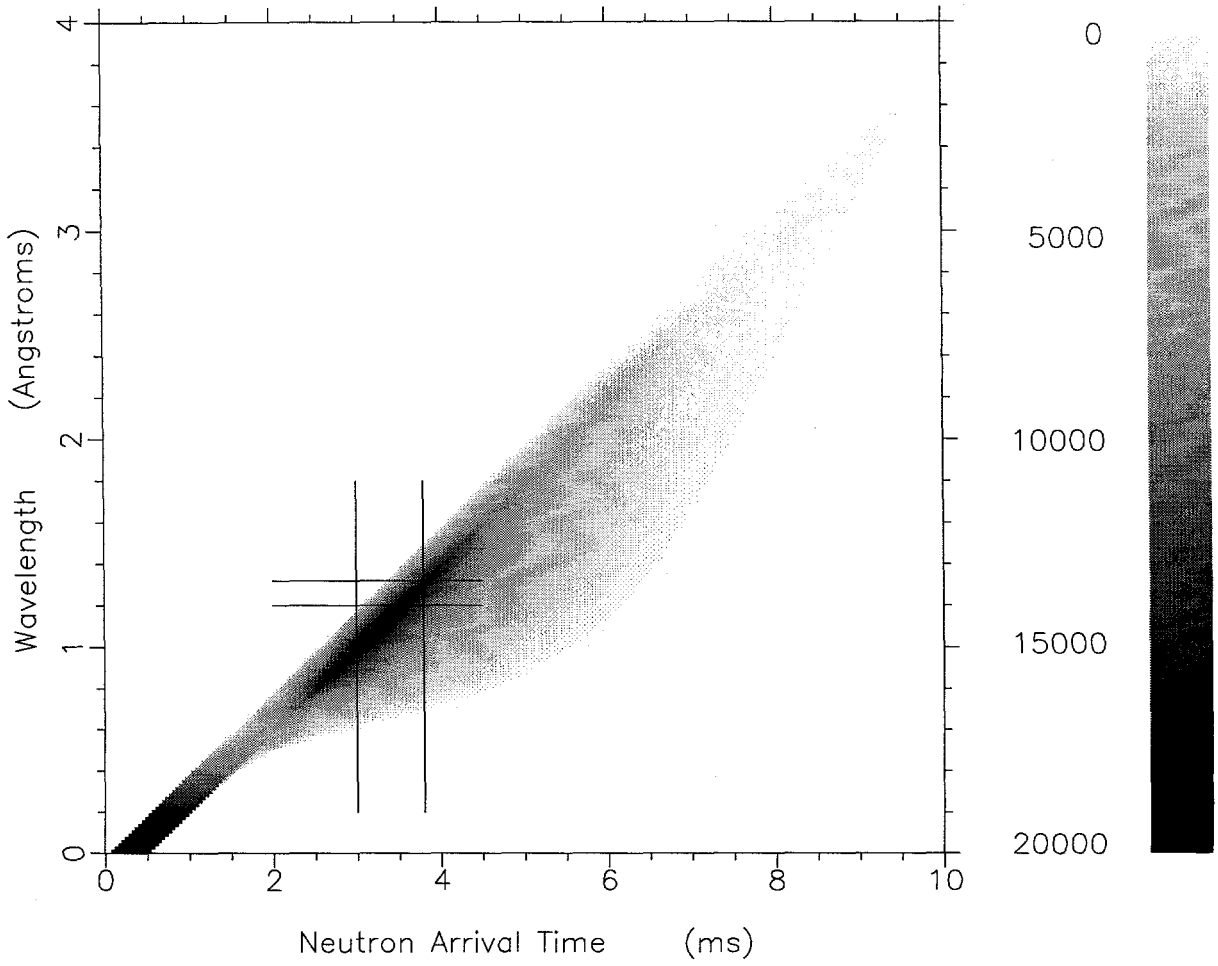

Fig. 5. Estimated instantaneous neutron differential flux per pulse (n/cm²/Å/μs) as a function of neutron wavelength and arrival time (nominal TOF) at a sample position 10 m from a water moderator at a 1-MW LPSS with a 500 μs proton pulse and 60-Hz operation. Estimates are based on the formalism of Bauer,[16] using data provided by Russell, et al.*[1]*

Protein Crystallography

In order to investigate the performance of an LPSS for protein crystallography, we compare with a myoglobin data set[13] collected at beam line H3A at the HFBR, working at that time at 60 MW. This data set was collected with a monochromatic-beam instrument using the 002 reflection from a graphite monochromator with $2\theta_B = 27.5°$. The incident beam divergence was 0.2°, giving $\lambda = 1.6$ Å, $\delta\lambda = 0.023$ Å. The measured flux on the sample was 6.7×10^6 n/cm²/s, corresponding to a differential flux of 2.9×10^8 n/cm²/Å/s. A 17×17 cm² area position-sensitive detector centered at a scattering angle of 22° and covering a 2θ range $2\Delta\theta = 16°$ was used to collect the reflections. The crystal was oriented so that the reciprocal lattice planes having the highest reflection density were horizontal, and reflections were scanned by rotating the crystal in 0.1° steps about the vertical axis. Scanning the crystal through a total angle of 90° required 720

minutes, and 995 reflections were collected in this process. On average, about 9 steps (0.9°) were required to scan through each reflection, giving an effective exposure time of about 7.5 min/reflection. This implies that on average about 10 reflections were present in the detector for any given step, and that an integrated flux of ~3×10^6 n/cm^2 contributed to each reflection. The volume in reciprocal space sampled in this 90° ω-scan is similar to that shown in Figure 3b, although for clarity larger values of θ and $\Delta\theta$ were used in the figure.

We now consider what would be required to duplicate this process (approximately) at an LPSS instrument. For this instrument we use the TOF Laue technique with a wavelength band of 1-4 Å and the same detector setting. For the 60-Hz source this requires $L \leq 20$ m. The flux calculations were made for L = 10 m and with the 13×13 cm^2 coupled water moderator masked down to 7×7 cm^2, and it was assumed that the source produced a 500 μs pulse. These conditions produce an incident beam divergence of 0.2° and a wavelength resolution of $\delta\lambda = 0.2$ Å. (For a 1-ms source pulse, the instrument could be moved to 20 m and the whole moderator could be viewed. This would produce the same divergence and wavelength resolution, and essentially the same flux on sample.) The calculations of Russell[1] show that the time-averaged differential flux from a coupled water moderator at a 1-MW LPSS varies from a maximum value of 7×10^{12} n/cm^2/sr/Å/s at λ = 1 Å to 1.1×10^{11} n/cm^2/sr/Å/s at λ = 4 Å. For the conditions of the calculation, these correspond to a differential flux on sample of 3.4×10^8 n/cm^2/Å/s and 5.4×10^6 n/cm^2/Å/s, respectively. The integrated flux on sample over this 1-4 Å wavelength band is 1.6×10^8 n/cm^2/s, which is more than 20 times the flux on sample in the BNL case. An instrument having these parameters should be suitable for the study of unit cells with dimensions of 50-100 Å, provided the detector spatial resolution is adequate.

The data are collected using TOF binning, with each time step representing a monochromatic slice. The volume in reciprocal space sampled in one such TOF-scan using λ = 1-4 Å is schematically indicated in Figure 4a, although larger values of θ and $\Delta\theta$ were used in the figure for clarity. The calculations of Schoenborn[2] indicate that this TOF Laue instrument would collect data with comparable statistics for this myoglobin crystal 83 times as fast as was done in the original BNL crystal-monochromator measurements.

If we were instead to locate this TOF instrument at a 60-MW reactor, using a chopper to provide the pulses, then by the simple arguments we would expect the instrument to lose intensity by a factor of 17 because of the duty cycle, but to gain by a factor of 6-7 because of the higher time-averaged flux at the reactor. In other words, the TOF instrument at a 1-MW LPSS would be a factor of ~2.5 faster than would a TOF instrument at the 60-MW reactor. Comparison of the integrated flux on sample in the two cases suggests that the 1-MW LPSS TOF instrument might have data rates more than 20 times those at the BNL crystal-monochromator instrument. The TOF Laue technique can be much more efficient for protein crystallography than is the monochromatic beam technique, as indicated by the factor of 83 gain calculated by Schoenborn[2] for one particular unit cell size and geometry.

As was noted above, the quasi-Laue technique at the reactor produces data roughly equivalent to that from one time slice in the TOF-Laue technique. The incoherent background has an intensity that scales roughly as the neutron wavelength λ while Bragg-peak intensity scales as λ^2. Thus the best signal-to-noise ratio is achieved at the longest wavelengths that still provide information

at the desired d-spacings. In biological crystals, it is imperative to obtain data down to d ≈ 2 Å, which can be achieved in backscattering at a wavelength of about 4 Å. To minimize background, the bandwidth is limited (by a multilayer neutron optical device) to roughly that used for the one time slice, leading again to a loss of a factor of ~15 relative to the TOF Laue technique at the LPSS. However, this bandwidth can be set to be at the most intense part of the spectrum, giving an average gain factor of ~2 over the TOF case. Backgrounds should be the roughly same for both types of instrument in this case, since they are being integrated over the same bandwidth. When we consider the factor of ~4 for time-averaged flux from a cold moderator at the reactor, this gives a net gain of ~1.8 for the TOF Laue instrument at a 1-MW LPSS relative to a quasi-Laue instrument at a 60-MW reactor, provided both instruments utilize the same detector area.

However, this is not the whole story. The image plate detectors being used for the reactor instruments can be made quite inexpensively to cover very large solid angles. In the instrument designed by Lehmann and Wilkinson[12] the image plates are wrapped around a 30-cm diameter, 40-cm long cylinder, and the single crystal sample is at the center of this cylinder. This detector covers a solid angle of ~9 sr. The image plate is a thin (150 μm thick) phosphor doped with Gd_2O_3 as a neutron sensitive element. This novel detector has about 8×10^6 pixels, each about 200×200 μm^2. In a typical case about 15 pixels are required to span a Bragg peak.

The image plate detectors are integrating detectors, and so cannot readily be used for TOF measurements. In principle, it might be possible to move (oscillate, rotate, or cyclically step) an image plate in a manner synchronized to the pulsing of the LPSS, but this would lead to a detector considerably more complicated and probably covering a smaller solid angle than that used by Lehmann and Wilkinson. Gas proportional counters are one technology that does provide counting detectors useful for TOF measurements. For the LPSS TOF Laue instrument, Schoenborn[2,14] has proposed a ^{3}He counter having a 70 cm radius and covering 120° in 2θ with an active height of 17 cm. The detector resolution element would be 1.2×1.6 mm^2. This detector would cover a solid angle of ~0.5 sr, which is ~6 times more solid angle than covered by the detector in the BNL crystal-monochromator myoglobin measurements, but is still ~12 times less than the solid angle covered by the image plate detector described above. This is about the limit that is likely to be achieved with gas detectors. Scintillation detectors can also be used for TOF applications, and are readily adaptable to a variety of geometries. It should be possible to construct a scintillation detector with adequate resolution and covering a solid angle within a factor of 2 of the 9 sr achieved by the image plate detector. The emerging silicon diode technology for neutron detectors may also be suitable for this purpose. With such a detector the 1-MW LPSS TOF instrument and the 60-MW reactor quasi-Laue instrument would be roughly equivalent.

These arguments indicate that a current quasi-Laue instrument using image plates at a 60-MW reactor or a TOF Laue instrument using a large scintillation detector at a 1-MW LPSS would collect protein crystallography data at least two orders of magnitude faster than was the case for crystal monochromator instruments at a reactor. These large increases in speed mean that full data sets, which previously required 2-6 months of instrument time, might then be collected in a few days. This type of data collection speed could be expected to revolutionize the field. It should be cautioned, however, that neither type of instrument has yet measured a full data set and

analyzed it to determine a crystal structure, so there is as yet no direct measure of the quality of data which can be achieved by either of these techniques.

For the 20-m version of the LPSS instrument described here, the 1-ms pulse width and the 15-ms usable time frame provide just the resolution and bandwidth required by this instrument. A similar instrument would work equally well at a 1-MW SPSS with a coupled moderator, but there would be no further data-rate advantages at the SPSS because the flight path length is dictated by angular resolution requirements. However, locating the instrument on a coupled moderator at an SPSS rather than an LPSS might offer improvements in the signal/background ratio, even though the data rates would be the same at the two types of sources (at the same beam power).

Single Crystal Diffraction with Smaller Unit Cells

The protein crystallography instrument discussed above is able to study protein crystals up to unit cell volumes of 10^6 Å^3. These techniques can be applied to smaller unit cells as well.

From a resolution point of view a single crystal machine suitable for protein crystallography can also be used for smaller unit cells, since the number of detected peaks is approximately proportional to V, the unit cell volume for the scattering sample. In order to increase the number of simultaneously-recorded peaks as V drops, the value of λ_{min} should probably be decreased to say 0.5-0.7 Å. Even down to a relatively small unit cell size (~100 Å^3), each of the time-slices in the TOF Laue data set will contain (on average) at least one peak, and the full duty-cycle advantage over a reactor is maintained. Note that this is only true in the case where a relatively large detector is used. If only a smaller detector is available, some of the measured time slices may contain no useful data, and since the crystal monochromator instrument can avoid such regions, it begins to win in this case.

According to Jauch and Dachs[15] the minimum d-spacing that can be accurately integrated when the pulse width is δt (FWHM) is given by

$$d_{min} = \left(\frac{0.00420\,\delta t}{L \sin\theta} \right)^{1/2} \qquad (8)$$

for δt in μs and the path length L in m. For backscattering with L = 20 m and δt = 1000 μs, this gives d_{min} = 0.45 Å, which is probably adequate for all but the highest resolution measurements. If higher resolution is required, a shorter pulse or a longer flight path will be necessary.

Measurement of Diffuse Scattering

TOF Laue single-crystal diffractometers have already shown themselves to be good for diffuse scattering studies. Such studies do not require high wavelength resolution, and can be done on an instrument designed for small-unit-cell crystallography. The TOF Laue technique automatically scans all of the reciprocal space within the region defined by the instrument settings, and not just the regions around the Bragg peaks, as is the usual case with crystal-monochromator instruments. The diffuse scattering is automatically measured, as are any

superlattice peaks or any other features which fall between the normally expected lattice peaks. Thus the TOF Laue instrument is excellent for survey purposes. Since all of the regions between the Bragg peaks need to be scanned in such measurements, the TOF Laue technique will win out over the crystal-monochromator technique.

Single-Crystal Diffraction Summary

As a general conclusion, it appears that large-unit-cell single-crystal crystallography could be done ~2 orders of magnitude more effectively at a 1-MW LPSS than at a crystal-monochromator instrument at a 60-MW reactor, provided suitable large detectors can be developed. Such an LPSS instrument would be roughly as effective as an image-plate quasi-Laue instrument at a 60-MW reactor. This is true for both protein crystallography and for crystallography with smaller unit cells. The TOF technique is particularly useful for diffuse scattering and survey measurements, and in this case the spallation source instruments can be expected to win by a large margin over crystal monochromator instruments at a reactor, but probably not over image-plate quasi-Laue methods at a reactor. Since all of these techniques require relatively low resolution, the SPSS does not offer any particular data rate or dynamic range advantages over the LPSS. However, in some cases the improved resolution offered by a coupled moderator on an SPSS can lead to significant improvements in signal/background. The SPSS also offers some advantage for very high resolution measurements on small-unit-cell crystals. It appears that a state-of-the-art protein-crystallography instrument with a large detector at an LPSS could offer neutron crystallography data rates 1-2 orders of magnitude better than those to which protein crystallographers have been accustomed, with the amount of gain depending on unit cell size and geometry, and that the image-plate instruments being developed at reactors will be at least as effective as the best 1-MW LPSS instrument. A protein crystallography instrument should be considered for inclusion among those planned for any new 1-MW LPSS or SPSS, provided suitable large-solid-angle detectors can be developed.

Before a a single-crystal diffractometer for protein crystallography is built at the LPSS, a number of issues warrant further exploration. These include:

- Detailed comparison between the crystal-monochromator, image-plate quasi-Laue, and TOF Laue instruments, taking proper account of the variation of flux with wavelength and the sources of background in the three cases. Both analytical treatments (e.g., along the lines of Jauch and Dachs[15]) and Monte-Carlo or other numerical methods should be explored.
- Monte Carlo investigation of the background effects due to the long tails associated with coupled moderators.
- Testing of a prototype TOF Laue protein crystallography instrument at an existing SPSS. This could help ascertain what background problems might occur, verify the data rate relations obtained above, and help demonstrate the validity of the technique. It should also help to point out any additional problems requiring R&D.
- R&D relating to the use of focusing devices such as toroidal mirrors for such an instrument.

- R&D aimed at producing detectors suitable for TOF Laue protein crystallography, which cover a large solid angle, are fast and have good position resolution.

Small-Angle Scattering

Contributors: Harald Conrad, KFA; Charlie Glinka, NIST; Rex Hjelm, LANL; Glenn Olah, LANL; Phil Seeger, LANL; P. Thiyagarajan, ANL; George Wignall, ORNL

Scientific Opportunities

Small-angle neutron scattering (SANS) is a key technique for the characterization of polymers in solution and melts, of colloids, and amphiphillic mesophases. With the continued development of new materials and systems, these will remain important areas. There is, however, an increasing interest in more detailed structural information associated with more detailed labeling schemes and internal structure. There is a trend towards the study of complex fluids and multi-component systems, with the inherent range of dimension scales. This trend applies to amphiphillic/polymeric systems and in material science, such as in composites and porous media. There is currently much growth in the use of SANS to study ordered structures on longer length scales, for example template methods to generate novel zeolite structures. There are potential applications in kinetic studies and in the study of non-equilibrium phenomena, such as phase behavior, clustering, and aggregation in polymeric systems. Recent studies have demonstrated the possibility of using SANS to study structure in thin films and at interfaces, to provide information complementary to reflectometry. There is an increasing requirement to study systems in more complex environments, and subjected to different external fields such as stress and shear and high pressure. Samples subjected to external stress and/or shear also involve relaxation phenomena and imply kinetic or non-equilibrium phenomena, and provide the opportunity to study morphology in systems and environments of industrial relevance, such as extruders. Measurements at high pressure include the study of super-critical fluids.

In biologically related areas the expansions in applications of SANS are likely to be in the study of biomimetic systems, in food science and pharmacy (with strong overlaps with the more established and conventional use of SANS in colloids, etc.).

The use of polarized neutrons in combination with SANS provides unique opportunities for the study of magnetic phenomena, such as magnetic domain sizes and distributions.

These trends and developments in the applications of SANS imply requirements for increased neutron flux, wider Q range (broader band), and in many cases the need for improved resolution.

Scientific Requirements

To cover the scientific areas indicated above, a modern SANS instrument or suite of instruments should satisfy the following criteria:

- Q-range covering at least from 0.001 to 0.5 $Å^{-1}$
- Ability to vary resolution $\sigma(Q)/Q$ (rms) from at least 2% or less to 15%

- Ability to use different sample sizes and geometries
- Low backgrounds.

Throughout this section the symbol σ is used to indicate an rms variation in a variable.

Relative Performance of 21-m SANS Instruments

On the first day of the workshop, Phil Seeger presented the results of Monte Carlo simulations for a specific configuration of a small-angle-neutron-scattering (SANS) instrument at an LPSS.[3] The specific configuration was chosen to match one of the most frequently used configurations at the D11 instrument at ILL. Pinhole collimation was used, with a 3×5 cm^2 incident-beam aperture located at the LPSS moderator, a 1 cm diameter aperture at the sample 10.5 m from the incident beam aperture, and a 64×64 cm^2 area detector 10.5 m from the sample. These Monte Carlo simulations showed that data collection at such an instrument viewing a coupled liquid hydrogen moderator at a 1-MW 60-Hz LPSS having a 1-ms pulse would be a factor of ~2.2 faster than at that configuration for the present D11 at a neutron wavelength of 10 Å, and approximately a factor of 3.8 faster at 6 Å.

The SANS subgroup focused on this particular instrument configuration, and considered in detail some of the factors which contribute to the performance of the LPSS instrument. The Monte Carlo calculations compared the hypothetical LPSS instrument with the actual D11 instrument, but the comparison with a hypothetical optimized instrument at a reactor is perhaps more informative. When the inefficiencies of the cold source, guides, and velocity selector of D11 are included, the rough scaling arguments work. Therefore, simple scaling arguments can be used to understand the approximate relative performance of LPSS, SPSS and reactor (CW) instruments.

Consider a measurement on the LPSS hypothetical instrument and a D11 style instrument that might be built on the cold source CS-2 at ILL to cover the Q-range 0.002 to 0.26 Å^{-1} with reasonable overlap. For the 60-Hz, 1-ms LPSS instrument at 21 m, Eqs. 2 and 3 indicate a bandwidth and wavelength resolution of $\Delta\lambda \cong 3$ Å and $\delta\lambda \cong 0.19$ Å FWHM. A wavelength of ~10.5 Å is required to reach a Q_{min} of 0.002 Å^{-1} at this distance. Several different chopper settings giving different wavelength bands will be required to cover out to a Q_{max} of 0.26 Å^{-1}. Similarly, the CW instrument will need to move the detector to positions closer to the sample, and to change the incident beam collimation accordingly, in order to cover the higher Q values. Alternatively, the LPSS instrument could be designed to move its detector in a manner similar to the CW instrument. In this case, the LPSS instrument could move the detector to achieve the desired Q range, and would use TOF to select the wavelengths to be used. The full TOF bandwidth would be useful. A fixed geometry instrument is more easily shielded, and the intensity gains at the higher Q values are greater when using shorter wavelengths instead of using shorter distances. However, when crystalline samples are being studied or when the sample is in some apparatus (e.g., pressure cell) containing crystalline material, wavelengths below 4-5 Å may have to be excluded because of contamination from double-Bragg scattering. In this case, the moving-detector instrument would have an advantage for reaching the higher Q values. (Alternatively, the stationary-detector instrument could have its area detector supplemented by additional detectors at higher scattering angles.)

For these parameters, two chopper settings are needed to cover this Q range with the LPSS instrument if the detector is not moved. The CW instrument requires two camera settings and one wavelength change. In an actual measurement it would be good practice to use three or four chopper settings at an LPSS and three camera settings and one wavelength change at a CW instrument, as shown in Table 3. At 21 m and λ = 10 Å, the 3 Å bandwidth for the TOF case gives $\Delta\lambda/\lambda \approx 30\%$ FWHM, to be compared with the $\Delta\lambda/\lambda \approx 12\%$ FWHM for the CW case. Since a 1-MW LPSS is equivalent to (1/4) ILL, the net gain for the TOF case is (30/12)(1/4) = 0.6 with respect to a hypothetical optimized instrument at ILL. It should be noted, however, that the resolution of the stationary-detector LPSS instrument is a factor of at least 2 better than that of the CW instrument for most of the Q values measured. Since the wavelength resolution is already very good for the LPSS instrument, there is no advantage to using the same instrument at an SPSS operating at the same frequency unless much larger values of Q_{max} are desired.

Table 3 -- Settings Required for LPSS and CW SANS Measurements*

Stationary-Detector LPSS Instrument						
Total length (m)	mean λ[a] (Å)	$\sigma(\lambda)/\lambda$ (%)	Q_{min}[b] (Å^{-1})	Q_{max}[c] (Å^{-1})	$\sigma(Q)/Q$[d] (%)	relative flux on sample[e]
21	10	1	0.0024	0.022	2	0.6
	7.6	1.2	0.0031	0.038	2	1.9
	5.3	1.7	0.0045	0.050	2	9.5
	3.0[f]	3	0.0080	0.13	3	31

Ideal CW Instrument						
Total length (m)	mean λ (Å)	$\sigma(\lambda)/\lambda$ (%)	Q_{min}[b] (Å^{-1})	Q_{max}[c] (Å^{-1})	$\sigma(Q)/Q$[d] (%)	relative flux on sample[e]
21	10	5	0.0024	0.020	5	1
11	10	5	0.0046	0.039	5	3.6
5	6	5	0.016	0.14	5	120

* Note that resolutions are specified here as rms values (σ) rather than as the FWHM values (δ) used in other sections of this report

a Center of 3 Å bandwidth

b Based on mean λ and 35 mm penumbra

c Based on minimum λ and 32 cm radius on detector

d Based on 1-cm pixel at 25 cm radius on the detector

e Relative to 21-m CW settings at 60-MW reactor (gain factors at 10 Å explained in text, gains at other settings are based on relative solid angle and source spectrum)

f This setting may not be usable in cases where double-Bragg scattering is important.

The moving-detector TOF case would employ the same three settings as the CW case. Flux on sample would differ by this same factor of 0.6 for the two settings with λ = 10 Å. However, at λ = 6 Å, $\Delta\lambda/\lambda$ increases to 50% FWHM for the TOF case, making the relative flux on sample (50/12)(1/4) = 1.0 times that for the CW instrument.

For this pinhole-collimation configuration, the geometric factors dominate for the LPSS, which means that the instrument has to be long to achieve the desired Q_{min}. Furthermore, for a 1-ms pulse with an exponential tail (375 μs decay time) the instrument must be at least 20 m long to achieve the desired wavelength resolution $\sigma(\lambda)$ (rms) at λ_{min}. Thus the bandwidth is much narrower than could otherwise be used. As a result, the TOF gain is only ~3, rather than the factor of ~15 which might otherwise be possible. If the 1-MW LPSS were to operate at 30 Hz, the usable bandwidth would double, and the gain of the LPSS instrument would increase by at least a factor of 2. Similarly, if the source were to operate at 120 Hz, there would be a loss of more than a factor of two.

Based on the discussion above, we conclude that to first order sources as listed in Table 4 would give the same count rate for a 21-m D11 style instrument at $Q = 0.01$ Å^{-1}, $\sigma(Q)/Q = 0.1$.

Table 4 -- Configurations giving the same data rate at $Q = 0.01$ Å^{-1}, $\sigma(Q)/Q = 0.1$ for a 21-m pinhole SANS instrument*

	λ (Å)	Relative count rate	σ(Q)/Q	Q_{min} (Å^{-1})	Q_{max} (Å^{-1})
20-Hz SPSS @ 0.3 MW	1-9	1	0.10	0.0027	0.19
60-Hz LPSS @ 1 MW	8.6-11.3	1	0.10	0.0021	0.022
CW @ 30-40 MW	10 (12% FWHM)	1	0.11	0.0023	0.020
present D11 @ 130 MW	10 (12% FWHM)	1	0.11	0.0023	0.020

* Note that resolutions are specified here as rms values (σ) rather than as the FWHM values (δ) used in other sections of this report.

These tabulated values are based on :

1) for comparisons of the LPSS and CW sources the calculations of the time averaged brilliance of the ILL D_2 source CS-2,[17] and of the H_2 flux-trap moderator[1] are used. This comparison predicts that the ratio of moderator brilliance is LPSS/CW = 16 P, where P is the ratio of the power of the LPSS source to the power of the CW (ILL/CS-2) source.

2) For SPSS, LPSS and the hypothetical CW instruments the assumption is that the instruments are ideal. That is there are no guide losses, etc. However, losses due to the velocity selector or choppers are accounted for.

3) For the SPSS instrument it was assumed that the pulse maximum scales with the source power. The source operates at 20 Hz, using a coupled H_2 moderator. Thus the pulse has a 375 μs exponential tail.

4) The LPSS operates at 60 Hz using a 1-ms pulse width and using a coupled H_2 moderator. The time constant of the exponential tail is 375 μs.

5) The hypothetical CW instrument is placed on the CS-2 cold source. The velocity selector is CONSTANZ and is placed at the bulk shield. The sample is 10.5 m from the velocity selector. The source aperture is the same as that used on D11, 5 cm × 3 cm. We assume a velocity selector with 0.8 transmittance. The total increase in count rate over the present D11 calculated from the data of Lindner *et al.*[18] and Ageron[17] is 3.3-4.3 and comes mostly from the use of ^{58}Ni-coated guides.

6) The comparison with the present D11 is based on the calculations of Phil Seeger and Glen Olah (with the CONSTANZ velocity selector).[3] These calculations show a gain of 2.2 using time-of-flight and an LPSS moderator.

7) Q_{max} is based on the minimum λ and a 32 cm radius on the detector.

Alternative Configurations for SANS Instruments

The above comparison was based on the use of pinhole collimation geometry SANS instruments, which have proven to be extremely effective at CW sources. In this geometry the geometrical resolution forces the flight path to be long. At a CW source this does not lead to any intensity penalties, but at a pulsed source the long flight path makes the wavelength resolution much better than is usually desired, and limits the bandwidth which can be utilized in a single instrument setting. A geometry which is much more favorable for TOF SANS instruments is the converging-multiple-aperture collimation geometry. This geometry allows the use of a large area of the moderator and a large sample size (when desired), while permitting good resolution with a short source-detector distance. The SANS instrument SAD has been successfully operating at the 30-Hz IPNS pulsed source using this geometry for a number of years. This instrument works reliably down to a Q_{min} of ~0.006 $Å^{-1}$, with a source-detector distance of only 9 m. This short path allows this instrument to use all wavelengths in a 1-14 Å band, giving this instrument competitive data rates despite the relatively low power of the IPNS source.

The time available in the workshop did not permit exploration of the performance of a multiple-converging-aperture instrument at the LPSS. This should be a subject of future analyses. Other geometries, such as focusing geometries using curved mirrors focused on the detector, should also be explored. The converging-multiple-aperture geometry has not yet been employed in a routine manner for instruments operating to lower values of Q_{min}, so it is not yet clear whether the collimator technology can be developed to design a short flight path instrument with the desired Q_{min} for the 1-MW LPSS. To do this, it might be necessary to use an additional chopper to trim the tail off the pulse. These might be fruitful areas for R&D efforts.

SANS Conclusions

As has been often noted, a pinhole collimation (long flight path) SANS instrument is particularly well suited to a CW source largely because the angular resolution of the instrument (determined by its geometrical parameters, i.e., length and aperture sizes) is decoupled from the wavelength resolution. Hence, in principle, the detector count rate can always be optimized (at a particular Q, but not at all Q-values covered with a particular instrument configuration) by balancing the angular and wavelength contributions to the overall Q-resolution.

For any pulsed source, pinhole collimation, SANS instrument, the wavelength resolution and the angular resolution are not independent but are coupled through the choice of instrument length, which, in turn, depends on the neutron pulse width and the repetition rate of the source. As a result, the characteristics of the source are crucial to the performance that can be achieved. This analysis has shown that relatively long neutron pulses, such as can be achieved at either an LPSS or an SPSS through the use of a properly designed cold, coupled moderator, are advantageous for SANS because they result in wavelength resolution that, in general, more closely matches the angular resolution than can be achieved if the neutron pulses are shortened at the expense of intensity, as with a decoupled moderator or a pulse-definition chopper. For the particular 1-MW LPSS model considered, a 20-30 m pinhole-collimation SANS machine could be built that would, in the most favorable situations, nearly match what could be achieved with an optimized instrument at the ILL reactor. Such an LPSS SANS instrument with fixed sample-detector

distance would cover a wide Q-range (~0.002 to 0.25 $Å^{-1}$), although not as wide as at an optimized reactor instrument with a movable detector (0.001 to 0.5 $Å^{-1}$), with a count rate for equivalent resolution from ~0.5-1 in the most favorable cases, to ~0.2-0.3 in less favorable cases. Such an instrument would surpass all existing SANS instruments in the US.

SANS with pinhole collimation does not benefit fully from the TOF gain factor, as the geometric resolution, Q_{min}, and wavelength resolution at λ_{min} force a long flight path. This long flight path makes the wavelength resolution very good for the TOF instrument, and to the extent that an experiment requires higher resolution, then the gain is proportionately larger. At 60 Hz there is no benefit to making the SANS instrument longer, as the band width passes the point where there is less than a single resolution interval in the band and gain is lost. Therefore, 20-30 m is a good compromise as a work-horse/general-use spectrometer covering the Q-domain from 0.002 to 0.26 $Å^{-1}$ with 2-15% $\sigma(Q)/Q$. A smaller source repetition rate at the same power is better. Shortening the proton pulse width to less than 1 ms does not help much at low Q, as the resolution is dominated by the instrument geometry. Shortening the pulse decreases λ_{min} for the same resolution, allowing the instruments to be shorter and to reach larger Q_{max}. Thus the main advantage of SPSS instruments over LPSS instruments is in the higher-Q range, and consequently, in the greater dynamic range of the instrument.

A number of topics deserve further exploration. Among these are:

- Use of other geometries, such as the multiple-converging-aperture geometry, which allow shorter instruments and sampling more of the moderator for the same resolution and Q_{min}
- Effects of source pulse shapes
- Use of a pulse-definition chopper to shorten the pulse when high Q values are required
- Potential parasitic scattering from the bandwidth-limiting and t_0 choppers, which are all located within the incident-beam collimation on the LPSS instruments. It likely will be necessary to incorporate features in the design of these components (such as single crystal windows, beveled edges, etc.) that will eliminate sources of parasitic scattering. This will require an R&D program.
- Development of higher-data-rate detectors. Instantaneous data rates are higher at the LPSS and SPSS instruments for the same time-averaged data rates.
- How can we achieve lower Q at an LPSS or SPSS
- How important is a fixed instrument geometry and/or a fixed sample size
- Design to allow the use of larger apertures when intensity is required at the expense of resolution
- The use of detector banks at larger scattering angles to extend the range for Q_{max} when short wavelengths cannot be used (because of double-Bragg scattering).

Reflectometry

Contributors: Gian Felcher, ANL; Mike Fitzsimmons, LANL; Bill Hamilton, ORNL; Jeff Penfold, ISIS; Tom Russell, IBM; Sunil Sinha, ANL; Greg Smith, LANL.

Scientific Opportunities

In recent years neutron reflection has developed as a technique to study the structure of thin films, surfaces and interfaces. The existing scientific program includes the study of thin polymer films and interfaces, multilayers, L-B films, adsorption of polymers, surfactants, proteins, and lipids at the air-liquid and liquid-solid interfaces, and on solid substrates. Key features of the technique are the penetrability and the ability to alter contrast (principally by H/D substitution). The application of polarized neutron reflection has given rise to the investigation of magnetization profiles in magnetic thin films and multilayers, and in the study of flux penetration in superconductors.

In the future the scientific program is envisaged to develop in a number of directions. There is an increasing interest in kinetic, time dependent phenomena, such as interdiffusion at interfaces, time dependent adsorption, and surfaces under shear. There is a trend towards the study of complex multi-component systems and in the study of adsorption at more complex interfaces, such as buried interfaces, liquid-solid, and liquid-liquid interfaces, and in the study of *in situ* electrochemistry. In terms of complex interfaces/environments there is interest in the study of molecules in confined geometries, such as polymer segment density profiles in the force apparatus. In biological systems there is the potential for the study of membrane/protein interactions and in membrane transport phenomena. In magnetic systems there is increasing interest in magnetic thin films and multilayers exhibiting GMR, in the directional nature of moment distributions in-plane, and in the study of magnetic diffuse scattering associated with domain structure.

These trends and developments in the applications of neutron reflection imply requirements for increased neutron flux and wider Q range (broader band), and in many cases the need for improved resolution.

Estimates of Relative Performance of Instruments at Different Sources

Comparisons of the intensity, background, and resolution for specular and diffuse scattering experiments and the use of polarized neutrons at three different sources were made. The sources are a 15-MW reactor source (1/4 ILL) utilizing constant wavelength techniques, and long (LPSS) and short-pulse (SPSS) spallation sources. The long-pulse source considered would provide 1-MW power in 1-ms (FWHM) pulses at a rate of 60 Hz. The operating parameters considered for the SPSS were those proposed by the ESS and are 1 MW in 0.3 ms pulses from a coupled liquid hydrogen moderator at a rate of 10 Hz. To provide a better comparison with the LPSS source, we also include the performance of an SPSS having the same parameters but operating at 60 Hz.

The bandwidth available at the LPSS and SPSS depends upon the length of the flight path used. We assumed between 20 and 60 m for the LPSS instrument, which yields $\Delta\lambda$ of between 1 and 3 Å, and a 20 m flight path for the SPSS instruments, yielding bandwidths of 20 Å at 10 Hz and 3 Å at 60 Hz.

A reflectometer at an LPSS might utilize a short bandwidth to measure a reflectivity profile by fixing λ_{min} and λ_{max} and changing the angle of incidence onto the sample, much like a CW experiment. Alternatively, the angle of incidence can be fixed and λ_{min} and λ_{max} can be incremented in steps of $\Delta\lambda$. The latter measurement would be much like that done at the SPSS. One technique or the other might be better suited, depending upon the information desired. The flexibility of using both techniques at the same instrument might be an advantage of the 60-Hz sources. One advantage of the large bandwidth available at a lower-repetition rate or short-flight-path SPSS instrument is to survey a large region of reciprocal space. An equivalent bandwidth can be achieved at the LPSS using only one in six neutron pulses at the expense of intensity. One can envision a user using this mode to make a short survey of reciprocal space in order to identify regions requiring more detailed exploration with the smaller bandwidth of the full 60-Hz beam. For example, the position of a Bragg reflection from a multilayer could be determined using the survey mode. Once found, the integrated intensity of the reflection could be monitored as a function of an external parameter, e.g. magnetic field, stress or temperature, while achieving the full TOF gain available at the LPSS.

A number of areas in which intensity gains might be anticipated are indicated in Table 5. This increased intensity would make <u>new</u> science possible in several areas, including:

- much smaller footprints reduce path length for absorption for studies of liquid/liquid and liquid/solid interfaces
- real time experiments of dynamic processes
- increased dynamic range (larger Q)
- Q_x,Q_y,Q_z (SANS in reflection geometry and grazing incidence diffraction)

This higher intensity may lead to saturation problems in the neutron detectors presently available. For measurements utilizing a small bandwidth, attenuators can be used to mitigate saturation of the detector. This in not so easily done when larger bandwidths are used.

<u>Multiplexing</u>

Neutron guides are employed at CW sources to allow multiple experiments to view the same cold source (multiplexing). If temporal resolution were obtained using long flight paths (ca. 60 m) at an LPSS, multiplexing instruments on the same guide might also be possible. If for example, $\Delta\lambda$ were taken to be 1Å, four or five reflectometers might view the same moderator using different portions of the spectrum peak obtained using a series of multilayer mirrors to reflect neutrons of the proper wavelength outside the guide. These mirrors would have to be transparent to neutrons having wavelengths shorter than those reflected. Multiplexing instruments at the same moderator might also be possible at a shorter flight path TOF instrument, however, many short flight paths might not fit close to the bulk shield.

Table 5 -- Reflectometer Parameters and Intensity Gain at 1-MW LPSS and SPSS

Instrument parameters	60-Hz LPSS	60-Hz SPSS	10-Hz SPSS	note
Moderator	c-H_2	c-H_2	c-H_2	1
Flight path length (m)	60-20	20	20	
Bandwidth $\Delta\lambda$ (Å)	1-3	3	20	
Source pulse width (ms)	1.0	0.3	0.3	
λ resolution $\delta\lambda$ (Å)	0.07-0.2	0.06	0.06	
Gain factors				2
Source flux	0.25	0.25	0.25	3
Monochromator	1.25	1.25	1.25	4
Illumination	1.0	1.0	1.0	5
Focusing	1.0	1.0	1.0	6
TOF Gain	12-15	49	326	7
Useful $\Delta\lambda$	1.0	1.0	0.7	8
Footprint	1.0	1.0	1.0	9
Spectrum	1.0-0.8	0.8	0.3	10
TOTAL GAIN	3-4.7	12	21	

Notes for Table 5:

(1) Reflectivity experiments typically require resolutions $\delta Q/Q$ of a couple to few percent, so all sources benefit by using cold coupled moderators with long time constants. This gives a gain of roughly a factor of 6 in time-averaged flux, when compared to the decoupled cold moderators presently in use.

(2) Gains are calculated relative to an optimized crystal-monochromator instrument on the ILL cold source.

(3) 1-MW LPSS and SPSS coupled liquid H_2 moderator time-averaged flux is 1/4 that of the ILL cold source.[1]

(4) CW techniques utilize monochromators with reflectivities around 80%.

(5) Focusing monochromators can be utilized to illuminate samples by the full height of the neutron guide in CW experiments. Pulsed sources typically accept radiation from the full height of the moderator. The assumption made here is that the neutron guide at a CW source would be comparable in size to a moderator (moderator size is 13 cm by 13 cm).

(6) All sources can utilize focusing mirrors to reduce the footprint size of the sample. Focusing mirrors might be easier to use on small-bandwidth instruments (up to about 1-3 Å). If one chooses to measure the reflectivity profile by changing wavelength band at the LPSS rather than the angle of the sample, then the mirror would need to be readjusted for each measurement.

(7) TOF gain for the LPSS was determined through Monte-Carlo simulation by Mike Fitzsimmons.[4] The gain of 12-15 includes the reduction of the detector frame so that the chopper penumbra would not occur during the pulse on target, i.e. reduced by about 2 ms from the 16.7 ms frame available at 60 Hz. The gain from the simulation is between 70 and 90% of the reciprocal of the duty cycle or $\Delta t/\delta t$. The value for the TOF gain for an SPSS is based on this relation with a 2-ms reduction in time frame as well.

(8) While all reflectometry experiments would fully utilize a $\Delta\lambda$ of 1-3Å, most would probably not require more than 15 Å.

(9) Simple calculation suggests 1 for all techniques, but simulation is needed to confirm this calculation.

(10) The spectrum falls off rapidly at longer wavelengths, so the average intensity must be discounted when the bandwidth is large.

Background

Sources of background include the instrument and sample. At pulsed sources there exists a neutron "glow" during the proton pulse. Data acquired during the pulse might be contaminated; therefore, the period of time where data can be collected is reduced at the expense of bandwidth. This is one reason why the TOF gain realized in the Monte-Carlo simulation was reduced to between 12 and 15. The claim made by the reactor community is that there is no background for those instruments which view neutrons from a guide. Nevertheless, one method used at reactor sources to minimize background is to use analyzer crystals after the sample. Similarly, analyzer mirrors could be readily used at the LPSS if needed. Analyzer mirrors could also be used at the SPSS but at the expense of bandwidth.

Resolution

The resolution required for most reflectometry experiments ranges from 2-10% (FWHM) with most experiments requiring perhaps 4% (FWHM). For specular scattering experiments the geometrical contribution to the resolution is predominantly determined by the width of a detector element and by the sample size. This contribution is the same for all sources. The wavelength contribution at a CW source is determined by the divergence of the neutron guide and the mosaic spread of the monochromator. Typically graphite crystals are utilized and yield $\delta\lambda/\lambda$ of about 2% FWHM. For better resolution, crystals with less mosaic spread would be used. For TOF measurements $\delta\lambda/\lambda = \delta t/t$ where t is the neutron time of flight. The time of flight is determined by the wavelength used and the length of the instrument. For an LPSS, $\delta t/t$ would typically be between 1 and 2% (FWHM). This component of the resolution can be reduced further by lengthening the instrument. Alternatively, a pulse-definition chopper can be used to shorten the 1-ms pulse. The choice of path length on both LPSS and SPSS instruments allows a trade-off between bandwidth and resolution, and should be carefully considered when the instruments are designed. Instruments at both types of pulsed sources would benefit if the source were to be operated at the same power and pulse width but at a frequency lower than 60 Hz, since this gives a greater usable bandwidth at the same resolution.

Off-specular Scattering

Off-specular scattering is a very comprehensive topic, which includes scattering from disorder within the plane of the reflecting surface as well as a 2D ordered structure. Even considering diffuse scattering, a further separation needs to be made. Scattering in the x-direction, or within the reflection plane, reveals objects of length 50-5000 nm. Along y, or out of the reflection plane, objects of sizes 0.5-50 nm can be measured. For completeness both ranges should be measured; however at present only scattering along x is usually studied

Diffuse scattering can most easily be surveyed with a large-bandwidth instrument. A smaller-bandwidth TOF instrument might however be equipped with a "survey button" that eliminates some of the pulses to amplify the bandwidth available. The least useful in this respect is the CW source, since it requires detailed scanning over a region whose size has to be guessed in advance. However, it might be most advantageous to measure diffuse scattering with the beam at very low

angle of incidence and with tight collimation. The reflected beam is then totally reflected, the beam does not penetrate into the sample and the diffuse, incoherent scattering is minimized. On the other hand, the dishomogeneities at the surface give rise, in this geometry, to the highest (in absolute terms) non-specular intensity. These measurements can probably be done most efficiently with a narrow-bandwidth instrument, so on the whole no one type of instrument appears to have a large advantage relative to the others for off-specular scattering.

Grazing Incidence Neutron Diffraction

Measurements of surface diffraction or truncation rods is accomplished by illuminating a flat sample with a neutron beam at grazing incidence. When this angle is on the order of the critical angle an evanescent wave is created in the near-surface region. Through the adjustment of the sample about its surface normal, this wave can be diffracted by the periodic arrangement of atoms or magnetic spins. The intensity of the diffracted neutron radiation is sharply peaked in departure angle off the sample surface around the critical angle. The peak can be made broader by using a more divergent beam, however, this is accomplished only by sacrificing depth resolution. In other words, the divergence of the beam is usually small in order to sample only the near-surface region.

Typically, the divergence of the incident beam is on the order of 0.01°, and for Ni and using 4 Å neutrons the angle of incidence is about 0.4°. If the wavelength resolution is comparable to the geometric resolution (yielding $\delta Q/Q$ of about 4%) then the bandwidth admitted by the sample is 0.1 Å. Thus only 0.1 of the bandwidth of the 60-m LPSS reflectometer could be utilized. What bandwidth is utilized, however, is fully useful as far as measuring single diffraction peaks. The intensity for such measurements at the 1-MW LPSS would be (1/4) ILL×15×0.1 = 0.38 times an optimized instrument at ILL. (The equivalent ILL instrument is EVA.)

Polarized Neutrons and Reflectometry.

The state of the technology for polarizers in 1995 is the following:

CW: polarization by transmission of multilayers. Excellent polarization.

LPSS: polarization by reflection from supermirror. Excellent polarization over several Å bandwidth.

SPSS: polarization with the same device as for LPSS. The limited bandwidth will reduce the efficiency on large-bandwidth instruments.

For flippers, all sources use either the Mezei flipper (wavelength dependent) or adiabatic flippers (Drabkin, Rekveldt or Korneev types) for white beams. Some decreased efficiency (down to 80%) has been observed in the broad-band filters for long wavelength neutrons. These limitations are most important for large-bandwidth instruments. Most of the limitations of the present devices are expected to be eliminated in the future, for example, by the continuing development of polarizing multilayers. In addition, transmission filters based on polarized nuclei (^{3}He) are expected to become operational within a few years.

Conclusions

A 1-MW LPSS would be very powerful for reflectometry. At least the full TOF gain of ~15 would be realized, and it should be possible to achieve data rates 3-4 times those at a 60-MW reactor. This increased intensity will lead to considerable improvement in conventional reflectometry measurements (e.g., many more types of time-dependent phenomena can be studied in real time), and will also expand the field into other areas (e.g., off-specular scattering, grazing-incidence diffraction). However, the dynamic range and the resolution of the LPSS instruments are limited in comparison with the SPSS instruments, and even greater gains would be possible at a 60-Hz 1-MW SPSS and especially at a 10-Hz 1-MW SPSS.

In order to fully utilize these gains, R&D must be pursued in several areas, including:

- Detectors. Position-sensitive detectors having better spatial resolution and capable of handling higher data rates may be required, depending on the instrument parameters selected.
- Additional studies (Monte Carlo?) to produce a clearer picture as to the relative importance of resolution and bandwidth for various types of science with reflectometers.
- Studies (probably Monte Carlo) of the effects, if any, of the long pulse tails from the coupled moderators on the quality of the data for various types of science.

References

[1] G. J. Russell, E. J. Pitcher, and P. D. Ferguson, "Calculated Performance of a Benchmark Target-Moderator System for a 1-MW LPSS", these proceedings.

[2] B. Schoenborn, "Calculated Performance of Laue Diffraction for Protein Crystallography", these proceedings.

[3] P. Seeger and G. Olah, "Monte Carlo Simulation of Neutron Scattering at CW, LPSS and SPSS", these proceedings.

[4] M. Fitzsimmons, "Monte Carlo Simulation of a Reflectometer at CW, LPSS and SPSS", these proceedings.

[5] G. Smith, "Monte Carlo Simulation of the SPEAR Neutron Reflectometer", these proceedings.

[6] A. D. Taylor, *SNS Moderator Performance Predictions*, Rutherford Appleton Laboratory report RAL-84-120 (1984).

[7] Y. Kiyanagi, N. Watanabe, and H. Iwasa, "Experimental Studies on Neutronic Performance of Coupled Liquid-Hydrogen Moderator for Pulsed Spallation Neutron Sources," *Nucl. Instrum. Methods* **A312**, 561-570 (1992).

[8] F. Mezei, "From Reactors to Long Pulse Sources", these proceedings.

[9] G. S. Bauer, J. P. Delahaye, H. Spitzer, A. D. Taylor, and K. Werner, "Relative Intensities and Time Structure of Thermal Neutron Leakage from Various Moderator-Decoupler Systems for a Spallation Neutron Source", proceedings of the 5th Meeting of the International Collaboration on Advanced Neutron Sources (ICANS V), Jülich, Germany, 22-26 June, 1981, Kernforschungsanlage Jülich report Jül-Conf-45. pp 417-444.

[10] V. L. Aksenov, A. M. Balagurov, V. G. Simkin, Yu. V. Taran, V. A. Trounov, V. A. Kudrjashev, A. P. Bulkin, V. G. Muratov, P. Hiismaki, A. Tiitta, and O. Antson. "The

New Fourier Diffractometer at the IBR-2 Reactor: Design and First Results", proceedings of the 12th meeting of the International Collaboration on Advanced Neutron Sources (ICANS-XII), held at Abingdon, UK, May 24-28, 1993, Rutherford Appleton Laboratory report 94-025, 1985. pp I124-I131; A. M. Balagurov, "High Precision Structural Refinement from High Resolution Fourier Neutron Powder Diffraction Data," *Materials Science Forum* **166-169**, 261-277 (1994).

[11] *Scientific Opportunities with Advanced Facilities for Neutron Scattering*, proceedings of a workshop held October 23-26, 1984, Shelter Island, New York. Brookhaven National Laboratory report CONF-8410256, 1985. pp 51-53.

[12] F. Cipriani, F. Dauvergne, A. Gabriel, C. Wilkinson, and M. S. Lehmann. "Image Plate Detectors for Macromolecular Neutron Diffractometry", *Biophysical Chemistry* **53**, 5-14 (1994); F. Cipriani, J.-C. Castagna, M. S. Lehmann, and C. Wilkinson. "The Application of Neutron Image-Plates for a Large Position-Sensitive Detector", proceedings of the workshop on New Tools for Neutron Instrumentation, Les Houches, France, June 6-9, 1995.

[13] S. E. V. Phillips and B. P. Schoenborn. "Neutron Diffraction Reveals Oxygen-Histidine Hydrogen Bond in Oxymyoglobin", *Nature* **292**, 81-82 (1981).

[14] B. P. Schoenborn, "Area Detectors for Neutron Protein Crystallography", Proceedings SPIE, Volume 1737, 235-242 (1992).

[15] W. Jauch and H. Dachs, "Single Crystal Diffractometry at the SNQ and at a Steady State Reactor", Proceedings of the Workshop on Neutron Scattering Instrumentation for SNQ, Maria Laach, Germany, 3-5 September, 1984, Kernforschungsanlage Jülich report Jül-1954. pp 31-52.

[16] G. S. Bauer, "Source Characteristics of a Long Pulse Spallation Source and the Use of Multiplexing Techniques", these proceedings.

[17] P. Ageron, "Cold Neutron Sources at ILL", *Nucl. Instrum. Methods* **A284**, 197-199 (1989).

[18] P. Lindner, R. P. May, and P. A. Timmins, "Upgrading of the SANS Instrument D11 at the ILL", *Physica B* **180-181, pt B**, 967-972 (1992).

INELASTIC SCATTERING RESEARCH AT A 1 MW LONG PULSE SPALLATION NEUTRON SOURCE

Inelastic Scattering Working Group Report

Colin J. Carlile (ISIS, RAL), Chairman

Team Members: G. Aeppli, AT&T; B. Alefeld, KfA Jülich; M. Arai, U. Kobe; J. Axe, BNL; G. Bauer, PSI; C. Broholm, Johns Hopkins U.; C.J. Carlile, ISIS; L. Daemen, LANL; G.J. Kearley, ILL; T. Mason, U. Toronto; F. Mezei, HMI, Berlin; H. Mook, ORNL; H. Mutka, ILL; R. Osborn, ANL; L. Passell, BNL; R. Robinson, LANL; S. Shapiro, BNL; U. Steigenberger, ISIS; F. Trouw, ANL; R. Pynn, LANL; A.D. Taylor, ISIS.

The Brief to the Instrument Groups

The brief was, with respect to the LPSS bench mark design supplied (60 Hz, 1 MW, 1msec proton pulse, with a split, non-fissile target and 4 moderators in a flux trap geometry design), to identify a set of instruments, and to assess their performance with respect to *existing* spectrometers on other sources. Any modifications to the existing instruments which would make them more effective on the bench-mark source, or conversely, any modifications to the source bench-mark required by the proposed instruments were to be identified, as were any uncertainties in the estimated performances, or any R & D needed to make the proposed instruments viable. Any new instrument concepts specifically matched to the long pulse itself were to be identified and assessed. This process was to result in an indicative list of instruments for the source. A figure of around 10 spectrometers was to be aimed for.

A Suite of Spectrometers

Any neutron scattering facility would need to consider the following types of spectrometers if it wished to cover the whole range of scientific fields available to inelastic neutron spectroscopy.

Instrument Type	**Application**	**Existing (or Proposed) Spectrometers**
Spin echo	Atomic & molecular diffusion	IN11 (ILL) IN15 (ILL) SPAN (HMI)
High resolution at low $\hbar\omega$	Molecular tunnelling, diffusion & crystal field splitting	IN5 (ILL) IN6 (ILL) IN10 (ILL) IRIS (ISIS) LAM80 (KENS) QENS (IPNS) (MUSICAL)
Crystal analyzer instruments	Molecular spectroscopy & catalysis	IN1B (ILL) TFXA (ISIS) FDS (LANSCE)
Electron volt spectrometer	Momentum distributions in quantum fluids and chemical systems	eVS (ISIS)

S(Q,ω) powder spectrometers	Magnetic excitations, dynamics of amorphous materials and chemical systems	IN4 (ILL) HET (ISIS) MARI (ISIS) HRMECS (IPNS) LRMECS (IPNS)
Single crystal spectroscopy	Phonon & magnon dispersion curves, phase transitions and critical diffuse scattering	TAS (ILL,BNL etc.) (RITA (Riso)) PRISMA (ISIS) ConstQ (LANSCE) HET (ISIS) (MAPS (ISIS)) SPINS (NIST) MARI (ISIS)

Initial Assumptions

The Inelastic Scattering Working Group decided, wherever possible, to compare any proposed spectrometers to those which are already operational and for which we have direct knowledge. There is of course a valid argument for carrying out comparisons with "upgraded" spectrometers on "upgraded" sources. This method is however prone to generate large uncertainties and the Inelastic Group decided to restrict itself to qualitative comments in these areas rather than attempting to generate quantitative numbers. For the purpose of this study therefore we only need to factor in source gains or losses when projecting forward to a proposed LPSS from the known performances of the ILL reactor and the ISIS pulsed source, which represent our main benchmarks, as far as the source flux and pulse shapes are concerned.

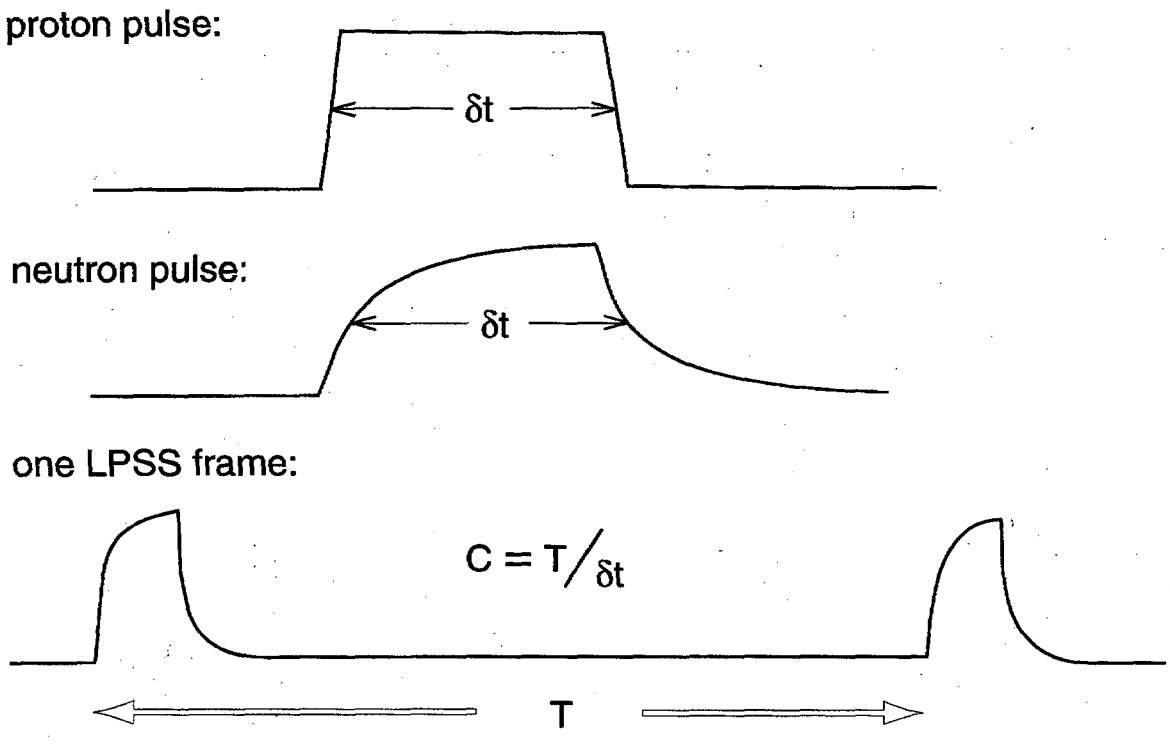

Fig. 1. The shape of the incident proton pulse and the resultant cold neutron pulse from a 1 MW coupled moderator on LPSS

In the first section we restrict ourselves to a consideration of cold neutrons. We have assumed, following the paper by G. Russell, that the 1MW LPSS would provide, time averaged, 25% of the ILL cold flux at 58MW. Assuming that the proton pulse width of LPSS is 1ms with a 60Hz repetition rate, the neutron pulse would asymptotically rise to a maximum at 1ms and decay exponentially for a further 1 ms or so as illustrated in Figure 1. Faster reflectors such as lead could be used to generate more rectangular neutron pulses (G Bauer).

We assume that the ratio of the neutron peak height to the average neutron intensity is 1/c (R. Pynn) where c is the duty cycle ($T/\delta t$) of the source. T is the period of the source (16.7 msec) and δt is the pulse width (1 msec). For LPSS this factor is therefore 16. When considering the comparison with crystal analyzer instruments on a sharp pulsed source (SPSS) such as ISIS, we have assumed that the 1ms neutron pulse can be chopped mechanically whilst preserving to a large extent the peak intensity. Depending upon the pulse length required this may pose a severe technological demand on those choppers which need to be positioned within 3 meters of the moderator. In such cases, identified below, full radiation damage studies must be carried out, taking into account mechanical and geometrical considerations, before the gains quoted below can be taken as valid.

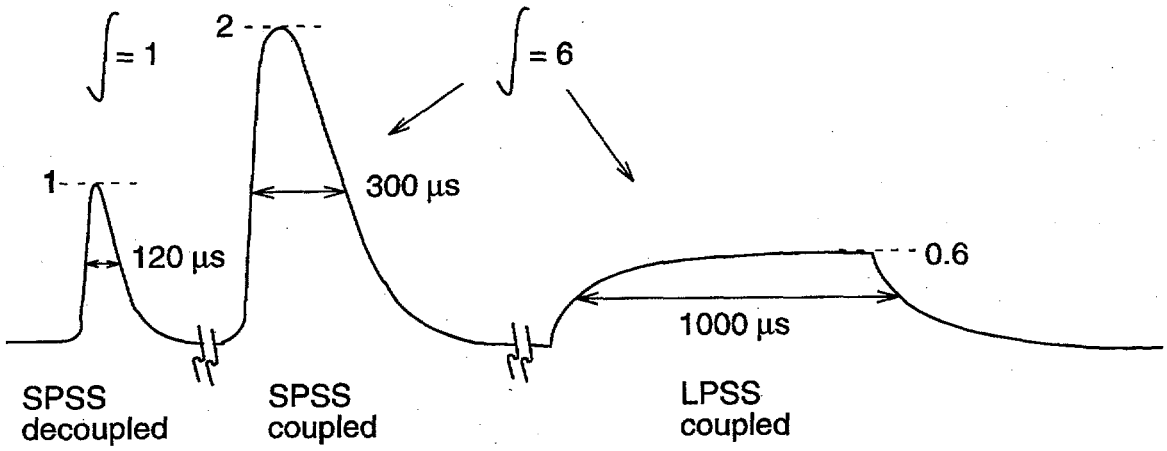

Figure 2

Fig. 2. A schematic illustration of the nominal peak shapes, peak heights and peak widths from (i) a decoupled sharp pulse source such as ISIS, (ii) a coupled sharp pulse source and (iii) a coupled long pulse source such as LPSS -- for the same proton current.

LPSS will have moderators which are neutronically coupled to the reflector, whereas ISIS is a sharp pulsed source (400ns) with decoupled moderators. For the same 400ns proton pulse length, considering cold neutrons, coupling has the effect, in round figures, of increasing the attainable peak neutron intensity by a factor of 2 and the integrated neutron intensity by 6 on an SPSS, while stretching the neutron pulse by a factor of about 3. For the same proton current, stretching the proton pulse to 1 msec will stretch the neutron pulse also to approximately 1 msec and drop its peak intensity to 0.6, as illustrated in Figure 2. For ISIS at 160 kW power and LPSS at 1 MW power the ratio of peak fluxes (LPSS:SPSS) is therefore 3.75 whereas the integrated

flux ratio is 37.5. This assumes that neutron flux scales with proton power, which may prove to be a valid assumption since opposing effects, for example increased coolant fraction as power increases and the opportunity afforded to optimise target moderator design, will tend to balance each other out.

These benchmark figures allow us a well-specified platform upon which to base our comparisons of proposed instruments for the LPSS with our experience of existing spectrometers on existing sources and we shall now deal individually with those instrument types listed in the table at the beginning of this report.

Time of flight multi-chopper spectrometer IN5

IN5 is a direct geometry time of flight instrument which uses a four-chopper monochromating system which could be transferred without modification to the LPSS. The first chopper would be phased to the maximum intensity of the required incident wavelength which would produce a narrow pulse in time. A 40 or 80 μsec triangular pulse is selected at IN5. As the first chopper opens there would only be a limited wavelength range present at LPSS, whereas at a reactor a full white beam is always present, within the limits of transmission of the neutron guide. This would reduce the possibility of impurity wavelengths passing through the chopper system, which might give better backgrounds in the LPSS instrument. For the LPSS it might be possible to use only a three chopper monochromating system for the same performance instrument, but this would require further study. A schematic diagram of IN5 is shown in Fig 3. Other more modern instruments, using counter-rotating choppers, but based upon the IN5 principle, are operating at Orphée (MIBEMOL) and HMI Berlin (NEAT), and a further instrument is under construction at NIST.

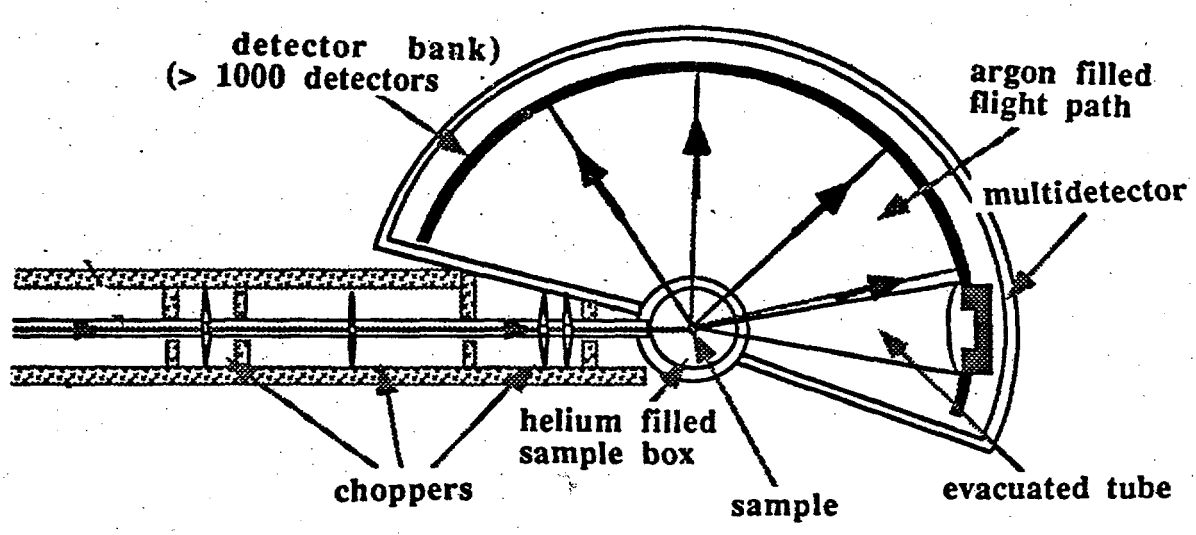

Fig. 3 A schematic layout of the IN5 spectrometer at ILL

The neutron intensity falling on the sample is related to the peak flux of LPSS. The ability, which IN5 has, to vary the pulse repetition rate to suit the individual requirements of each

experiment would be lost on LPSS. The effective intensity of the LPSS instrument compared with IN5 is therefore as follows:

0.25	x	16	x	0.5	=	2 x gain
source		gain per		non-optimum		
factor		pulse 1/c		frequency		

If we were able to increase the LPSS frequency to 120 Hz whilst halving the pulse length (i.e. still a 1 MW source) then the predicted gain will rise. As the peak flux will only reach ~90% of the asymptotic limit as illustrated in Fig 4 then in this case the gain of the instrument would be 3.6 x.

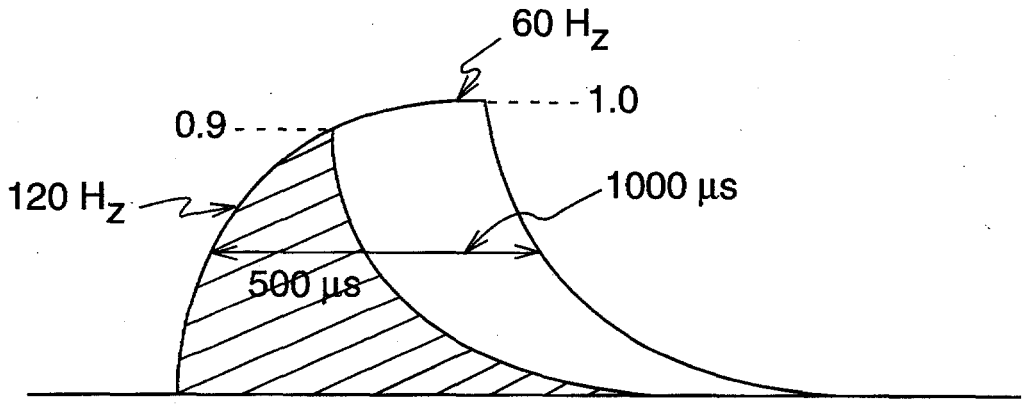

Fig. 4 *The effect on neutron production of increasing the LPSS frequency to 120 Hz*

The Time Focusing Spectrometer IN6

The crystal monochromator time of flight spectrometer IN6, with its focusing chopper in front of the sample, could be transferred as it stands providing gains similar to IN5. A schematic diagram of the instrument is shown in Figure 5.

The time-focusing requires a wavelength band $\Delta\lambda$ which is ~5% wide. If the spectrometer were placed 8 meters from the moderator, this represents a neutron "dwell-time" at the monochromator of ~900 µs for an incident wavelength of 6Å, which would be within the wavelength-time pulse "lozenge" of LPSS at this distance. Because of the reverse correlation required by this instrument for focusing purposes however (i.e. slow neutrons must arrive at the chopper first), there will be an illumination loss amounting to a further 20%. At 120 Hz because of the narrower pulse further intensity (totalling ~40%) would be lost due to non-illumination of this acceptance lozenge. The overall gain would therefore be 1.6 x at 60 Hz and 2.4 x at 120 Hz for an instrument like IN6.

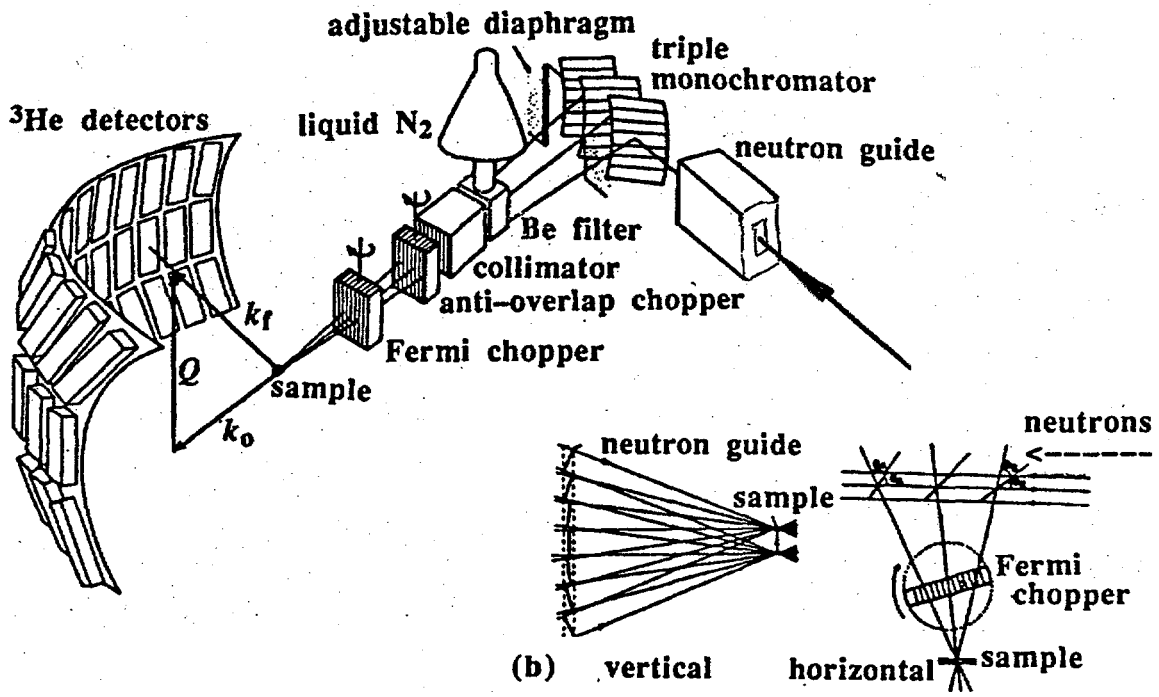

Fig. 5 *The IN6 time-focusing geometry inelastic spectrometer at ILL*

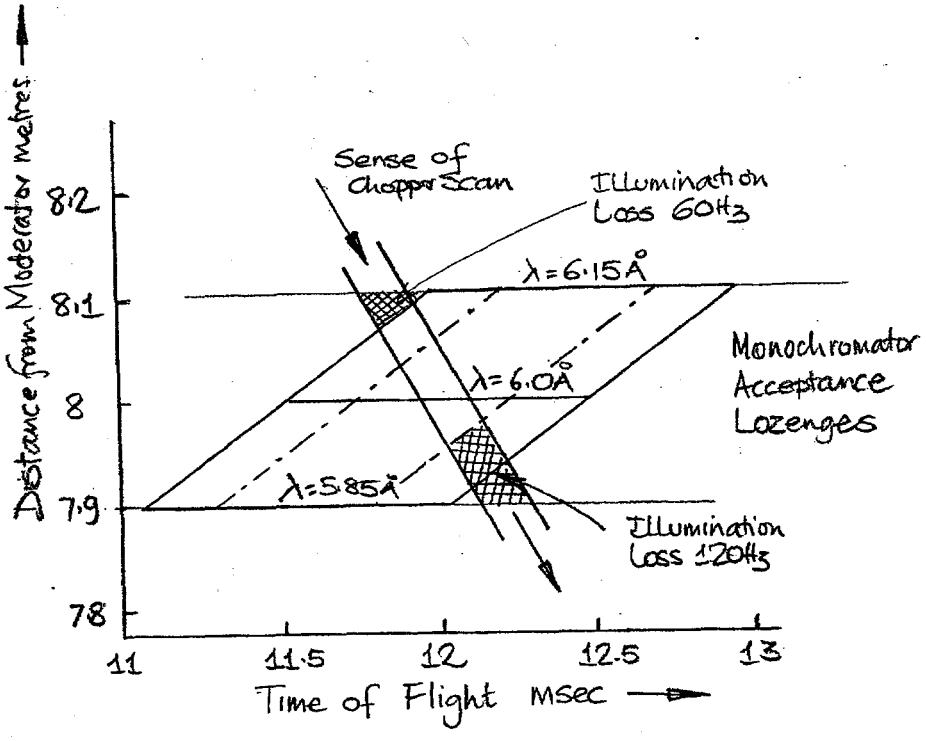

Fig. 6 *The scan of the focusing chopper through the "monochromator acceptance lozenges" for LPSS at 60 Hz (full line parallelogram) and 120 Hz (chain dotted) and for an IN6-type instrument (faint line)*

60 Hz:								
0.25 source factor	x	16 gain per pulse 1/c	x	0.5 non-optimum frequency	x	0.8 illumination loss	=	1.6 x gain
120 Hz:								
0.25 source factor	x	16 gain per pulse 1/c	x	1.0 non-optimum frequency	x	0.6 illumination loss	=	2.4 x gain

Moving the instrument closer to the source, say to 6 meters, would reduce the non-illumination problem, but could cause crowding with other instruments unless the large angular array of detectors were in the vertical plane. These effects, which are illustrated in Figure 6, require further study to fully quantify the losses and to optimise the instrument design.

One further point which must be considered is whether the fast neutron component of the long pulse passing through these instruments would be a source of background. This is illustrated in Figure 7. It can be seen that a section of the dynamic range of the spectrometer might be affected. Because both instruments concentrate upon near-elastic measurements rather than broad inelastic spectra, this would pose a particular problem only if the time of flight of the incident wavelength neutron pulse was close to the period between pulses. For a 120 Hz source any such effect, were it to be significant, would be more troublesome. Experience on ISIS suggests that this is not a limiting problem but further study is recommended here.

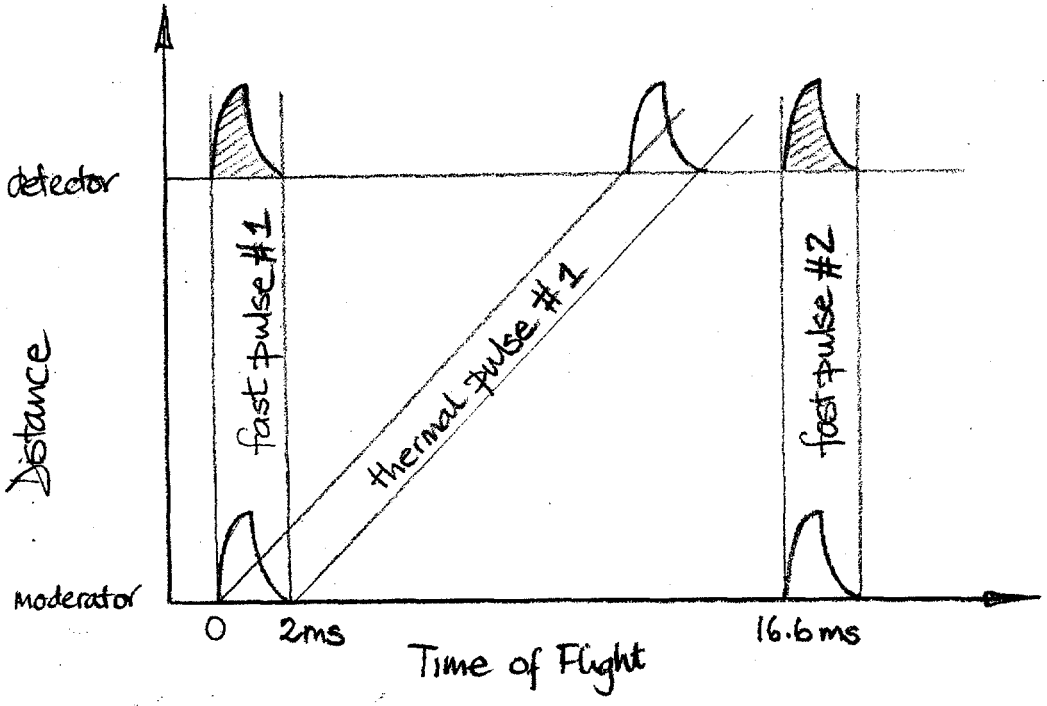

Fig. 7 *A length-time diagram for a direct geometry spectrometer such as IN5, IN6 or MARI, showing the regions in which the fast neutron pulse might affect the spectroscopic range for a 60 Hz source. The shaded fast pulse at the instrument will be reduced by a factor of ~10^3 by accelerator and target station shielding*

The Inverted geometry TOF backscattering machine IRIS

IRIS is an inverse geometry spectrometer operating at the ISIS pulsed source. ISIS is a 160 kW sharp pulsed source rather than a 1 MW long pulsed source. IRIS uses large area graphite and mica analyzers after the sample, which is illuminated by a white beam transmitted through a 36 m neutron guide to achieve the necessary resolution. The instrument is shown in Figure 8.

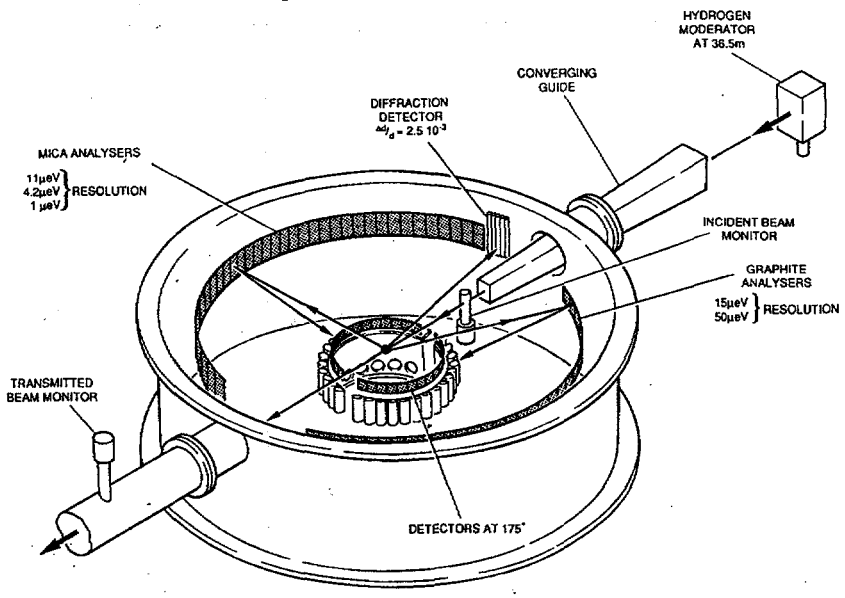

Fig. 8 The IRIS crystal analyzer instrument, which operates at ISIS.

The pulse width from the ISIS liquid hydrogen moderator is 120 μsec and therefore, to transfer the instrument as it stands, it would be necessary to chop out a similar length pulse from the 1 msec LPSS pulse using two disc choppers, one at 3 meters, inside the LPSS biological shield, and a second wide-band chopper at say 15 meters. The count rate of the instrument is reduced by the drop in peak flux per kW of source power and the fact that the flux falling on the sample in the white beam is lower than that at the peak of the long pulse by about 20% on average. This can be seen by reference to Figures 1, 2 and 4.

0.6	x	6.25	x	0.8	=	3.0 x gain
ratio of peak fluxes LPSS/SPSS		power of LPSS/ISIS		average to peak		

In order to be confident of realizing the instrument at LPSS it must be demonstrated that it is feasible to chop the pulse width down and yet retain, in terms of intensity and energy range, the quality of the white beam. However, for this instrument, we do not need to be limited to the 120 μsec pulse width which would simulate IRIS, but could optimise the pulse length to the required instrument performance. This would allow us to contemplate building a shorter instrument which would not simply be cheaper but would benefit from an increased L_2/L_1 factor, which would improve the S/B in certain experiments because of a reduction in the effect of simultaneous analyzer reflections (Kearley et al.). The dynamic range of the instrument for a given set-up would be doubled for an 18 m machine (60 μsec pulse). As long as the peak flux is

maintained, and information exists within the whole of the dynamic range, the data rate is unchanged by shortening the instrument. In order to fill the time frame of the LPSS (16.7 msec at 60 Hz) the ratio of the distances from the δt-definition chopper to the instrument (L_{12}) and to the moderator (L_{11}) must equal the duty cycle c of the source as shown in Figure 9.

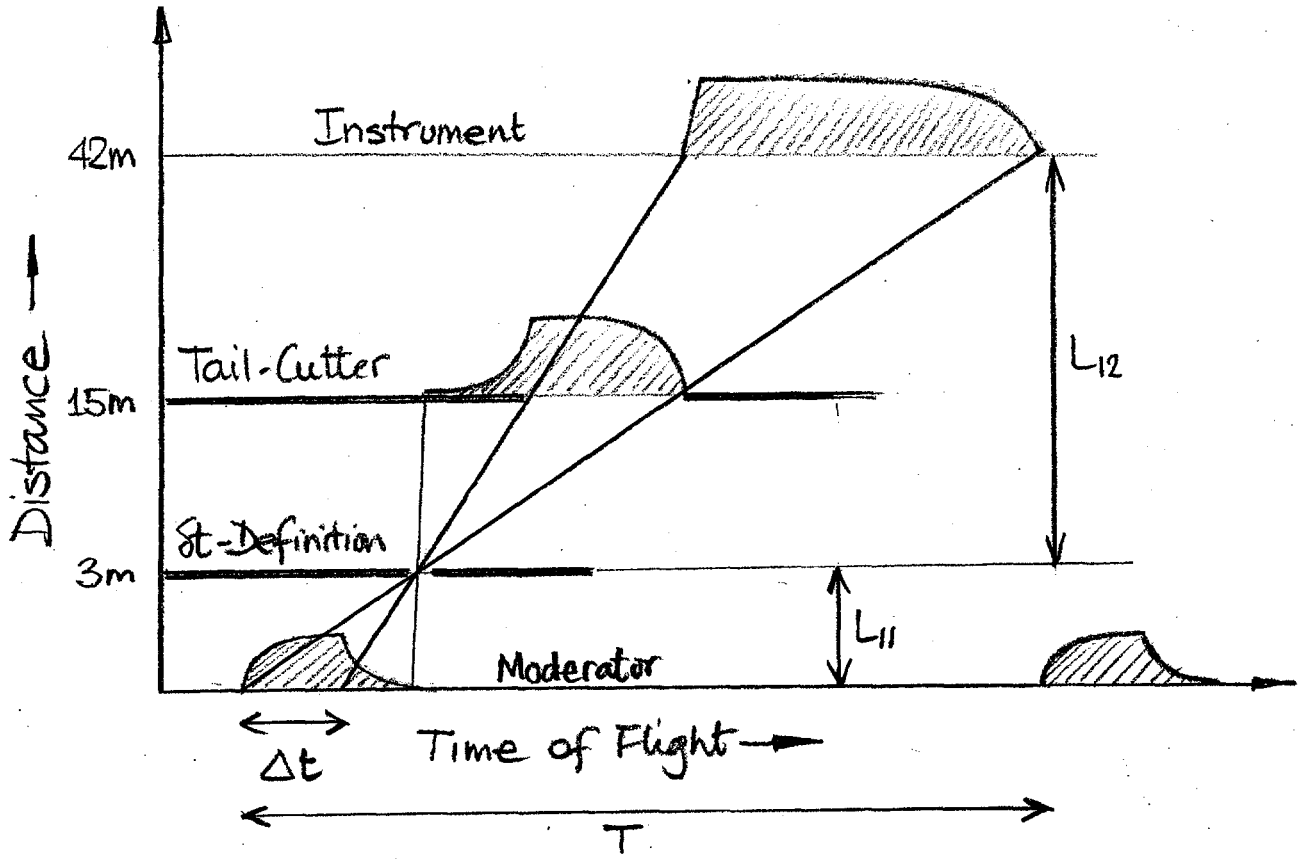

Fig. 9. Chopping a long pulse down to generate a short pulse whilst retaining the white beam quality of the incident beam requires the ratio $L_{12}/L_{11} = T/\Delta t$

This criterion requires choppers close to the moderator and favours longer primary flight path instruments however. Even an IRIS lookalike instrument would not achieve a full frame with the δt-chopper at 3 meters. 2.25 meters is required which will pose a difficult technical problem. Chopping a long pulse will give a symmetrical resolution function. Depending upon your point of view, this loss of the sharp leading edge on the IRIS resolution function, which will remove the higher Fourier components in the instrumental resolution function, is an advantage or a disadvantage. On LPSS the resolution function will be symmetrical and probably Gaussian-like when the effect of the crystal analyzer is convoluted in.

The TOF backscattering spectrometer

Let us consider moving the 1 μeV resolution backscattering crystal analyzer spectrometer IN10, which operates at ILL, to the LPSS. The function of the Doppler drive monochromator will be provided by the TOF white beam. This is a logical progression of the IRIS instrument, which

indeed was considered at one stage. If we aim for 1 μeV resolution, then this can be achieved by various combinations of pulse length and incident flight path length. The length of the instrument also determines the energy transfer range which the instrument can access at a single setting of the choppers and therefore, provided information exists in the energy transfer window, the shorter the instrument the better. For a 25 μsec pulse, the instrument length necessary for an overall resolution of 1 μeV is 92 m with a δt-defining chopper at 6 meters and a tail-cutter at 20 meters. The spectrometer is illustrated in Figure 10. It is not an unrealisable instrument to build, and would give a very generous 450 μeV energy transfer range. To attempt to chop the beam much below 25 μsec requires the highest technology disc choppers.

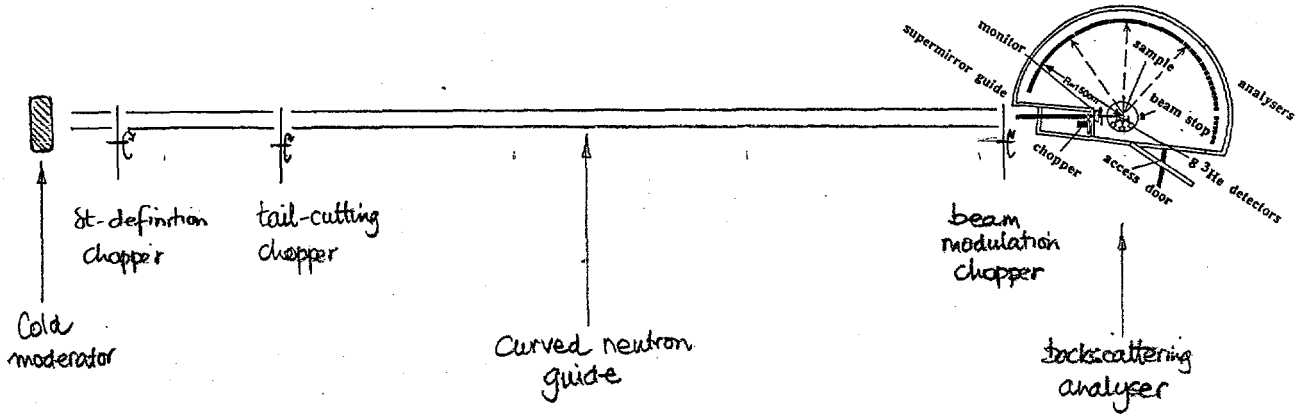

Fig. 10 A TOF version of the IN10 backscattering spectrometer

The data rate can be estimated, as for IN5 above, for an LPSS instrument compared to IN10, as follows.

0.25 source factor	x	16 gain per pulse 1/c	=	4 x gain

One advantage of a TOF backscattering machine is that the energy transfer range can be offset by simply rephasing the choppers. Thus energy transfers up to 1000 μeV with 1 μeV resolution would be feasible. The instrument is too long to benefit from second order separation as proposed for a short IRIS, and the effect of time dispersion after scattering through such (relatively) large energy transfers needs to be assessed. This effect would result in the realisable energy transfer range being reduced. Very importantly however, the count rate of such an instrument is very much sample-response dependent, since, unlike IN10 where the Doppler drive can be slowed down to reduce the energy transfer range and yet retain a constant total intensity falling on the sample, it is not possible to do this when using TOF as the monochromating element.

If therefore we compare the *count rate per resolution element* of the two instruments, which can be done by dividing through by the dynamic ranges, we see that the LPSS instrument is then down by a factor of 3.8 on IN10. By increasing the LPSS frequency to 120 Hz (and as a

consequence decreasing the dynamic range to 225 μeV) this factor would fall to 1.9 times down. This "gain" factor of 0.5 has to be seen in the context of the IN10 dynamic range of only +/- 15 μeV. The LPSS instrument would access a factor of 15 wider dynamic range for a single setting of the instrument. Note however that a new instrument, IN16, is now in the commissioning phase at ILL which promises gains in intensity of greater than 5 over IN10. An equivalent gain could probably not be realized on a pulsed source instrument because IN16 utilises a large focusing array of monochromators on the Doppler drive. The two types of instrument have sufficiently different characteristics and yet similar performances as to be rated as complementary.

The MUSICAL instrument

A 1 μeV resolution time of flight IN10-type spectrometer at an LPSS can be realized by a flight path of 92m and a pulse length of 25 μsec as shown in the previous section. The relative dynamical range is given by the ratio of $T/\delta t$, where T is the time between two pulses and δt is the pulse length. This value amounts to 666 for the above instrument. Because backscattering μeV spectroscopy is associated with notoriously low intensity, it is advantageous to be able to match the dynamical range to the physical problem to be studied because the intensity available for an experiment is inversely proportional to the dynamical range necessary for the experiment. The dynamical range of a TOF-type instrument can only be reduced by increasing the pulse length and the total length of the instrument. The MUSICAL instrument offers the possibility of realising a flexible dynamical range independent of the distance between the source and the analyzer. The minimum dynamical range which can be realized is the time which is available between two consecutive pulses divided by the pulse length of the LPSS. This value amounts to 16 for a source with a 1 msec pulse length and a frequency of 60 Hz. With 16 monochromator

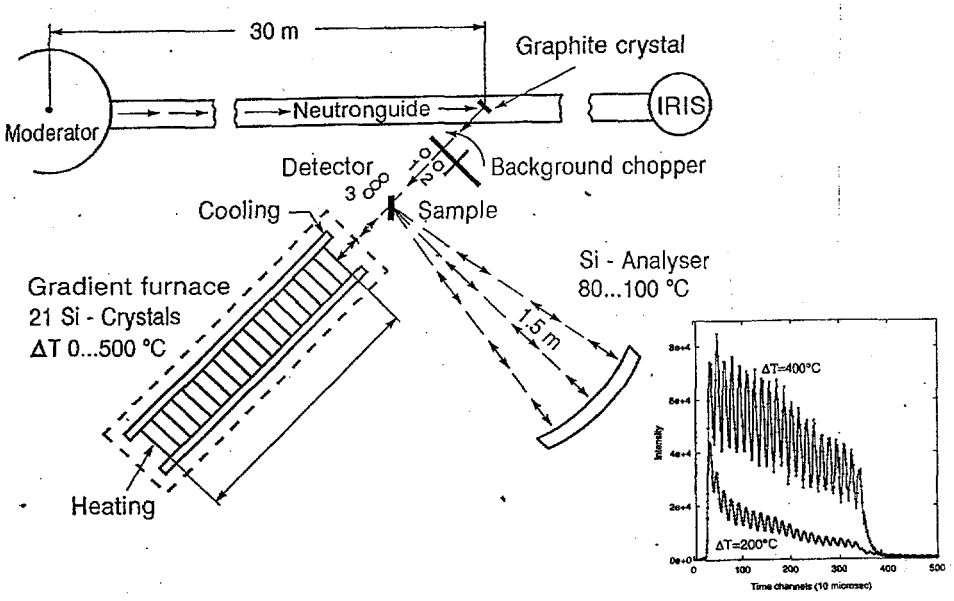

Fig. 11 The MUSICAL spectrometer prototype set-up and an inset of the generated "white beam".

crystals, positioned at slightly different distances and with slightly different lattice spacings, the MUSICAL instrument can be realized. A prototype MUSICAL set-up which recently operated successfully on the IRIS beam is shown in Figure 11.

If the crystals can be heated, as has been done for the single monochromator on IN10 at the ILL, the dynamical range, which is relatively low, can still be extended to values comparable to those of a TOF-type instrument. The advantage of LPSS for a MUSICAL-type instrument is the fact that only a few crystals (16) are needed, and therefore absorption in the monochromator assembly does not play such an important role as in the case of an SPSS instrument, where many crystals (100) would be needed. The gain of such an instrument would be a straight factor of 4 (i.e. 16 x 0.25) compared with IN10 and could represent a more appropriate instrument for an LPSS than the IN10-type instrument described above. MUSICAL is an instrument which is ideally suited to the LPSS pulse structure but further work to prove its principle of operation would be worthwhile.

Neutron Spin Echo

NSE spectrometers in most experiments require only a coarsely monochromated beam with $\Delta\lambda/\lambda$ ~ 15%, similar to that needed for small angle scattering. This is usually produced on a continuous source with the help of a helical velocity selector. There are however a number of NSE experiments, accounting for some 10% of the use of IN11, in which a lower value of $\Delta\lambda/\lambda$ is necessary. In such cases a graphite analyzer is used at 4-6Å in order to achieve $\Delta\lambda/\lambda$ ~ 3-5%. In view of the long monochromator-to-sample distance, a crystal monochromator before the sample leads to a beam intensity reduction due to the additional divergence imposed upon the monochromatic beam by the crystal mosaic spread. The IN11 instrument is shown in Figure 12.

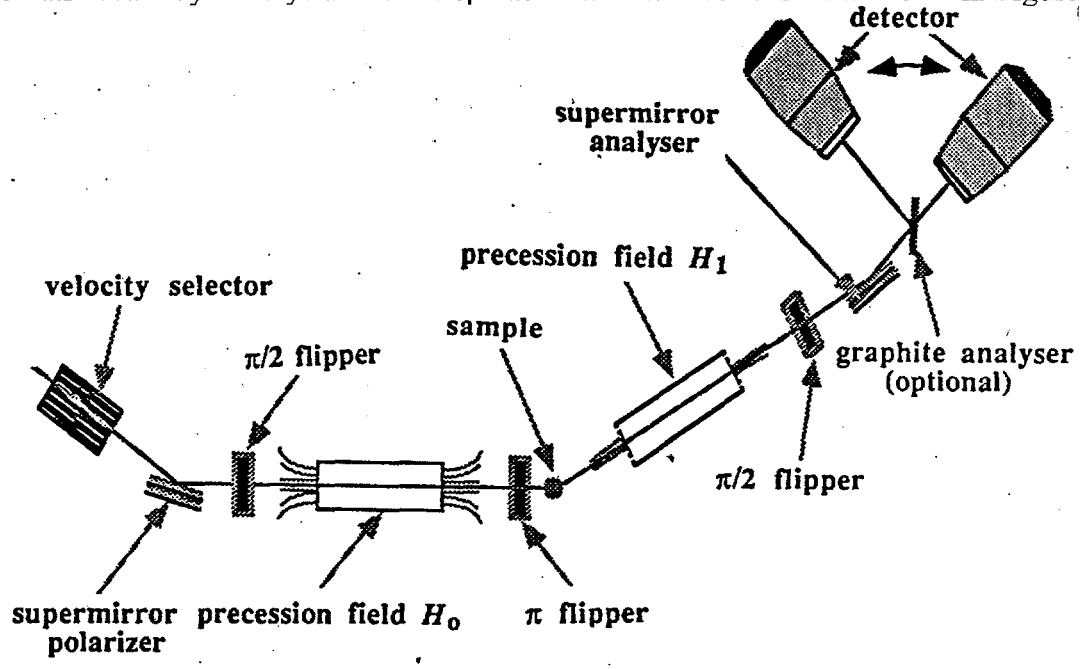

Fig. 12 The IN11 neutron spin echo spectrometer operating at the ILL reactor

Newer versions of NSE spectrometers (IN15, IN11C and SPAN at HMI) utilise multidetectors. On LPSS the function of the velocity selector would be taken over by TOF monochromation where transmission, reflectivity or divergence losses are eliminated. This requires the spin flippers to be phased to the instantaneous neutron velocity. The electronic control system required for this mode of operation has already been built under the framework of the HMI-ILL-KFA project, IN15, and will soon be tested, together with the chopper TOF monochromator system installed on IN15 as an alternative to the velocity selector. On the LPSS, with 1 ms pulses and 60 Hz repetition rate, the long neutron pulse provides sufficient $\Delta\lambda$ resolution (7% FWHM at 4 Å and better for longer wavelengths) at a 15 m moderator-to-detector distance, the shortest conceivable in view of the length of the instrument itself (7-8 m). This distance already assumes that on one side two neighbouring instruments are shorter than 10 m. At this distance, the wavelength band $\Delta\lambda$ is 4 Å, so at an average wavelength of 7 Å, the $(\delta\lambda/\lambda)/(\Delta\lambda/\lambda)$ ratio is 0.25, while the source duty cycle is only 0.07. Thus only about 30% of the ideal peak flux can be made use of, or in other words, some 4 times the average cold flux. This means that for NSE spectroscopy, instruments built on a 1 MW 60 Hz long pulse spallation source would be equivalent to those built at the ILL.

Additional advantages of the spallation source are the better wavelength resolution, if required, and the wider dynamic range of the NSE scan in a single geometrical setting where several Q-values are of interest, as is usual. In addition to the field scan H, a wavelength scan would extend the range by a factor of $(\lambda_{max}/\lambda_{min})^3 = 5$.

As in the case of SANS, a higher repetition rate for NSE would be detrimental because of the inevitable reduction of the wavelength band. A lower repetition rate would be of considerable advantage. It would allow the instrument to be pulled out to some 25 m from the moderator with no penalty on the wavelength band (a polarized guide is used in any case) thus easing the space requirements.

Thermal and Epithermal Neutron Quasielastic and Inelastic Spectrometers: QENS, TFXA and FDS

The time-averaged thermal flux produced by the LPSS is calculated to be ~ 15% - 20% that of the ILL. In addition, SPSS sources such as ISIS, IPNS and LANSCE generate increasingly narrow neutron pulses as the neutron energy increases into the epithermal range, giving access to comparatively higher peak fluxes and high resolution instrumentation. Both factors mitigate against such instruments on LPSS.

Inverted geometry (or crystal analyzer) spectrometers on the three sources, TFXA, QENS and FDS, therefore obtain their high performance figures by a combination of wide energy transfer range, out as far as 1eV, with very good energy resolution ~ 1 - 2%. The combination of white incident beam and low final energy allows measurements to be made in neutron energy loss configuration with the sample kept cold. This is ideal for molecular and magnetic spectroscopy.

It has not yet been demonstrated that pulses which become shorter as neutron energy rises can be effectively generated from a long pulse even though methods have been suggested. Accordingly,

the Inelastic Group considered that this instrument was not well-suited to LPSS, particularly when considering the ideal match which there is with such instruments on SPSS pulsed sources.

Direct Geometry Chopper Spectrometers

Direct geometry chopper spectrometers for thermal neutrons have proved to be very successful for studies of $S(Q,\omega)$ over a broad range of Q and ω with high resolution. Such measurements include vibrational spectroscopy in liquid and amorphous materials, phonon densities–of–state, molecular spectroscopy and magnetic inelastic scattering in polycrystalline materials. They have also been used on pulsed sources to measure single–crystal excitations up to very high energy transfer and have been particularly successful in studies of low–dimensional systems. The MARI spectrometer is shown in Figure 13.

Figure 13.

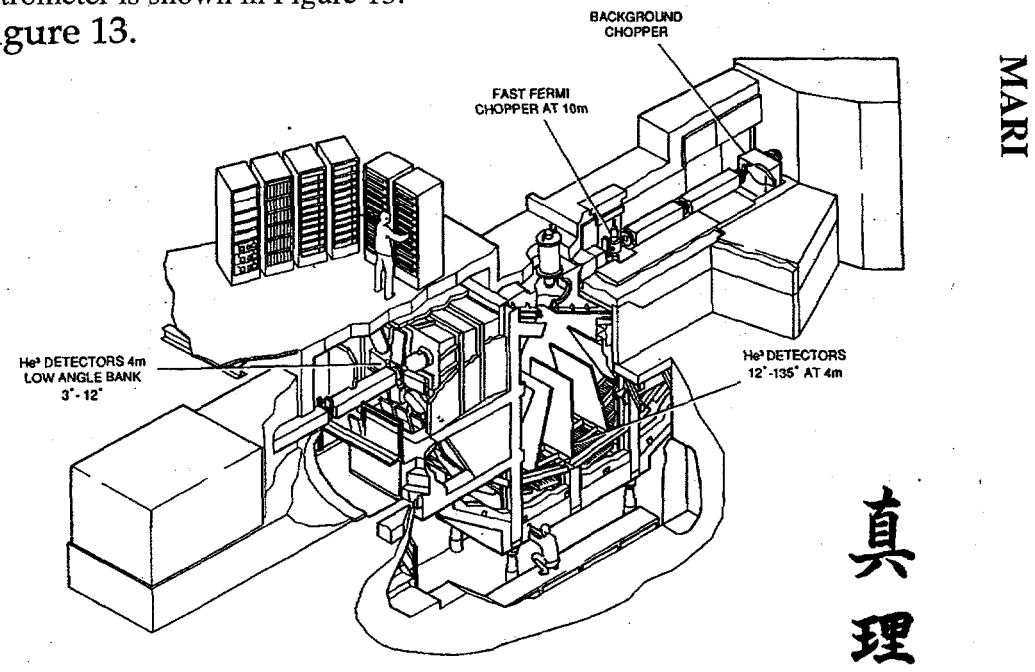

Fig. 13 The direct geometry spectrometer MARI which operates on the ISIS SPSS.

The Inelastic Group considered the value of building such an instrument as HET or MARI but concluded that the flux penalty and the need for very narrow (down to 1 μsec) monochromatic pulses meant that there was not a strong case for building such an instrument at a long pulse source. Instead an instrument based on the design of IN4C, presently under construction at ILL, which has a hybrid monochromator (crystal plus chopper) and is optimized for count rate rather than resolution might be a more well-adapted candidate. Since such instruments still require quite narrow chopper burst times (~ 10 to 20 μsec), only a small fraction of the 1 ms pulse available on LPSS would be used. There is the advantage however that the monochromator can be phased to use the peak flux in the pulse and so has a gain (1.25 x) over the average flux in the pulse (refer to Figure 4). In addition a focusing monochromator, accepting an angular divergence of about 1°, will enhance the incident flux, as it would on a reactor source.

Our comparison is based on the optimized IN4C currently being built at ILL. The gain factors are dependent on incident wavelength because, on a reactor, it is possible to optimise the repetition rate of the instrument precisely to the required time frame, which is not possible to do on LPSS. In our calculations, we have assumed that the optimum time frame starts at the infinite energy transfer time channel and ends at $E_f = 0.9xE_i$. This produces a conservative (lower) gain factor since, in practise, the longer time frame is useful for determining backgrounds. In general, for the wavelengths considered, the gain would be greater with a higher source frequency (though not faster than 120Hz at the longer wavelengths) and shorter pulse length. Therefore a coupled short pulse source would give higher gains at the same source power, assuming the peak flux is higher (see Figure 2).

Table 1. A 2% resolution Direct Geometry Spectrometer ($L_2 = 2m$)

Moderator–sample L_1	11m
Sample–detector L_2	2m
Chopper burst time	10μs
Energy resolution	$2\%E_i$

Wide–angle bank of detectors (gas tubes or multi–wire)
Focusing monochromator with 1° angular divergence

			Gain	Total
	Source flux		0.2	
	Peak flux enhancement 1/c		16	
Duty cycle	E_i = 5 meV	150 Hz	0.4	1.3
	E_i = 10 meV	210 Hz	0.3	1.0
	E_i = 20 meV	300 Hz	0.2	0.65
	E_i = 80 meV	300 Hz	0.2*	0.65

Table 2. A 1% resolution Direct Geometry Spectrometer ($L_2 = 4m$)

Moderator–sample L_1	11m
Sample–detector L_2	4m
Chopper burst time	10μs
Energy resolution	$1\%E_i$

Wide–angle bank of detectors (gas tubes or multi–wire)
Focusing monochromator with 1° angular divergence

			Gain	Total
	Source flux		0.2	
	Peak flux enhancement 1/c		16	
Duty cycle	E_i = 5 meV	75 Hz	0.8	2.6
	E_i = 10 meV	100 Hz	0.6	1.9
	E_i = 20 meV	150 Hz	0.4	1.3
	E_i = 80 meV	300 Hz	0.2*	0.65

* Current chopper technology does not allow a shorter (optimum) time frame at higher energies.

These gains would be increased by designing a higher resolution spectrometer, increasing the monochromator take–off angle (and matching the mosaic spread of the monochromator) and lengthening the secondary flight path. For example a 4 m secondary flight path would increase the resolution to 1% E_i but would increase the time frame by a factor of two. The duty cycle (and overall) gains would be increased by a factor 2 compared to an equivalent reactor spectrometer. This would require a longer time frame and therefore reduce the duty cycle losses. This would require some R&D to improve the quality of monochromator crystal mosaics (e.g. fabrication of anisotropic mosaic crystals). Backgrounds would in general be expected to be lower than an equivalent reactor machine which would enhance the useful energy transfer range. This cannot be quantified easily.

There are some applications which require a considerably relaxed energy resolution spectrometer. This could be realized by increasing the chopper burst time, to say 100 μs. Since the energy is coupled to Q, the Q–resolution would also be relaxed but only parallel to k_i. The gain factors compared to an equivalent reactor spectrometer would be identical to the above, since the peak flux would still be used. A coarse resolution machine could also be built by removing the crystal monochromator and using a broader band chopper. Since the flight path of the secondary spectrometer would need to be increased to maintain 20% resolution with a 500 μsec pulse, the time frame is better optimized to a 60 Hz source.

Table 3. Coarse resolution Direct Geometry Spectrometer

Moderator–sample L_1	10m
Sample–detector L_2	5m
Chopper burst time	500μs
Energy resolution	20 %E_i
Movable bank of detectors (+/- 10°)	
Guide with focusing funnels at entrance and exit (1° at 20 meV)	

			Gain	Total
	Source flux		0.2	
	Peak flux enhancement 1/c		16	
Duty cycle	E_i = 5 meV	60 Hz	1.0	3.2
	E_i = 10 meV	90 Hz	0.7	2.1
	E_i = 20 meV	120 Hz	0.5	1.6
	E_i = 80 meV	240 Hz	0.25*	0.5 (loss of focusing)

The removal of the crystal monochromator provides a significantly higher count-rate than would be obtained with a hybrid monochromator instrument. There is also some reduction because of the loss of focusing at the highest energies where the guide divergence is smaller. The crossover energy would be about 20 meV (no loss below, factor 1.5 loss at 80 meV).

Coherent excitations spectrometers at LPSS

Magnetic and vibrational excitations in condensed matter with energy scales from 0.5 to 8 meV may be studied using triple axis spectrometers at reactor-based cold neutron sources. Such instruments exist mainly in Europe, at ILL and Riso for example, where they are heavily oversubscribed and have made unique contributions in many areas of condensed matter physics. The only such spectrometers available in the U.S.A. are the SPINS instrument at the cold neutron source at NIST, and the instrument at Brookhaven.

Single Analyzer Instruments

To assess possibilities for LPSS let us first of all conceptually move a classic cold-source triple axis spectrometer like IN12 at ILL, with focusing graphite analyzer and graphite monochromator, to the long pulse source and adapt it to the specific capabilities of the LPSS. The proposed instrument would use both horizontal and vertical focusing. The aim is to keep the instrument as short as possible (~6 m) without using a neutron guide. The layout is shown in Figure 14.

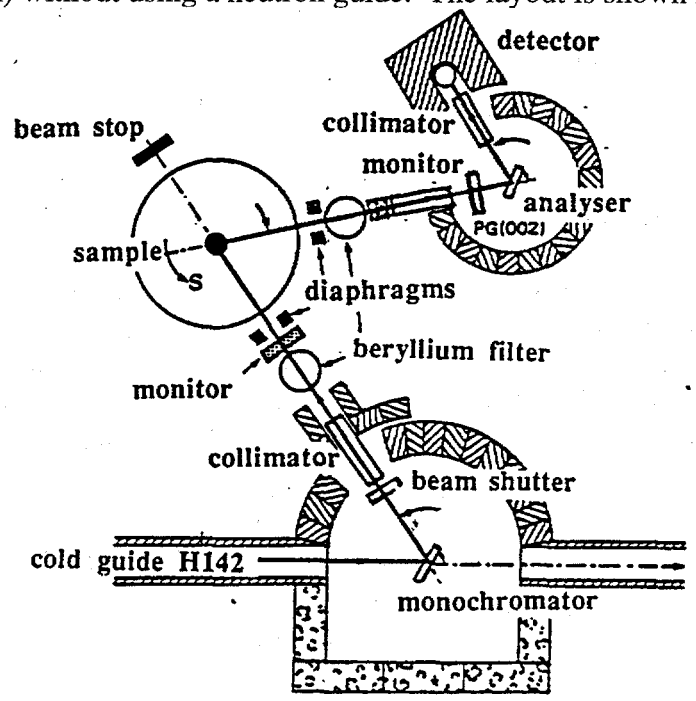

Fig. 14 The cold neutron triple axis spectrometer IN12 at ILL

Incident energies from 2 meV to 14 meV will be used. Operating in a point-by-point mode, the performance of such an instrument will scale as the average flux of the two sources, making the LPSS TAS ~ 0.25 of the count rate of IN12. Significant improvements in performance (1.25 x) would result from not requiring a graphite filter or velocity selector for order contamination removal in the monochromator, which would be timed out on LPSS, as would fast neutron background only generated during the 1ms pulse. The time-independent background might be reduced by a factor approaching the duty cycle of the source (16.7) from this effect.

Because of the high energy neutrons in the direct beam, the shielding drum around the monochromator may need to be increased in size compared to a reactor instrument. Geometries allowing as much as 26 degrees radially on one side of the instrument to scan the sample, analyzer and detector at 90 degrees will be needed, as it would of course at a reactor source. The instrument could, in principle, be adapted to polarisation analysis mode as for similar reactor instruments. A non-polarized instrument however is an attractive option for LPSS with count rates ~ 0.33 of ILL instruments.

Extending the analysis to a thermal triple axis spectrometer, we obtain a conclusion which is not so sanguine. Firstly to avoid the first two milliseconds of the frame when the fast pulse is produced and still have access to a significant energy transfer range, means that the instrument must be sited at least 10 m from the source, with the monochromator at 7 m (c.f. the 3 m at Brookhaven). Options for the design of the moderator, such as having a tall narrow face, may gain count rate by allowing the vertical divergence to be increased. A t-zero chopper placed at 3 m will eliminate the 1 ms fast pulse and be fully open to pass 50 meV incident neutrons on to the monochromator.

Given the fall in relative flux with respect to the LPSS cold moderator (and the loss in solid angle because of the need to site the instrument further from the source) the Inelastic Group were not convinced that a thermal triple axis spectrometer was a viable candidate for LPSS.

Multiple analyzer Instruments

Optimized spectrometers employing focusing techniques and large solid angle detection (referred to as RITA, the reinvented triple axis spectrometer) are currently being developed at NIST and at Risø. Typical energy and wave-vector resolutions are $\delta E = 0.1$ to 0.5 meV and $\delta Q = 0.02$ to 0.1 $Å^{-1}$ covering energy transfers $h\omega$ from -1 to 8 meV and wave-vector transfers from 0.1 to 2.0 $Å^{-1}$. Since $|h\omega/\delta E|$ is comparable to the duty cycle of LPSS, such instruments are well suited to

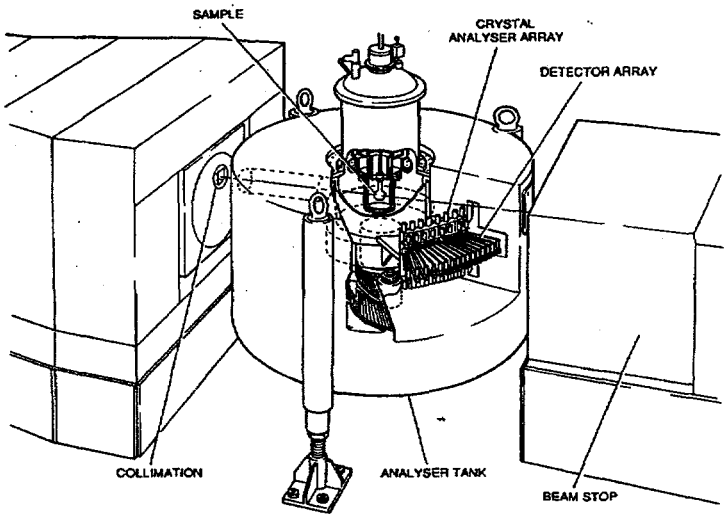

Fig. 15 *The PRISMA multiple analyzer coherent excitations spectrometer operating at ISIS.*

this type of spallation source. Because of the long pulse width, the optimal configuration of such an instrument at LPSS employs a long incident flight path, a pulsed white incident beam and a crystal analyzer assembly after the sample. The instrument therefore conceptually resembles a cold neutron version of the multiple double analyzer instrument PRISMA at ISIS, which is illustrated in Figure 15. In the wavelength range (2Å<λ<6Å), which characterizes neutrons used in cold neutron spectrometers, angular divergences can be relaxed to typically 2° to 4° in all directions, leading to large gains in sensitivity while maintaining sufficient wave-vector resolution for many experiments. The Inelastic Group assumed that, for the comparison, the secondary spectrometers would be identical for reactor, SPSS and LPSS versions of the instrument and has assessed only the performances of the primary spectrometers.

Crucial for the success of such an instrument at an LPSS would therefore be the ability to view an area of the moderator comparable to the sample size (~3 x 3 cm) with angular divergences of at least 2° x 2° at a distance of ~ 30 m although a 38 m instrument may be more efficient for single point measurements. This may be possible through the use of the so-called eye-of-a-needle phase-space transformer proposed by F Mezei, which employs supermirror guides. The outline and technical specifications of the proposed instrument are as follows:

Specification:

Total flight path : 30 meters
Chopper at 4 meters from source + waveband defining choppers
Eye-of-the-needle neutron guide
Double analyzer configuration
0.6° horizontal and up to 4° vertical collimation on analyzer system
Energy acceptance of the analyzer system : 0.15 meV

Selecting a 200 μs window, typically, results in a 2.5 Å to 4.5 Å wavelength band (4 - 13 meV). Benchmarking for E_i = 8 meV, E_f = 5 meV and δE = 0.2 meV and assuming 0.8 x average pulse intensity to peak. (A reactor instrument would lose a factor 0.8 due to a velocity selector or a filter so this factor is recovered) and a 14 msec useable counting time would result in a performance 0.5 to 3.3 times ILL, where 0.5 corresponds to a horizontal collimation of 2° on the reactor experiment and 3.3 corresponds to a horizontal collimation of 0.6° on the reactor experiment. The instrument becomes increasingly efficient as E_i becomes smaller.

The LPSS instrument has an advantage over reactor-based instruments in that the fast neutron background from the spallation source is only present for ~ 2 ms out of the 16.7 ms period. In our comparison we have assumed that this time is not used for counting signal. Therefore the LPSS would not have any fast neutron background contribution from the source.

This instrument appears to be particularly well matched to the performance of a 60 Hz source. Whilst not wishing to change the source repetition rate any reduction of the proposed pulse length (down to the proposed 200 μsec chopper burst time) which would increase the peak flux, would be beneficial.

As stated above, we have compared the performance of such an instrument to a fully optimized doubly focusing cold neutron spectrometer proposed for the cold neutron source at the 20 MW NIST reactor, and scaling up to the ILL power, and find that the LPSS instrument could be

approximately 3 times as efficient for energy transfers $\hbar\omega \sim 4$ meV in surveys of areas or volumes in Q-ω space. In the comparison it is assumed that the two instruments have identically large solid angles for the secondary spectrometers.

If we instead compare to the IN14C instrument which views the second ILL cold source through a neutron guide and has just a single analyzer/detector, using published numbers for the flux at the sample, then the LPSS instrument would be $15xN_{det}$ and even more efficient for surveying volumes of Q-ω space. The gain depends on the number of detectors, N_{det} employed at the LPSS instrument. If IN14C were equipped with a multidetector analyzer covering the same solid angle, the LPSS instrument would still be 15 times more efficient than IN14C. In situations where only selected Q-ω points are of interest, the efficiency of the LPSS instrument is reduced by a factor of up to 60 since then only one of the 225 μsec time slots in the 14 msec useful counting time would contribute to the signal of interest. For such purposes the LPSS instrument would therefore be approximately 4 times less efficient than IN14.

In terms of absolute efficiency, we estimate that the count rate accumulated in one 225 μsec time bin of a single detector would be

$$I = 1.9x10^3\lambda_i^3\exp[-(\lambda^{-3})/2.1]S(Q,\omega)\ n/cm^2/s/Å^3xmeVxsr$$

From this number we estimate that the average count rate from 0.05 moles of an S=1/2 magnet with a bandwidth of 10 meV for $\lambda_i = 3Å$ would be 30 counts/second in a 225 μsec time bin of a single detector. With such count rates it would be feasible to map out the dynamic spin correlation function of a large single crystal completely, a task which would certainly be out of the question with present day neutron scattering instrumentation.

It is important to note that the mode of survey is different for a reactor-based and an LPSS cold neutron spectrometer. The LPSS instrument can map areas in Q-ω space where Q is along a selected symmetry direction in a single crystal. This requires a multicrystal analyzer in which the final energy can be varied independently for each crystal analyzer as on PRISMA at ISIS. The reactor-based instruments on the other hand can map out a 2-dimensional zone in reciprocal space at a fixed value of the energy transfer and does not require the settings of each analyzer crystal to be varied independently.

Conclusions

The Inelastic Scattering Working Group, composed of reactor and short pulsed spallation source instrument specialists, were on the whole encouraged by possibilities offered by LPSS for neutron spectroscopy. Cold neutron instruments, in particular, offer opportunities for scientific applications which would be an advance on present-day facilities by up to a factor of 3. Set against these gains must be the inevitable advance in instrumentation which would take place elsewhere in the realisation phase of the LPSS project, although any general advances in techniques would feed through into the design of all instrumentation. There is a distinct lack of such facilities in the USA and even level pegging instruments which are able to open up investigations into complex chemical problems and materials science as well as more esoteric investigations must be regarded as attractive.

FUNDAMENTAL NEUTRON PHYSICS AT A 1 MW LONG PULSE SPALLATION NEUTRON SOURCE

Fundamental Physics Working Group Report

Geoffrey L. Greene (NIST), Chairman

Introduction

Modern neutron sources and modern neutron science share a common origin in mid twentieth century scientific investigations concerned with the study of the fundamental interactions between elementary particles. Since the time of that common origin, neutron science and the study of elementary particles have evolved into quite disparate disciplines. The neutron became recognized as a powerful tool for the study of condensed matter with modern neutron sources being primarily used (and primarily justified) as tools for condensed matter research. The study of elementary particles has, of course, led to the development of rather different tools and is now dominated by activities carried out at extremely high energies. Notwithstanding this trend, the study of fundamental interactions using neutrons has continued and remains a vigorous activity at many contemporary neutron sources. This research, like neutron scattering research, has benefited enormously by the development of modern high flux neutron facilities. Future sources, particularly high power spallation sources, offer exciting possibilities for the continuation of this program of research.

The scientific content of this research, which has come to be known as "fundamental" neutron physics, has important implications for particle physics, nuclear physics, astrophysics, for tests of fundamental phenomenology, for the determination of fundamental constants and for the investigations of the underlying symmetries of nature. In addition to their scientific importance, activities in this field have led to a variety of technical developments that have found extensive utility in other neutron activities. Neutron guides, modern neutron polarizers as well as a variety of neutron detectors that originally developed as a consequence of "fundamental" neutron activities are now widely employed at all modern neutron sources. Continuing instrumentation developments, which may be expected to have a significant impact on materials science studies, include novel methods of neutron polarization (based on optical pumping of ^{3}He) as well as intense sources of extremely low energy neutrons (UCN).

In anticipating a program of "fundamental" neutron physics at a 1 MW Long Pulse Spallation Source (LPSS) it is useful to note that the character of such research is qualitatively different from typical neutron scattering activities and condensed matter research. While most neutron scattering measurements use installed, fixed instruments (perhaps with some modification), fundamental neutron physics experiments often employ rather complex apparatus specifically constructed for *one measurement*. With rare exceptions, the support for the construction and operation of apparatus is provided by "outside" funding and is not directly provided by the neutron facility itself.

The fundamental neutron physics community is broadly diverse and reflects the interdisciplinary character of the field. Quite often, an experiment in this field arises from the realization that an

interesting problem, perhaps in astrophysics or particle physics, is best addressed, or is only addressable, at an intense neutron source. This insight is likely to develop among researchers outside the traditional neutron physics community. It is not uncommon for projects in this field to be "technique" driven in that they develop through the realization that a method from some other field can be applied to neutrons with good effect. There have, for example, been very fruitful interactions with the atomic physics, optics and low temperature physics communities. An intense neutron source should be viewed as an important resource for the broad scientific community. This contact with a very broad scientific community has very important positive implications for the tenor of scientific and technical activities that may be expected at a 1 MW long pulse spallation neutron source. A vigorous program in fundamental neutron physics at a 1 MW LPSS will encourage important scientific connections with an extremely broad scientific community.

As an aid in the review of this area of research, it is convenient to divide fundamental neutron research into two categories. The first, *fundamental and particle physics with cold neutron beams*, is concerned with elementary particle physics, tests of fundamental symmetries and the determination of fundamental constants using neutron beams. The second, *particle physics with stored ultra-cold neutrons*, concerns research with neutrons of sufficiently low energy that they can be "trapped," held and studied in material bottles for long periods (i.e. many minutes).

Several recent workshops have been held with the specific purpose of assessing the prospects for this type of research at future neutron sources [1, 2]. In addition, a detailed review of these scientific possibilities has been prepared [3]. The interested reader is referred to these summaries (and the references therein) for further information.

Fundamental and Particle Physics with Cold Neutron Beams

Fundamental research with cold neutron beams includes a rather considerable variety. This section will present only a brief survey of the field. More detail is readily available in the form of the proceedings of a series of international workshops and conferences[4, 5, 6 7] that have been devoted to this work.

In general, there are two reasons why cold neutron beams are well suited to the study of the neutron and its fundamental interactions. Experiments which measure static neutron properties (including decay properties) or which measure the interaction of free neutrons with laboratory fields typically benefit from the (relatively) long observation times (of flight) that are available with low energy neutrons. Experiments that require spin polarized neutrons profit from the relative ease with which intense cold beams can be polarized with high efficiency.

Accurate values for the properties of the free neutron, determined using cold neutron beams, have implications in a variety of fields.[1] The determination of the neutron magnetic moment can shed light on the quark structure of the nucleus. Limits on the neutrality of the neutron reflect on the more general question of the neutrality of matter and indirectly on the gauge invariance of the electromagnetic interaction. Measurements of the correlations in free neutron decay can shed

[1]Except where specifically appropriate, references will be restricted to the citation of reviews and conference proceedings in which more complete bibliographies may be found.

light on the origin of parity and time reversal symmetry violation as well as providing important information on the nature of semileptonic weak interactions. Measurements of the neutron beta decay lifetime are useful for detailed tests of the standard model of the weak interaction and provide a parameter of great importance in astrophysics and cosmology. The measurement of selected neutron cross-sections is important for stellar astrophysics, for the understanding of the details of the standard solar model and for the solar neutrino problem. Measurements involving polarized neutrons have been used to shed light on the details of the weak interaction between quarks. Another interesting program of research carried out over the last decade concerns the search for a baryon non-conserving "oscillation" between the free neutron and its antiparticle, the antineutron.

To date, investigations such as these have been carried out at high flux reactors rather than spallation sources. This reflects the need for cold beams of very high intensity. A spallation source with a flux of a few $\times 10^{14}$ $cm^{-2}s^{-1}$ would provide beams which beams of considerable interest. It has been suggested that some experiments could take advantage of the time structure of the spallation neutron pulses to reduce parasitic backgrounds.

Particle Physics with Stored Ultra-Cold Neutrons

Measurements of the neutron electric dipole moment (d_n) and the beta decay lifetime of the neutron (τ_n) which are possible using UCN [8, 9, 10], have proved to be extremely valuable in achieving a better understanding of the nature of fundamental forces and, in particular, the symmetry breaking components of those forces. The neutron is now viewed as a composite structure comprised of quarks and gluons bound together by the "strong interaction." In spite of the neutron's electric charge neutrality, this composite structure manifests itself in a non-zero neutron magnetic moment. Neutron interactions are also influenced by the "weak" force, which although its strength is 10^{-7} times that of the strong force leads to neutron beta decay. The weak force has a "handedness" which implies a violation of parity symmetry, P. As far as we know, this is not the case for the strong and electromagnetic forces. The relative "weakness" of the weak force is responsible for the relatively long neutron lifetime of approximately 888 ± 2 *s*.

In 1964 experiments on the decay of the K° mesons revealed another even weaker effect that violates both parity and time reversal symmetry, T. A force, which is perhaps 10^{-12} times the strength of the strong force, would also be expected to play a role in the internal structure of the neutron. In view of this minute strength, it is perhaps not surprising that other manifestations of this force have so far proved to be elusive. Thus, it has been difficult to develop a theory or indeed to even determine whether it is a new interaction or simply a novel manifestation of other interactions. The simplicity of the neutron makes it an attractive laboratory for the study of T violation.

The P and T breaking symmetry properties allow the possibility of permanent electric dipole moments (EDM's) in elementary particles. Naively we may anticipate that the size of the neutron EDM *may* be $d_n \leq 10^{-2}$ times the diameter of the neutron. That is, $d_n \leq 3 \times 10^{-26}$ *e cm* (It should be noted that the current, most widely favored explanation for the T violation predicts much smaller effects, with d_n being 5–7 orders of magnitude less). From experiments with stored UCN the present 1σ error is 4×10^{-26} *e cm*. There is a strong incentive to improve this precision.

The weak force with a relative strength of 10^{-7} is more accessible and consequently it is much better understood. It exists by virtue of exchange of the known heavy W^+, W^- and Z^0 particles and it is related in detail to the electromagnetic force in the "electroweak" theory. Beta decay is its most direct manifestation at low energies and the decay of the neutron is the simplest case for which quantitative low energy measurements can be made. The neutron lifetime, τ_n, and the asymmetry parameter for the correlation between the decay electron momentum vector and the neutron spin direction furnish simultaneous, linearly independent inputs that can be solved for the parameters g_V and g_A, which represent the strengths of the vector and the axial vector parts of the weak force for the nucleon. The same value of g_V, with some small corrections, will apply to all nuclear beta decays and to the decay of the muon. The shortage of precision in the neutron measurements has frustrated the pursuit of the finer details of this theory. In the last five years measurements with stored UCN have improved the precision of τ_n by nearly an order of magnitude and there has been improved consistency among different experiments. In the future, the asymmetry parameter may also be measured using UCN. Further improvements by a factor of 10 are highly desirable for both quantities as they will then provide one of the most stringent tests of the standard model for the weak interaction.

Compared with thermal and cold neutron speeds of approximately 2000 m/s and 500 m/s respectively, UCN have speeds less than about 6 m/s. They are characterized by the fact that they can be stored in "bottles" with material walls (or confined by laboratory magnetic fields). During storage they steadily disappear from the bottle due to beta decay and loss processes involving nuclei in the wall surface. Average storage times of hundreds of seconds can be obtained with clean, room temperature walls of suitable materials. During storage the neutrons continually bounce between the walls of the storage vessel, reflecting elastically from the walls and may cross the bottle many thousands of times before being lost. Observation times for individual neutrons in UCN experiments may be hundreds, or even thousands of seconds. This may be contrasted to observation times that are restricted to tens of milliseconds for cold beam experiments. This huge advantage is partly offset by lower counting rates, but the net improvement in precision can still be several orders of magnitude. In addition, UCN storage vessels can be displaced by several meters from the source line of sight. This results in very low background conditions. Nonetheless, the low absolute count rates associated with all UCN measurements to date have resulted in nearly all experiments being limited by counting statistics. All UCN measurements will therefore profit from higher UCN densities. Indeed, it is likely that the most exciting prospects for fundamental neutron physics at a 1 MW spallation source will involve the use of UCN. As will be discussed below, there are intriguing prospects for a new class of UCN source which is particularly well suited to a LPSS.

At present, the most intense source of UCN in the world is at the Institut Laue-Langevin (ILL). The number density of UCN up to the speed of 6 m/s at the output of the turbine blades is about 80 cm^{-3}. Another intense source is that at the WWR-M reactor of the Petersburg Nuclear Physics Institute (Russia) where the density is about five times less, reflecting the comparably lower source thermal neutron flux. These sources have been in use since 1986 and there are no immediate plans for more intense sources at these institutions. Both of these sources are "thermal" in character in that the UCN which are extracted correspond to that portion of a thermal Maxwell-Boltzman distribution near zero energy (the UCN regime). This total phase space in this regime is only a minute fraction of the total neutron density (on the order of 10^{-13}).

The UCN density is a strong function of moderator temperature (proportional to T^{-2}). Practical considerations limit the temperature of a fully moderated source to a few tens of Kelvin. Thus, in the absence of the availability of new neutron sources with greatly increased fluxes, no significant increase in the UCN density from thermal sources appears feasible.

The production of UCN is not limited to thermal sources alone. So called "super-thermal" sources utilize processes (typically downscattering by phonons) which are not limited by the Maxwellian phase space density. In such sources, the neutron energy distribution is NOT in thermal equilibrium with a moderator. This thermal disequilibrium results from very different rates for the production and loss of UCN. The production of UCN occurs when a thermal (or cold) neutron creates a phonon which has an energy equal to the kinetic energy of the neutron (thus leaving the neutron in the UCN regime with nearly zero kinetic energy). The rate for this process depends upon (in addition to other parameters) the phase space available for phonons having energies comparable to thermal neutron energies. The "loss" rate of UCN in the moderator (ignoring capture) results from the excitation of a UCN by absorption of a phonon. This rate is determined by the density of those phonons, in the moderator, capable of transferring energy to a UCN. It is important to note that these two rates can be vastly different. This production method has been demonstrated for several moderators [10]

A particularly exciting prospect for a 1 MW spallation is a proposed superthermal UCN source based on a solid D_2 down-converter maintained at approximately 5K[11]. Such a source might produce a continuous UCN flux with densities approaching 10^4 UCN cm^{-3}. This technology, offering the possibility of a two order of magnitude increase in UCN density, would truly revolutionize the field of ultra cold neutron research. Such a source, if shown to be practical, could lead to very significant advances in fundamental neutron research and could, as well, open a variety of opportunities for the study of materials with UCN.

Summary: Unique Opportunities for Cold and Ultracold Neutron Physics at a 1 MW LPSS

The development of intense neutron sources has seen the parallel development of a rich research program in which the neutron (and its fundamental interactions) are the object of study. This research, employing a rather wide variety of experimental approaches and techniques, has produced results of importance in particle physics, in nuclear physics, in the determination of fundamental constants, in astrophysics and in the study of fundamental quantum phenomenology. While the scope and sensitivity of this research has expanded with the refinement of measurement techniques, it is a particular characteristic of this area of study that advances in both the quality and quantity of results follow directly from improvements in source intensity.

A 1 MW spallation source provides a unique and potentially extremely valuable facility for the investigations discussed above.

- The pulse structure can be useful to a number of fundamental physics experiments which are performed on cold neutron beams. For example, in the study of the neutron-nucleon weak interaction through the measurement of neutron spin rotation, time-of-flight (TOF) can be used to determine the rotation angle as a function of neutron energy. This is of

crucial importance in regard to systematic tests and is not possible without a crippling loss of intensity at a continuous beam facility. TOF techniques are also useful, for example, in determining the efficiency of ^{3}He polarizers as a function of incident neutron energy and precise determination of neutron polarization.

- The ability to place cryogenic apparatus near the cold moderator of a spallation source can be exploited to provide extremely high densities of Cold and Ultracold neutrons, exceeding that of existing sources by orders of magnitude. Such close placement in a reactor is probably impractical, primarily because of reactor physics and safety questions, and because of radiation heating of and damage to the cryogenic apparatus.

- As has been proposed, providing a large solid angle view at close range to a spallation source liquid D_2 moderator will provide a unique opportunity for new Cold, Verycold (VCN), and Ultracold neutron sources. Such moderator access can be used directly for a source of 20–50 Å neutrons. *At present there is NO existing source for such neutrons.*

- Use of a thick D_2 target has been suggested as a UCN and VCN source, and such a target placed near a spallation source moderator would provide a continuous source exceeding the intensities of existing sources by orders of magnitude. Construction of such a source would, for example, make long wavelength neutron scattering, as has been applied only sporadically and in demonstration, a truly useful tool for condensed matter research. Such scattering probes a unique region of $\omega - Q$ space, particularly useful to large biological systems. This source would also provide UCN and VCN for a number of experimental investigations as described in the references, all of which benefit from the increased intensity.

- Use of inelastic scattering of 8.9 Å neutrons in superfluid ^{4}He has been suggested for a non-steady state source of UCN and is particularly applicable to neutron lifetime or electric dipole moment measurements. By placing 5 liters of superfluid ^{4}He in close proximity to a spallation source liquid D_2 moderator, it might be possible to collect up to 10^9 UCN in a 900 second accumulation period. Use of such a source for measurements performed directly in the superfluid bath have been described, specifically in regard to the neutron lifetime and to the neutron electric dipole moment where one or more orders of magnitude might be eventually possible. Close access to a spallation source moderator will allow this techniques to be developed to their fullest potential. The performance possibilities at a spallation source appear significantly better than those at a 50 MW reactor of the ILL class.

References

[1] D. L. Price and J. J. Rush, editors, *Neutron Sources and Applications*, Department of Energy Report DOE/ER-0607P, 1993.

[2] G. Aeppli and B. Brown, editors, *Technology and Science at a High-Power Spallation Source*, Argonne National Laboratory, 1994, US Government Printing Office publication 1994-547-499.

[3] A. Michaudon, editor, *Basic Physics with Spallation Neutron Sources*, Los Alamos National Laboratory, 1994, Los Alamaos National Laboratory Report LA-UR-94-1320.

[4] T. von Egidy, editor, *Fundamental Physics with Reactor Neutrons and Neutrinos*, Institute of Physics, 1977.

[5] B. Desplanques, F. Gonnewein, and W. Mampe, editors, *Proceedings of the Workshop on Reactor Based Fundamental Physics*, J. Physique Colloque **C3**, 1984.

[6] G. L. Greene, editor, *The Investigation of Fundamental Interactions with Cold Neutrons*, National Bureau of Standards Special Publication 711, U.S. Government Printing Office, 1986.

[7] D. Dubbers, W. Mampe, and K. Schreckenbach, editors, *Proceedings of the International Workshop on Fundamental Physics with Cold Neutrons*, Nucl. Instr. and Meth. **A284**, 1989.

[8] L. Koester and A. Steyerl, *Neutron Physics*, Springer-Verlag, 1977.

[9] V. K.Ignatovich, *The Physics of Ultracold Neutrons*, Clarendon Press, Oxford, 1990.

[10] R. Golub, D. J. Richardson, and S. Lamoreaux, *Ultra-Cold Neutrons*, Adam Hilger, 1991.

[11] A.Serebrov, V.A. Mityukhlyaev, A.A.Zakharaov, V. V. Nesvizhevsky, and A. G. Kharitonov, JETP Lett. **59**, 757 (1994).

Contributed Papers

FROM REACTORS TO LONG PULSE SOURCES

F. Mezei

European Chair, Department of Atomic Physics, Eotvos University, Budapest,
and Hahn–Meitner Institut†, Glienicker str. 100, D—14109 Berlin

Abstract

We will show, that by using an adapted instrumentation concept, the performance of a continuous neutron source can be emulated by one switched on in long pulses for only about 10% of the total time. This 10 fold gain in neutron economy opens up the way for building reactor like sources with an order of magnitude higher flux than the present technological limits. Linac accelerator driven spallation lends itself favorably for the realization of this kind of long pulse sources, which will be complementary to short pulse spallation sources, the same way continuous reactor sources are.

Introduction and Overview

Neutron scattering has proven itself in the past four decades as one of the several indispensable tools in the research of condensed matter – including chemistry, solid state and liquid state physics, material science, molecular biology – as it was high-lighted by the 1994 physics Nobel prize awarded to two founders of the field, Cliff Shull and Bert Brockhouse. With the advent of very high intensity X-rays provided by synchrotron radiation facilities the complementary of neutron and X-ray scattering methods remains as valid as it ever was, with the borderline between these two fundamental microscopic probes shifting somewhat in view of the new capabilities offered by synchrotron radiation intensities, e.g., inelastic scattering at the higher thermal and epithermal energies. The tremendous development of other complementary methods also calls for increasing the power of neutron scattering, which primarily implies improving the source flux. Much of the neutron scattering work has been and is being done on sources not primarily dedicated to neutron scattering or only rebuilt, refurbished or modified for this purpose, sometimes as a parasitic usage. The very few facilities built from the outset for neutron scattering as primary goal (e.g., HFBR at Brookhaven, the ILL reactor and the IBR-2 pulsed reactor at Dubna) come rather close to the technical limit of reactor technology, basically limited by the power density of heat production in the core. Indeed, the about factor of 4 increase of the power density over the 1.5 MW/l value of the ILL reactor, as planned in the recently abandoned Advanced Neutron Source (ANS) project, proved to be so expensive that some 4 ILL reactors could be built for the same price. This leaves us with the only feasible way to progress: to give up continuous (CW) reactor sources for the future and to turn to another approach.

Neutron generation by spallation offers a possibility of generating considerably less heat per fast neutron produced than fission (actually about 6 times less taking into account that from the 2.45 neutrons emitted per fission in ^{235}U 1.4 are necessarily reabsorbed by the fissionable nuclei in order to maintain the chain reaction.)

†Permanent address.

Another way of reducing the heat load per useful neutron flux on the sample is to make use of a larger fraction of the moderated neutron spectrum. This is actually achieved by making the source pulsed, both with reactors (Dubna) and with spallation (IPNS, ISIS, LANSCE, KENS...). In actual fact, however, on these successfully operating pulsed sources the primary function of the pulse structure is to provide for sufficient resolution of the time-of-flight type neutron scattering instruments installed, hence the trend to make the pulses as short as feasible.

The main subject of the present paper is to analyze the potential gains in heat load per useful neutron flux offered by pulsed operation as opposed to CW operation. In order to achieve this, we will consider first the use of beam monochromatization techniques on CW sources, and it will be shown that adequate chopper systems (proposed to be named time-of-flight (TOF) monochromators) can efficiently, sometimes advantageously replace conventional CW monochromators also on continuous reactor sources. These monochromators only "look" at the source for a fraction of the time, so the source could be switched off between the short periods it is needed to be "on." This can be accomplished by a "long" pulse (pulse length in the ms range) operation, and the analysis of various standard neutron scattering techniques used on research reactors shows, that about 10–15% duty factor is sufficient to provide all of these instruments with the full flux corresponding to the "on" power of the source. This gain in the efficiency of utilization of the source power, together with the lesser heat load in case of spallation would provide us at the same heat load with 30–40 times higher effective neutron flux than a CW reactor source. (In actual fact the most efficient way of using the proton beam power in spallation is to use a target volume considerably smaller than the active zone of a reactor so that the optimal flux/power ratio is further improved somewhat.) The main problem with high power spallation sources becomes the radiation damage instead of the heat load, but the technical limits can be certainly stretched by the proposed "brute force" solutions such as liquid metal or rotating targets. So, as far as one can guess at this stage, long pulse spallation sources (LPSS) offer the technical possibility to emulate CW reactor type performance in neutron scattering applications with effective neutron fluxes some 50 times or more higher than that of ILL. This potential is by an order of magnitude out of reach for the stationary reactor approach and it represents a tremendous jump in performance if we compare it with the mere factor of 5 flux improvement achieved by now compared to the Chalk River NRU reactor (at which Bert Brockhouse accomplished part of his Nobel prize winning research) put into operation in 1957!

In the following chapters we will first consider the TOF-monochromator concept and some of its applications on CW sources. Than we will introduce a Long Pulse Source by the requirement of emulating a CW source for a set of TOF-monochromator instruments. Finally, as a new development since the workshop, we will show that the TOF-monochromator approach also allows us to improve the efficiency of inelastic TOF spectrometers on pulsed sources.

Neutron monochromators

In all neutron scattering experiments on a CW source a small, more or less precisely monochromatic fraction of the Maxwellian spectrum of the moderator is selected by eliminating the rest. Actually the precision of this monochromatization determines in nearly all cases the resolution of the experiment, with the exception of Neutron Spin Echo (NSE) and TOF Fourier

Diffraction. The clue of these Fourier methods is exactly the intensity gain offered by that they require poor monochromatization compared to the resolution offered. Unfortunately, such "simultaneous" methods, in which the signal from various wavelengths is detected at the same time and sorted out by in other modern experimental techniques standard signal processing methods (such as, e.g., in pulsed NMR) can only be used in a few special cases with neutrons, due to the inherent quantum noise of neutron signals. Namely neutron scattering spectra contain a very small number of quanta (neutrons) compared to microwave or light signals, for instance, so that the statistical Poisson noise is inevitably large. In simultaneous data processing this leads to masking the low intensity part of the spectra, which contain the hard-to-observe pieces of the information. (This was the reason of the practical abandon of correlation spectroscopy, a promising idea from the 1960's).

There are basically three types of successful monochromator devices used on CW sources, none of them without substantial drawbacks though. Crystals transmit not only the desired wavelength λ, but higher orders $\lambda/2$ and/or $\lambda/3$, etc. too, which has to be most often removed by a filter. Furthermore, the reflectivity of many crystal monochromators is considerably less than 100% and the resolution curve shows up long tails. The optimal adjustment of the resolution, requiring a set of exchangeable crystals, is of limited flexibility. Last but not least, crystals also display other scattering processes than Bragg reflection. This often leads to "spurion" signals, which are time consuming and not always easy to be sorted out. Helical slot velocity selectors suffer from none of these drawbacks of crystal monochromators, but they cannot provide comparable resolution due to mechanical limitations of the speed of rotation. Actually their are limited to some 5% best resolution and this for cold neutrons only. In contrast to these two continuous beam, (CW) monochromators, disc chopper systems of the type of IN5 at ILL provide a clean, tunable beam and to crystals comparable resolution, but only for a fraction of the time with duty factors around 1% or less. Such a pulsed monochromatic beam is fine for TOF inelastic spectroscopy, but for nothing else.

The idea of TOF – monochromators is just to use disc choppers systems in a way that they produce useful, monochromatic neutrons for nearly all the time i.e. with a duty factor close to 100%. The idea goes back to the very old proposal of TOF diffraction by Buras [1] which, however, could not guarantee useful beam availability for most of the data collection time.

In a neutron scattering experiment on a CW source one starts with choosing an optimal incoming neutron wavelength. This choice is never a unique, single value, it is rather one of many equivalent ones within a given more or less broad wavelength band. Conventionally a single wavelength within this "useful band" is selected for extended data collection periods. In many cases the best compromise between intensity, resolution and dynamic range requirements is, however, achieved by dividing the beam time between runs with several incoming wavelengths within the useful range.

A TOF-monochromator provides a monochromatic beam at any instant of time t with a wavelength $\lambda(t)$ and a resolution $\delta\lambda(t)$, with $\lambda(t)$ and $\delta\lambda(t)$ periodically changing in time following a sawtooth pattern within a band $\lambda_{max} - \lambda_{min} = \Delta\lambda$. Thus instead of using one single wavelength the measurement is performed with a set of wavelengths stretching a range $\Delta\lambda$ which is chosen to be fully within the "useful range" so that each wavelength $\lambda(t)$ provides roughly equally useful information. Fig. 1 illustrates how this can be realized with a set of disc

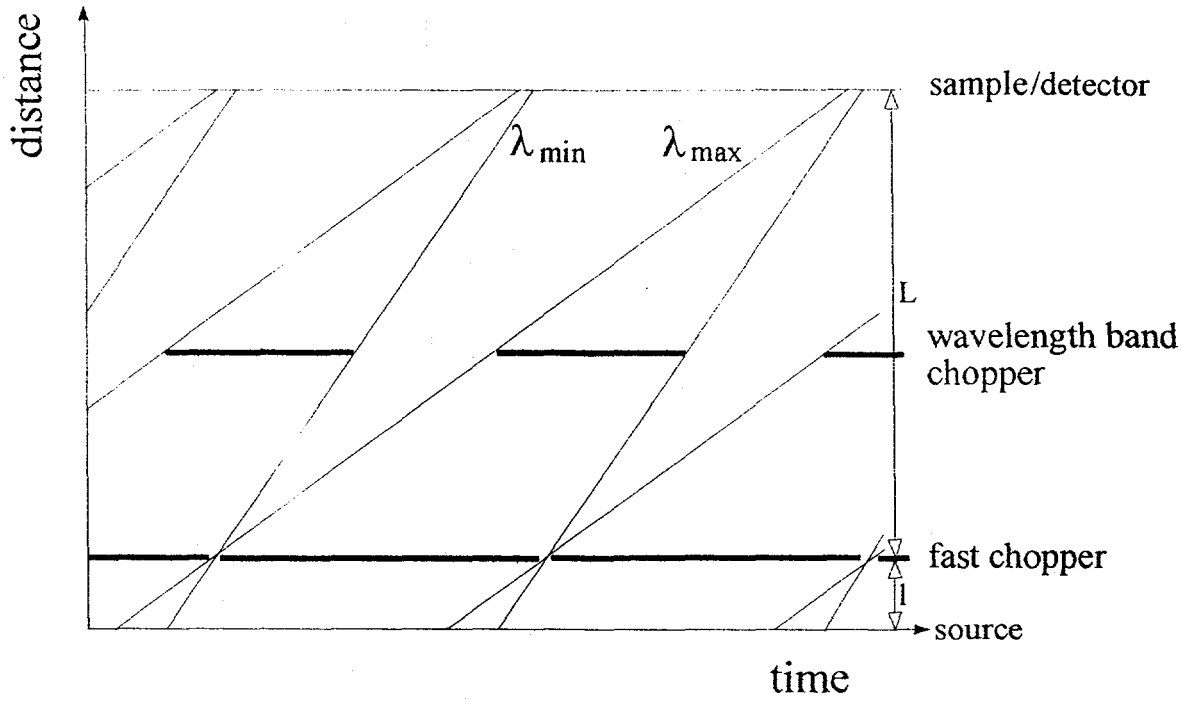

Fig. 1. The principle of TOF monochromators, after Ref. [2].

choppers. On this distance vs. time TOF-diagram the trajectory of an incoming neutron is a straight line with the slope corresponding to the velocity $v = h/m\lambda$.

The essential point is that the TOF monochromator delivers useful neutrons for nearly all the time onto the sample and maintains all the advantages of chopper systems (no higher orders, clean, well defined lineshape without tails, tunable resolution, 100% transmission at the center of the line) compared to crystals. The price to be paid for is the more complex data collection (i.e., adding the additional parameter t which labels the various wavelengths $\lambda(t)$ used and combining the information content of data sets corresponding to a set of single wavelength bins $\lambda_1, \lambda_2, \lambda_n$). This complexity is, however, rather small compared to state-of-the-art methods in, e.g., nuclear physics, and to a large extent well under control on existing spallation sources.

The clue to making the whole wavelength band of a TOF-monochromator uniformly useful is to make it narrow enough. In some cases, e.g., TOF-diffraction, this restriction is rather mild since the relevant intensity parameter $\lambda^4\phi(\lambda)$ is flat over a large range of λ (where $\phi(\lambda)$ is the quasi-Maxwellian neutron flux distribution of the moderator) [1]. In other cases, such as triple-axis spectroscopy, where one wants to concentrate on a small range of momentum and energy transfer $\vec{q}$ and ω, $\Delta\lambda$ might be chosen as small as 20%. We will show now, that under the condition of selecting an uniformly useful wavelength band (λ_{min}, λ_{max}) the time averaged flux produced by the TOF monochromator at the sample is equal to that of CW-monochromator (assuming equal resolution, beam collimations and neglecting losses such as finite crystal reflectivities, filter absorption etc.) [3]. Indeed:

$$\Phi_{CW} \cong \phi(\lambda)\delta\lambda \qquad (1)$$

and

$$\Phi_{TOF} = c\phi(\lambda)\Delta\lambda \tag{2}$$

where c is the duty factor of the fast chopper in Fig. 2, and it is given as c = $\delta t/\Delta t$, i.e. the ratio of the chopper opening time δt to the pulse repetition time Δt. On the other hand

$$\delta\lambda = \frac{h}{m}\frac{\delta t}{L} \quad , \quad \Delta\lambda = \frac{h}{m}\frac{\Delta t}{L} \tag{3}$$

where L is the neutron flight path from the fast chopper to the detector or – in inverted geometry inelastic experiments — to the sample. Thus we find that

$$c = \frac{\delta t}{\Delta t} = \frac{\delta\lambda}{\Delta\lambda} \tag{4}$$

Substituting (4) into (2) and comparing to (1) we get the mean flux (MF) theorem:

$$\Phi_{TOF} = \Phi_{CW} \tag{5}$$

i.e., that the time averaged flux on the sample for the TOF monochromator is the same as that for the conventional CW monochromator of equal resolution (for equal beam collimations and neutron transmission efficiencies) if the wavelength band $\Delta\lambda$ is uniformly useful.

The second half of the previous sentence is the crux of the matter. Without making the band $\Delta\lambda$ narrow enough, i.e., working with just one fast chopper and making the repetition rate small enough so that there is no frame overlap between the fastest and slowest neutrons from contiguous pulses (as originally proposed by Buras or actually done on short pulse spallation

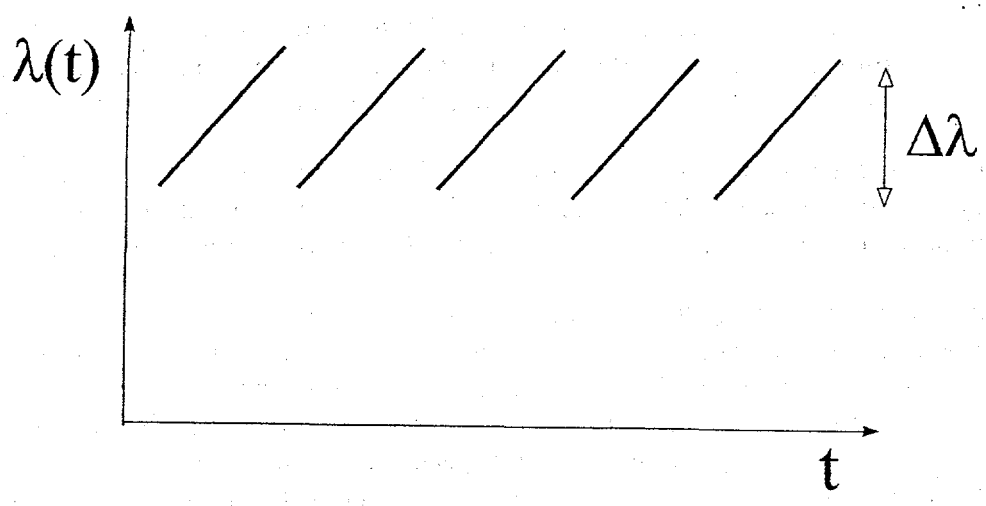

Fig. 2. Time dependence of the wavelength of the monochromatic beam in a TOF monochromator.

sources) $\Delta\lambda$ is not uniformly useful. One reason for this is the strong wavelength dependence of the Maxwellian distribution $\phi(\lambda)$ with eventually the low intensity parts contributing little to the information gathered. Also the strongly λ dependent resolution might limit the usable range. Thus a narrow enough $\Delta\lambda$ is a guarantee to make it all fully useful, which can be achieved by making L long enough and/or Δt short enough. (This latter applies to a CW source, where the chopper system can have any repetition rate mechanically feasible.)

TOF Monochromator instruments on CW sources

As already noticed early on by Buras, powder diffraction is a favorable case for TOF analysis. In this special case one can very efficiently work with surprisingly large $\Delta\lambda$. This is due to the fact that due to the Lorentz factor and the wavelength dependence of the cross section [1] the effective flux distribution is $\lambda^4\,\phi(\lambda)$, which is a very flat function between 1.5 and some 5 Å for a thermal beam. (Using a chopper system which produces a pulse length δt proportional to λ [2, 4], similarly to the moderator pulse length in the slowing down regime on an SPSS, we get $\lambda^5\phi(\lambda)$, which is even flatter.) Thus the TOF monochromators are particularly well adapted to powder diffraction work on CW sources and actually a performance considerable superior to the conventional crystal monochromator approach is expected on the basis of detailed quantitative analysis [5, 6]. Of course the MF theorem rules out, that either the TOF or the CW monochromator methods directly provides superior neutron intensity. The advantages of the TOF method in this case are physically explained by the difference between performing the whole experiment with a single wavelength (conventional crystal monochromator technique) or using a wide spread of wavelengths within the same total measuring time. This latter can offer an order of magnitude higher counting rates on a CW source due to the more favorable resolution conditions [5]. Let us stress here that in the TOF approach the wavelength band $\Delta\lambda$ as defined in eqs. (3) and determined by the particular chopper – instrument configuration is only a lower limit of the wavelength band used in an experiment. By varying the phasing between the fast chopper and the wavelength band choppers one has the freedom inherent to the method to shift this band $\Delta\lambda$ over the whole available wavelength spectrum.

The choice of $\Delta\lambda$, once narrow enough in order to make the simultaneously observed wavelength band (cf. Fig. 1) fully useful, is immaterial for the neutron economy: smaller $\Delta\lambda$ means higher duty factor c, i.e. no effect on the time averaged flux on the sample, cf. eqs. (2) and (4).

Besides neutron diffraction triple-axis-spectroscopy (TAS) and its special case, back-scattering spectroscopy (BS) are the other CW techniques relying on crystal monochromators. We will now show that in most cases TOF monochromators can be effectively or advantageously used instead.

The most important feature of the TAS method is that it allows one to concentrate the data collection time to a small domain of the ($\vec{q}$ ω) space, which is deemed to be only interesting in a given experiment. In comparison, in the tremendous 2 dimensional data set of a conventional TOF inelastic spectrometer with many detectors (typically 50.000 bins) each bin corresponds to a different $\vec{q}$, i.e., to a different point in the ($\vec{q}$ ω) space. Thus collecting a "constant q scan" on a single crystal sample requires a different run with a different orientation of the sample for each point in the scan and the counting efficiency compared to a TAS instrument with comparable resolution is reduced by the duty factor of the chopper, i.e., to ~1%. (For polycrystalline and

amorphous samples one can collect all the $|\vec{q}$ = const points from the TOF data sets, which improves the data collection rate by a factor roughly corresponding to the number of ω points required. If, in addition, several $|\vec{q}$ values are to be studied, a larger fraction of the simultaneously collected TOF data set becomes useful and the data collection rate rapidly exceeds that of the TAS machines.)

We can replace the crystal monochromator of a TAS (or BS) instrument by a TOF monochromator, which will be designed for providing a narrow wavelength band, say $\Delta\lambda/\lambda \cong$ 20%, so that we can concentrate on a small region in ($\vec{q}$ ω) space. (Fig. 3.) This wavelength band can be considered as a set of incoming momenta $\vec{k}_1, \vec{k}_2 .. \vec{k}_n = 2\pi / \lambda_n$ separated by a constant δk comparable to the resolution. Our next task is to arrange a set of analyzer crystals with selected momenta $k_1, k_2, \ldots k_n$ for example so that (Fig. 4)

$$\vec{k}_i' - \vec{k}_i = \vec{q}_i \qquad i = 1, 2 \ldots n \tag{6}$$

give $\vec{q}_i = \vec{q} = \text{const}$ for a constant $\vec{q}$ scan. (The orientation of the sample remains a free parameter, so there is no restriction on the phonon polarization studied.) We can set for one i, say for i = 1 both $\vec{q}_1 = \vec{q}$ and ω_1 freely, as usual in TAS work. With k_i predetermined, this will fix all the other energy values ω_i. Thus we will collect constant $\vec{q}$ data all the time, corresponding to a set of ω values ω_i, i = 1, 2 ... n. If the (ω_1, ω_n) energy interval is fully within the desired constant q energy scan, all of theses ω_i points are useful (i.e., the data collection is fully efficient, eq. (5) holds). If the ω_i points do not cover the whole scan looked for, in a next TAS like step we collect an additional set of ω_i points. If the span of the desired scan is less than (ω_1, ω_n) the data collection efficiency will be reduced corresponding to the number of useful ω_i points.

At the same time, however, with the TOF monochromator we obtain, instead of a single one, a whole set of constant q scans by combining other k_i, k_i' pairs:

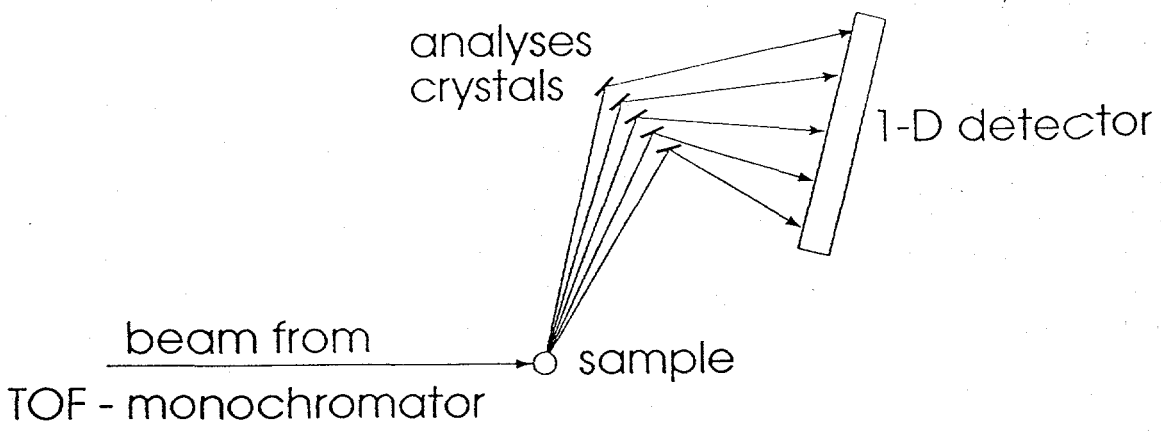

Fig. 3. Scheme of a triple-axis-spectrometer (TAS) with TOF monochromator.

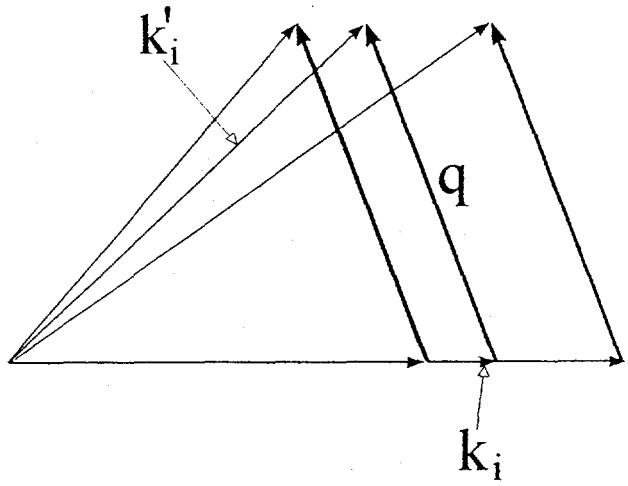

Fig. 4. Constant q scan on a TOF monochromator TAS instrument, cf. Fig. 3.

$$\begin{array}{ll} \vec{q}_1 = \vec{k}_i' - \vec{k}_{i+1} & \vec{q}_{-1} = \vec{k}_i' - \vec{k}_{i-1} \\ \vec{q}_2 = \vec{k}_i' - \vec{k}_{i+2} & \vec{q}_{-2} = \vec{k}_i' - \vec{k}_{i-2} \\ \vdots & \vdots \end{array} \qquad (7)$$

If one is interested in a set of constant q scans around a central value $\vec{q}$ (with $\vec{q}_l - \vec{q}$ being parallel to $\vec{k}$), this additional data points from the $(\vec{k}_i', \vec{k}_j)$ matrix contribute to an up-to an order of magnitude faster data collection rate by using the TOF-monochromator than by the conventional crystal monochromator single analyzer technique.

This kind of approach also has several precursors in the literature starting with a proposal from Poland [7]. The RITA-project from Riso [8] aims at using a set of several crystal analyzers and a crystal monochromator. In contrast to the above, constant $\vec{q}$scans cannot be simultaneously collected in this case. Inverted geometry crystal analyzer instruments on SPSS facilities operate much the similar way than the TOF monochromator TAS instrument described above for a CW-source, primarily PRISMA at ISIS [9].

In BS spectroscopy data collection is concentrated to a small ω range with a μeV or better resolution, but there is no restriction on the $\vec{q}$ variable. Therefore the monochromator only has to produce a very highly monochromatic beam, which can be easily achieved by disc chopper systems with a long chopper to sample distance: e.g., with 10 μsec pulse width and L = 80 m one has 0.3 μeV resolution at the usual wavelength around 6 Å. Apart from replacing the crystal monochromator system the rest of the spectrometer can be kept the same, including the usual 50% duty factor background suppression chopper in front of the sample (which can run either synchronously or asynchronously with the TOF – monochromator choppers). The substantial advantage of the TOF-monochromator is the flexibility it provides for selecting both the width and the center of gravity of the ω scan (the former one by adjusting the repetition rate of the TOF system.) This would extend the applicability of the method to much higher energy transfers (e.g., for the study of optical type excitations) than achieved by now.

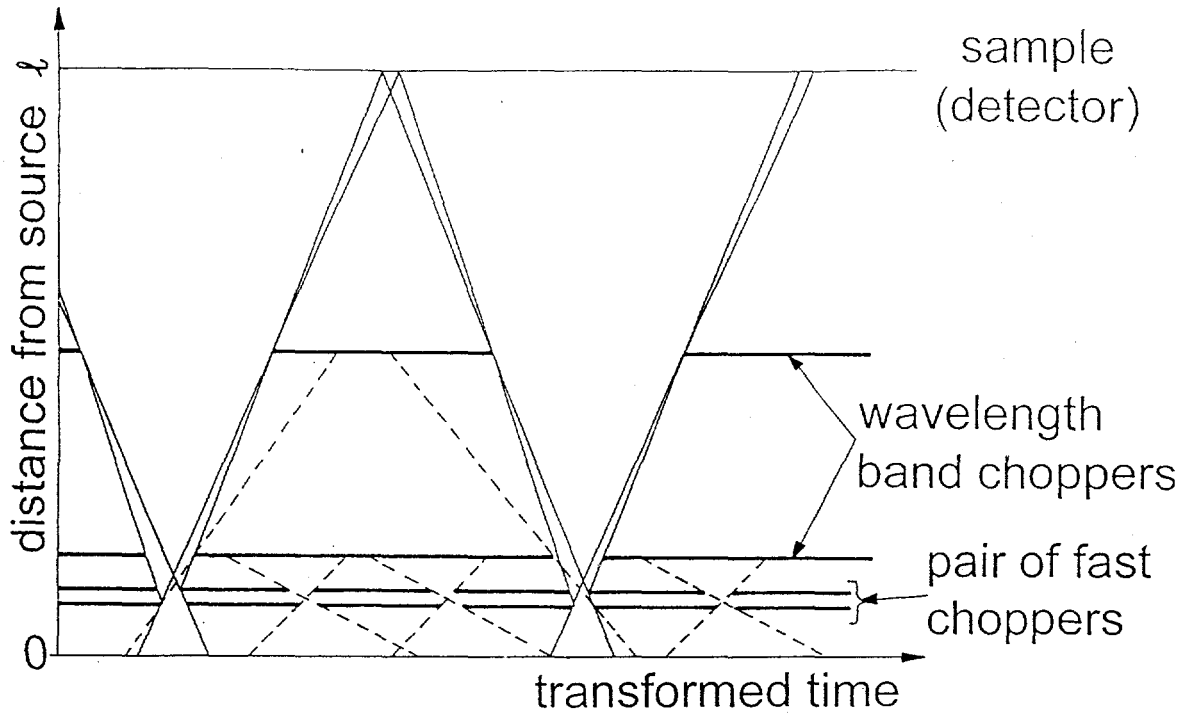

Fig. 5. *Scheme of a TOF monochromator chopper system. For easier representation a transformed time variable is used, which is measured relative to an average neutron velocity:* $t' = t' = t - l / v_o$

Finally let us note that a low resolution TOF monochromator can rather easily replace velocity selectors on small angle scattering (SANS) and NSE instruments with the potential benefits of providing better wavelength resolution, if needed, and an increased dynamic range, which latter can only be achieved now by combining a set of separate runs at different wavelengths. The option of using TOF as an alternative to the velocity selector has been installed on the new high resolution NSE spectrometer IN15, built at the ILL in collaboration with HMI, Berlin and KFA Jülich, will be soon tested in the course of commissioning of the instrument.

To conclude this chapter let us consider a few technical points of realizing TOF - monochromators. In general, one will need at least 4 disc choppers (Fig. 5.). The first two "fast" ones can either run in the opposite sense with narrow slits in order to produce the shortest pulses, or in the same sense with large slits in order to provide adjustable and eventually wavelength dependent pulse lengths. This pair of fast choppers placed at a few cm distance from each other also acts as a crude velocity selector with a pass band of some 4–20 Å width, which is an important feature for the leakage free design of the whole system. The repetition rate is defined by the first of at least two wavelength band choppers. The last of these choppers has to be not too far from the sample (less then half the sample to fast chopper distance) in order to reduce the penumbra at the beginning and the end of the wavelength frame. The time available for penumbra and frame-overlap free data collection can typically achieve 85–90% of the total data collection period.

Top of the line disc choppers can reach 500 m/sec peripheral speed, while 300–400 m/sec can be achieved at strongly reduced costs with light composite discs (carbon fiber, kevlar, etc.). These materials also have the great safety advantage, that the disc failure leading to its disintegration does not damage the vacuum housing of the chopper. The shortest pulse lengths can be obtained by counterrotating discs with slit width around 10 mm. (The height of the slits can be as much as some 10 cm.) By neutron optical phase space transformation methods one can squeeze neutrons transmitted in a 2–3 times wider neutron guide through an "eye-of-the-needle" slit [2] by using supermirror devices. Supermirrors and beam compression techniques [10] are also necessary to provide a reasonable vertical collimation, comparable to that of focusing crystal monochromators. As of today, large quantities of supermirrors can be produced by several laboratories and commercial manufacturers with a cut-off angle $2\theta_{Ni}^{C}$ and a few meters necessary for a beam "condenser" could be certainly obtained with $2\theta_{Ni}^{C}$ or more. Thus TOF monochromators can provide vertical beam divergences of at least $0.6^{\circ} * \lambda$, where λ is the wavelengths in Å units. The absence of reflectivity and filtering losses applicable to crystals essentially compensates for the reduced vertical focusing capability of TOF monochromators at shorter wavelengths.

The long distances one might wish to have between fast chopper and sample in order to improve resolution or reduce the wavelength band have to be bridged by neutron guides. The broad availability of supermirrors (20 years after their introduction) make by now feasible to build efficient guides for thermal neutrons too. The good transmission efficiency over a wide range of wavelengths is also essential, which can be achieved by a short supermirror reflector between two straight guide sections, as proposed by John Hayter [11], instead of the conventional curved guide approach.

In sum we can see, that recent technical developments, viz. light weight composite chopper discs, supermirror guides, neutron optical devices and new design concepts are essential pieces of the technology which allows us today to take full advantage of the benefits of some old ideas behind my present proposal of replacing crystals by TOF-monochromators on continuos neutron sources.

Long pulse sources

Beyond that they can advantageously replace crystals and contribute to the progress of instrumentation on CW reactor sources, TOF monochromators display a crucial property: they only need the neutron source to be switched on for a fraction of the total time (c.f. Fig. 1)

$$c_s = \left(\Delta t \frac{l}{L} + \delta t \right) / \Delta t = \frac{l}{L} + c \qquad (8)$$

where l is the distance from the source to the fast chopper. (Actually if the source pulse length is about equal or shorter than the chopper opening time δt required by resolution, there is no need for the fast chopper and we have to set $l = 0$ in eq. (8).) Thus, if we manage to shut off the source when it is not needed we gain a factor of $1/c_s$ in the actually very poor efficiency of utilizing the neutrons produced – without any loss in performance. Since heat production in the core is the

limiting factor, this means that $1/c_s$ times higher useful flux can be achieved by the same total power.

This leads us to the definition of a long pulse source: it is a pulsed neutron source with long enough, approximately uniform flux pulses so that the desired resolution can be achieved by methods also applicable on CW sources. This implies that the pulse lengths have to exceed considerably the time constant of the flux buildup in the moderator-reflector system.

It is interesting to note that one of the first neutron sources ever built for neutron scattering as the primary purpose, IBR-30 in Dubna, was a pulsed reactor, while continuous beam reactors are simple improved versions of earlier facilities built for the purpose of nuclear energy research. Clearly the pulsed option provides the better neutron economy, unfortunately pulsing reactors is not feasible at average powers of the order of 50 MW, so they can not represent the next generation of reactor sources with a gain factor $1/c_s \cong 10$. On the other hand, it is fully feasible to provide a similar long pulsed time structure with spallation by using, e.g., linac accelerators without pulse compressing storage rings.

The key problem in designing a long pulse source is to find a source duty factor c_s, which satisfies all instruments. (For the moment we will only consider TOF monochromator machines, IN5 type TOF-spectrometers will be considered in a separate chapter). In order to make full use of the "on" (peak) flux of the source, in view of the mean-flux theorem, we only have to fulfill eq. (4), i.e., other parameters such as repetition rate do not matter, in principle. However, choosing an ideal wavelength band $\Delta\lambda$ might require unreasonable distances, eq. (3), too short or too long, so this aspect is also of importance.

The following table shows the requirements of some experiments.

	$\delta\lambda$	$\Delta\lambda$	$c = \delta\lambda/\Delta\lambda$
SANS NES	~0.5 – 1Å	5 – 10Å	10 – 20%
TAS	0.05 – 0.1Å	0.5 – 2Å	3 – 10%
Diffraction	0.01 – 0.05Å	2 – 5Å	0.2 – 1%
High resolution diffraction	0.002Å	2 – 5Å	0.04 – 0.2%
BS	0.0006Å	0.5 – 2Å	$3 * 10^{-4} – 10^{-3}$

The hardest to fulfill is SANS, which actually sets the duty factor with $l = 0$ in eq. (6) to ideally not less then 10%. This choice of c_s satisfies all the others, but still there remains a compromise to be found to reconcile wavelength bands as different as 0.5 and 10 Å. This would imply a factor of 20 difference in instrument lengths L, which is not feasible. With 25 m, reasonably short source–detector total length, a SANS instrument can have $\Delta\lambda$ = 5Å at 30 Hz repetition rate,

which calls for a pulse length of about 3 msec in order to achieve c ≅ 10%. These parameters are fine for normal and high resolution powder diffraction, but they require some 100 m distance for a TAS or BS machine operating at 1.6 Å = $\Delta\lambda$ band width. 60 Hz repetition rate with 1–1.5 msec pulse length would be optimal for these too kinds of instruments, which would imply about a factor of two loss in SANS. The solution optimal for both cases would be a 60 Hz repetition rate with every second pulse of 3 ms length and the ones in-between 1 ms.

This optimization is valid under the boundary condition that the maximum peak current of the accelerator is given and it assumes of operating at an average power corresponding to $c_s \cong 12\%$ duty factor. Since it is much easier to achieve a given average current at a lower current and a higher duty factor, than the other way round this simplified boundary condition of getting the maximum out a given peak accelerator power is rather close to the real, complex constraints presented by accelerator technology. It has to be stressed that we only had to consider relatively modest compromises in looking for a source time structure suitable for all instruments types listed in the table above because we left out TOF-spectrometers and only took into account TOF-monochromator instruments. TOF-spectrometers only need neutrons for a very short time, typically 100 μs or less, but ideally require high repetition rates up to 300 Hz not feasibly with a linac accelerators and not compatible with the rest of the instrument. This problem was taken as an unsolvable one at the workshop. The reason I left TOF-spectrometers out here is that some new ideas described in the next chapter, which I came across after the workshop, essentially reconcile TOF-spectrometers with low repetition rate long pulses.

Repetition rate multiplication and constant $\vec{q}$ TOF spectroscopy [12]

We will show here, that some aspects of the TOF monochromator concept can also be applied to IN5 type multichopper TOF spectrometers, allowing us to run the instrument at a repetition rate up to 10 times higher than the that of the long pulse source. The key idea of the TOF-monochromator approach is that the same information can be obtained with using not only a single incoming wavelength, but a set of eventually close wavelengths λ_1, λ_2 ... λ_n and combining the information afterwards. Adding a fast chopper to the TOF monochromator set-up just in front of the sample with a repetition rate properly chosen for the TOF energy analysis in the secondary spectrometer and running synchronously with the source pulse and the TOF-monochromator, (i.e., with a frequency being the integer multiple of the that of the source) we get a set of short pulses with wavelengths λ_1, λ_2 ... λ_n, cf. Fig. 6. We obtain with each of these wavelengths a complete TOF spectrum of the sample, and the n spectra will carry essentially identical information if the total wavelength band $\lambda_n - \lambda_1$ is narrow, or eventually – and actually quite often – an improved data collection rate by extending the dynamic range of the data if $\lambda_n - \lambda_1$ is chosen to be substantial. Thus we arrive at an important generalization of the mean-flux theorem eq. (5) for the only case in neutron scattering not included there: the mean flux on the sample in a TOF spectrometer of any repetition rate ν installed on a TOF monochromator with a repetition rate ν/n (where n is an integer) is independent of n as long as the wavelength band $\lambda_n - \lambda_1$ is narrow enough

$$\Phi^{(\nu)} = \Phi_{TOF}^{(\nu/n)} \tag{9}$$

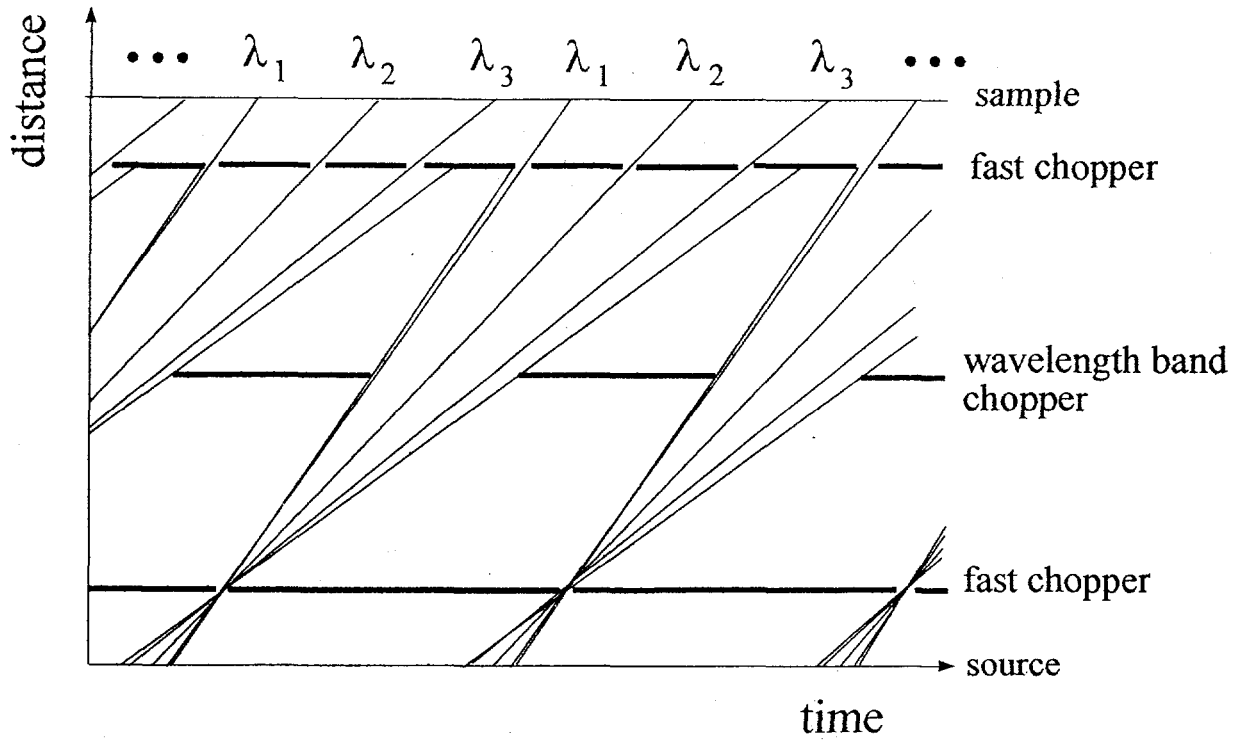

Fig. 6. Principle of TOF monochromator – TOF analyzer inelastic spectroscopy with repetition rate multiplication [12].

This idea was not available at the workshop, so the evaluation of the flux of the TOF-spectrometers as presented in this volume should be revised upwards by a factor of 2–5.

This TOF-monochromator – TOF secondary spectrometer combination offers another new possibility: constant $\vec{q}$ scans on single crystal samples on a single run using TOF technique only, a problem which was deemed to be unsolvable. Instead of phasing the fast chopper in front of the sample to the source – TOF monochromator system we let it run asynchronously, so that we get TOF spectra with a quasi continuous set of wavelengths (reasonably binned according to the resolution) within the $\Delta\lambda$ wavelength band, as we actually envisaged for the instruments discussed in previous chapters. The thus obtained 2 dimensional data set $I(\lambda_{in}, \lambda_{out})$ contains many constant $\vec{q}$ energy spectra in an extended 2 dimensional (with detectors covering a large vertical angular range, as usual, 3 dimensional) $\vec{q}$ domain. The method is mechanically simpler than the TOF monochromator TAS approach described above, although in principle it provides inferior data rates if a single or a small number a constant q scans are required due to the additional duty factor loss by the sample-end chopper. This disadvantage could be partially compensated for by the larger solid angles attainable with TOF and by having no reflectivity losses and higher order reflections in the analyzer system.

Conclusion

We have shown that by the use of TOF-monochromators one can get on the whole comparable and eventually more advantageous data collection rates in all types of neutron scattering experiments on a usual continuous reactor source than with the methods currently used. This applies both for cold and thermal neutrons, while the hot neutron regime is not relevant, since there continuous sources are at great disadvantage compared to short pulse spallation sources (SPSS) and this would not change with the use of TOF-monochromators. The crucial new feature of TOF monochromators is that they only need the source to be switched on for some 10% of the time, thus allowing us to save 90% of the source power or to increase the flux effectively seen by the instruments by a factor of 10 at equal power. Thus these sources simply are optimized neutron economy versions of continuous sources. This is the basic concept of long pulse sources. Practically the switching of the source on and off has to be done on the scale of a ms, which can be achieved by proton linac driven spallation.

We have compared here CW and LPSS sources by considering TOF-monochromator based instruments which are essentially identical on both types of sources. This instrumentation approach implies an increased degree of complexity in data processing and data analysis, which is not fully new, but not widespread in neutron scattering. (This complexity is still quite modest compared to the standards of accelerator experiments in nuclear or high energy physics.) Of course, TOF-monochromators represent just one possible instrumentation approach on LPSS, as they do on CW sources. From practical points of view, also including more traditional data analysis, the need to focus the experiment on a small enough region of the ($\vec{q}$, ω) space, or insufficient resolution, e.g., in backscattering with an improved resolution in the 0.1 – 0.2 μev range, etc. other instrumentation concepts will be preferred in a number of cases. The analysis based on TOF-monochromators meant to show that the theoretical limit, the peak flux, can be achieved under reasonable assumptions.

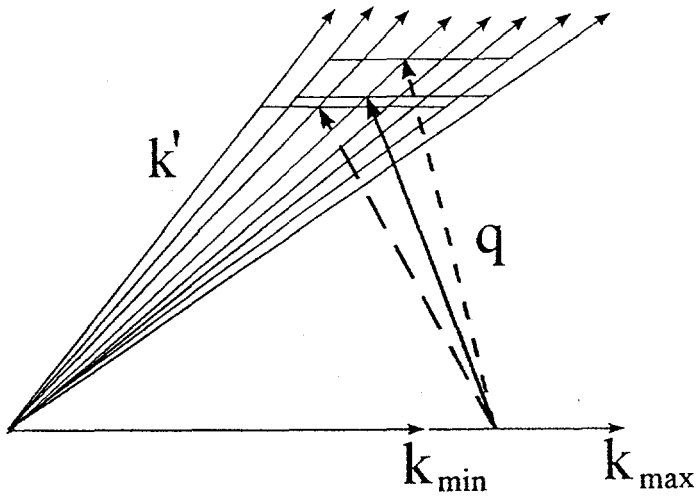

Fig. 7. Constant q scans on a TOF monochromator – TOF analyzer inelastic spectrometer. The horizontal bars at the end of the q vectors and equal to the incoming k band represent the constant q cuts across the quasi-continuous set of TOF data at various fixed angle detectors.

In comparing the performance of different kinds of neutron sources, one should consider sources which can be build for the same amount of money (actually the operational costs will come out rather similar, too.) Thus to build a reactor like that at ILL will cost about the same (in Europe, cf. the Munich reactor project) as a 1 MW SPSS with two target stations (cf. recent project studies in the US) or an about 4 MW single target station long pulse spallation source (extrapolation from the 1 MW projects and from preliminary results of the ESS study), i.e., about $500 M. At 4 MW average power with the 10% desirable duty factor the LPSS will display 40 MW peak power, i.e., thermal and cold fluxes, when switched on, equivalent to some 6 to 10 times that of ILL. By the use of the TOF-monochromator approach, including TOF spectroscopy too, this source would just outperform the neutron intensity of ILL in this ratio across the board in all applications of neutron scattering. (Choosing another duty factor will improve some applications and disadvantage others). Since one can transfer essentially the same TOF monochromator instruments from a CW reactor to a LPSS, the characteristics of the two sources are very similar. The SPSS displays, on the other hand, quite different characteristics. It outperforms both other sources in the hot neutron range ($\lambda < 1$ Å) due to its very short pulse lengths in the slowing down regime. In the thermal and cold neutron range however, its peak flux, will not exceed the "on" flux of the 4 times higher average power LPSS (compressing the proton pulse from 1 ms to 1 μsec only increases the peak height of the moderated neutron pulse by a factor of not more than 4). Thus the SPSS source is outperformed to various degrees in all thermal and cold neutron applications by an LPSS of similar costs. Compared to ILL, the 1 MW SPSS with a single target station can range from equivalent to some 5 times superior in thermal and cold neutron scattering experiments. However, the necessity of making the neutrons flight paths relatively short on a SPSS — quite the contrary to LPSS where long neutron guides similar to those at ILL are most often preferred -- induces the division of the total power between two target stations and reduces the relative merits of SPSS by a factor of 1.5 – 3, the higher losses tending to apply to the anyway less favorable cases. (The TOF monochromator concept could actually also help to eliminate the need of using two target stations on a SPSS).

In sum, from the point of view of the neutron scattering user the long pulse spallation source is just an improved (neutron) economy reactor source and both of them are complementary to short pulse spallation sources, which latter are known to be superior for applications essentially involving hot neutrons. This improved economy opens up the way to envisage building reactor like sources with a user side flux some 20 – 40 times superior to ILL by using current linac accelerator technology. A first, large step in this direction could be to harvest the 1 MW average power capability of the 15 years old LAMPF linac in order to provide the neutron community with a source already superior to ILL.

References

[1] B. Buras, AEC – ENEA Seminar, Santa Fe, New Mexico (1967); G. E. Bacon, Neutron Diffraction, 3rd ed. (Oxford, Clarendon Press, 1975) p. 144.

[2] F. Mezei, Proc. ICANS XII. (Rutherford Appleton Lab., 1994) p. I-377.

[3] F. Mezei, Neutron News, Vol. **5** issue 3 (1994) p.2.

[4] W. H. Kraan, private communication.

[5] F. Mezei, to be published.

[6] W. Schäfer, E. Jansen and G. Will, J. Appl. Cryst. **26** (1993) 660.

[7] E. Maliszewski, V. V. Nitc, I. Sosnowska and J. Sosnowski, in Neutron Inelastic Scattering Vol. II. (IAEA 1968) p. 313.
[8] K. N. Clausen, T. E. Mason, G. Aeppli, D. F. McMorrow and J. K. Kjems, Physica B. (in press).
[9] M. Hagen, U. Steigenberger, C. Petrillo and F. Sacchetti, RAL — Report 95 – 006 (Rutherford Appleton Laboratory, 1995).
[10] F. Mezei, in Thin Film Optical Devices, C. Majkrzak, editor. (SPIE, 1989) p. 10.
[11] J. B. Hayter, Proc. SPIE, **1738** (1992) 2.
[12] F. Mezei, in press.

SOME GENERAL REFLECTIONS ON "LONG PULSE" NEUTRON SOURCES

G.S. Bauer

Paul Scherrer Institute, CH-5232 Villigen PSI, Switzerland

Abstract

A long pulse spallation neutron source (LPSS) having about 20 times more time average thermal flux than its short pulse counterpart (SPSS) at the same proton beam power and featuring a pronounced time structure not available on CW sources (CWNS) of equal time average flux can in principle host instruments typical for both classes of facilities. While the need for additional choppers introduces some restrictions on inverted time of flight techniques typical for SPSS and high incident neutron energies are not easier to use on LPSS than on CWNS, taking advantage of the pulsed nature of the neutron flux can enhance significantly the performance of direct time of flight instruments and of crystal spectrometers or diffractometers. In the paper some of the options are reviewed in a general manner and criteria are discussed which can be used to optimize the performance enhancement.

What is a "long pulse" spallation neutron source (LPSS) and why should we want to build one?

"I understand reactors and short pulsed sources. A long pulse source seems to be somewhere in between, neither fish nor fowl. I wouldn't even know what knife to use". These are the words with which DOE-official Iran Thomas characterized pretty well the situation prevailing in a large part of the neutron scattering community. To shed some light on this issue and to identify those knives which might cut out the bits of science most efficiently from this "in between" thing was the purpose of this workshop. The purpose of this paper is to set the stage for the understanding of these deliberations and perhaps provide a feeling for how far one could expect to get in this kind of a first brain storming and what the next steps might be.

Besides reactors, there are at present four spallation neutron sources used for routine neutron scattering work: They are all short pulsed sources (SPSS) and three of them, KENS (Japan), IPNS (USA) and ISIS (UK) are based on rapid cycling synchrotrons delivering inherently short pulses. The fourth, LAMPF (USA), is fed by an 800-MeV Linac in conjunction with a proton pulse compressor to obtain the short proton pulses of less than 1 μs, required to produce short neutron pulses also in the slowing-down regime of the useful neutron spectrum (up to a few eV). All of these sources have relatively low proton beam power, i.e. less than 200 kW. As neutron scientists are demanding significantly more powerful sources in order to be able to tackle the more and more subtle problems in a growing number of scientific disciplines, the question arises, how such sources could be conceived. At present the discussion focuses on the power range between 1 and 5 MW, but there is no obvious reason, why this should not go further in the more distant future. In order to satisfy such demands, several technical problems will have to be solved on the accelerator side, as well as on the target side.

According to present thinking, the upper limit of the number of protons that can be accommodated in a ring is of the order of $2 \cdot 10^{14}$. Assuming that the upper limit of useful proton energy is around 3 GeV for spallation neutron sources this means that the maximum pulse energy can be $6 \cdot 10^{14}$ GeV or $\approx$ 100 kJ. In practice, the need to cycle the synchrotron magnets poses a limit to the repetition rate of such machines which is of the order of 60 Hz/GeV energy gain. In other words, a single ring will, according to present knowledge, not be able to accelerate significantly more than 2 MW. Synchrotron based spallation sources with higher beam power will therefore require more than one ring, which is a clear discontinuity in cost. Similar considerations hold for compressor rings fed by linac pulses at the full energy, with the added difficulty of the much more severe consequences of any injection losses at the ring. This, together with the cost of the linac, will limit the energy of such systems to 1.5 GeV or less. (According to present planning, the H^0-losses at the injection into the 5 MW ESS-2-ring compressors will be 60 μA out of 3.5 mA, i.e. 2%!). Accounting for the fact that 50 Hz is generally considered as an upper limit for the useful repetition rate of a SPSS, this clearly shows the problems in providing higher power.

On the target side, on the other hand, difficulties are no less severe. Numerous questions relating to heat removal, thermal stress, radiation damage and, last not least, target moderator coupling must be given careful consideration. The one point in which a SPSS is markedly different from a LPSS is that the full pulse energy (of the order of 20 kJ per MW average beam power) is delivered within a time that does not allow the system to accommodate the resulting pressure. As a consequence, pressure waves may develop in the target material, whose consequences are difficult to predict and to control.

In this situation it is obvious to ask the question, what a spallation source could look like that does not use a ring at all, thus avoiding its cost, its associated beam losses and the most serious problem in the target. Such a source would be fed directly from the linac with proton pulses of a millisecond duration or less and at a repetition rate which can be chosen more freely because there is no resonantly cycling system.

This provides us with an obvious definition for a long pulse source as opposed to a short pulse source: A SPSS is one whose proton pulses are shorter than the shortest time it takes to slow neutrons down to the energies at which they are to be used. A LPSS is one whose proton pulses do not meet this criterion and where the duration of the neutron pulses is therefore significantly affected by the duration of the proton pulse (100 to 1000 μs or even more).

In order to see how the proton pulse duration affects the shape of the neutron pulses we consider first the response of a target-moderator-reflector system to a very sharp proton pulse (Fig. 1). It is obvious that two times play a role. At very short times a flux builds up in the moderator whose time distribution is governed by the distribution of slowing-down times from the energies of the evaporation spectrum (around 2 MeV) to thermal energies. This flux starts to decay with the fundamental mode decay constant of the moderator which is of the order of 100 μs. At longer times different decay constants can be observed which, in the case shown, depend on the size of the reflector. This time constant is to a large extent responsible for the time average flux of the system (also given in the figure in relative units).

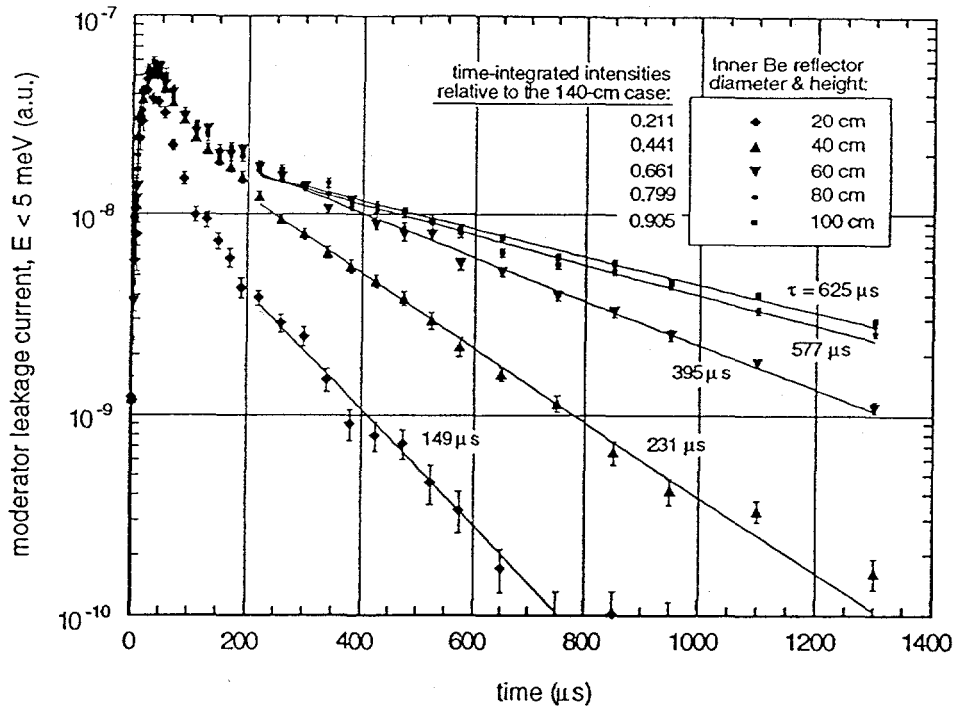

Fig. 1: Calculated response of the low energy neutron leakage current from a target-moderator-reflector system to an instantaneous proton pulse, given for various size Be-reflectors. The short term response can be seen to be about 50 μs wide (time distribution of the slowing-down process). For long times reflector-size dependent "effective" decay constants are obtained. Relative time-integrated intensities are indicated [1].

The response to a long pulse is then given by the convolution of the short pulse response with the time distribution (usually rectangular) of the proton pulse. The result is shown for three long time decay constants in Fig. 2 for a proton pulse duration of 1 ms.

It is obvious that the peak flux reached at the end of the proton pulse does not scale with the time average flux for different long time decay constants and the fraction of the total intensity in the trailing edge of the pulse becomes smaller as the decay constant becomes shorter.

To a first approximation we can use the convolution between the exponential decay and a rectangular pulse function to describe the pulse by

$$\begin{aligned} \phi(t) &= \bar{\phi} \cdot T / t_p (1 - \exp\{-t/\tau\}) && \text{for } t \le t_p \\ \phi(t) &= \bar{\phi} \cdot T / t_p (1 - \exp\{-t_p/\tau\}) \cdot \exp\{-(t - t_p)/\tau\} && \text{for } t \ge t_p \end{aligned} \qquad (1)$$

with τ being the decay constant, t_p the proton pulse duration, T the time between pulses and $\bar{\phi}$ the time average flux.

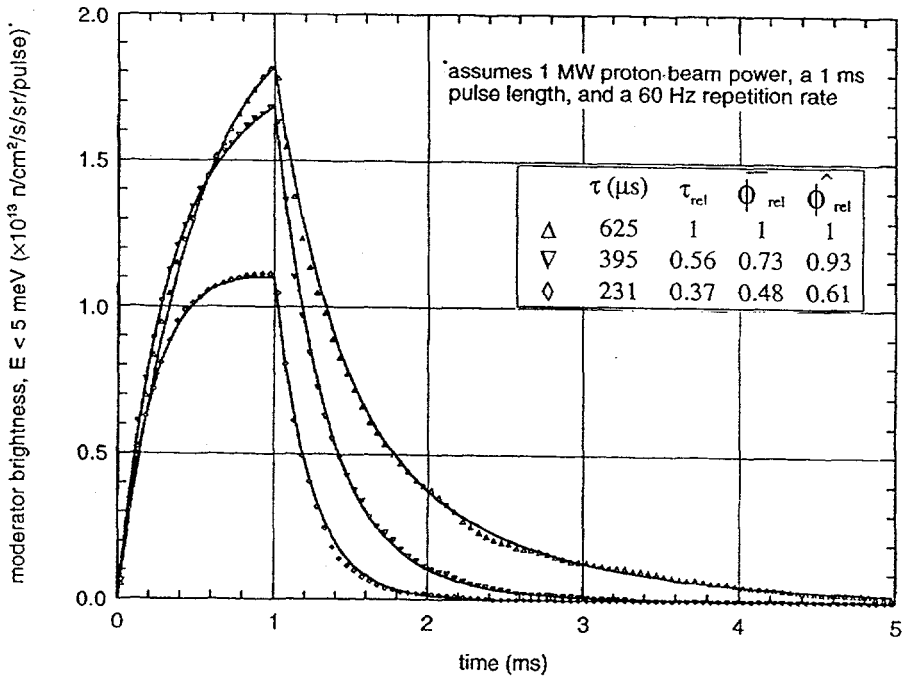

Fig. 2: Time distribution of the moderator leakage obtained from a convolution of the response given in Fig. 1 for different reflector sizes with a 1 ms long proton pulse of constant intensity [1].

Ways to use a long pulse source

There are essentially three classes of instruments to be distinguished, which make use of the flux of a neutron source in different ways, depending on whether crystals or time of flight are used to determine the neutron energy in the primary (before the sample) or in the secondary flight path (behind the sample).

Class of instrument	**Primary energy selection**	**Secondary energy selection**
Crystal spectrometer	Crystal	Crystal none (diffr.)
Direct time of flight spectrometer	Crystal Choppers	TOF
Inverted time of flight spectrometer	TOF	Crystal none (diffr.)

The most straight forward approach (and in fact the one adopted rightly in this workshop) is to look how these different classes of instruments would perform when transferred to a given benchmark LPSS and what modifications would help to improve this performance.

While the outcome of these deliberations is reported in the various working group accounts, some general features are worth to be stressed as they may affect later optimization efforts of the target-moderator reflector system and the accelerator parameters.

The benchmark data used for the accelerator are:

Time average beam power 1 MW

Proton pulse duration 1 ms

Pulse repetition rate 60 Hz
(note that this implies a linac current of only 17 mA at 1 GeV!)

For this system neutron spectra expected for a given (non optimized) target-moderator-reflector arrangement were calculated and were made available to the participants of the workshop. They are shown in Fig. 3. (The spectra used later in Fig. 8 do not agree precisely with those of Fig. 3 but are calculated as slowing-down and Maxwellian spectra according to simple diffusion theory for moderators with effective temperatures of 300 and 35 K.)

Crystal spectrometers

Crystal spectrometers are typical reactor, i.e. CW-source instruments and, at a first glance, do not seem to profit at all from the time structure of a source.

The space time diagram of such a spectrometer is shown in Fig. 4. Each wavelength band transmitted by the monochromator will have the time distribution of the moderator pulse (for that particular wavelength). Since the incoming and outgoing energies are essentially fixed by the settings of the monochromator and analyzer crystals there is an extra parameter, namely the predictable time of arrival of the desired neutrons at the detector, which can be taken advantage of. This can happen in two ways:

a) The detector can be electronically gated in such a way that it is only sensitive when the "good" neutrons arrive (case shown in Fig. 4). This enhances significantly the signal to background ratio and helps to eliminate spurious effects from higher order reflections which might otherwise be difficult to identify, if all neutrons were spread out over all times. As a consequence, filters can be omitted, avoiding their associated losses and giving more freedom in the choice of the experiment setup. The estimated overall gain G_F in measuring time over the same experiment on a CW source is of order three (say 2 to 6).

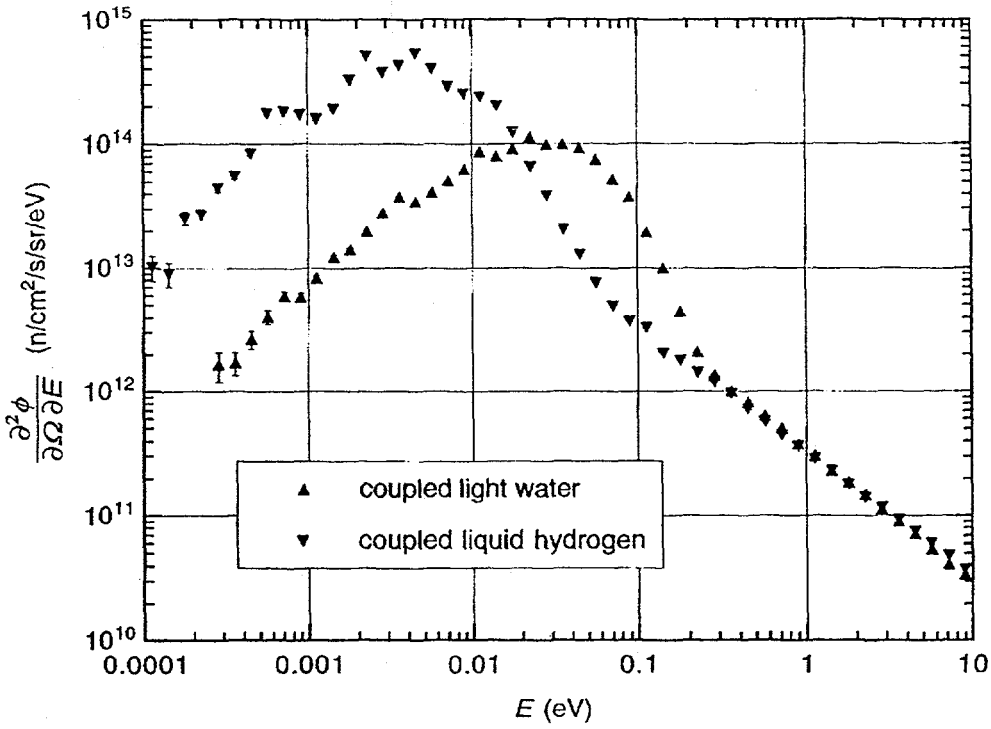

Fig. 3: Differential neutron spectra for a coupled ambient temperature water moderator and a coupled liquid hydrogen moderator for the baseline target-moderator reflector system considered [1].

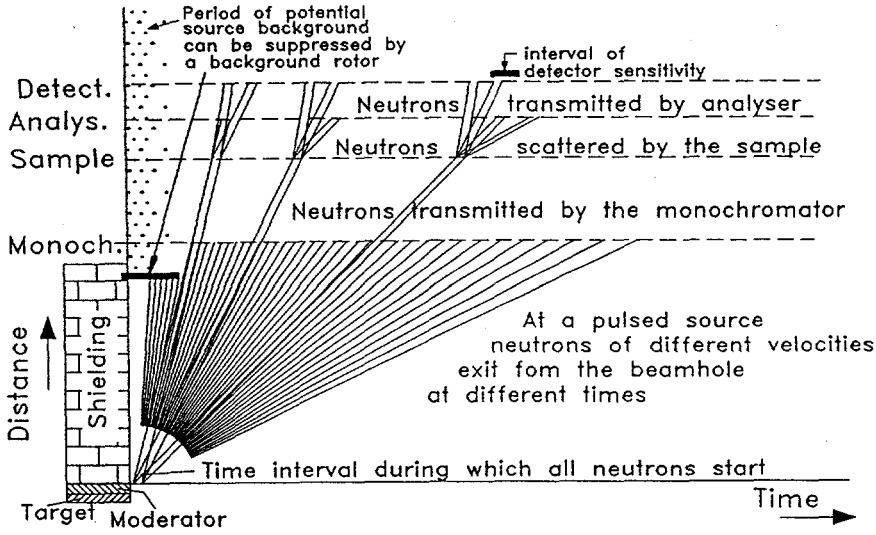

Fig. 4: Space-time diagram of a crystal (triple axis) spectrometer on a pulsed source. Each slope corresponds to a different neutron velocity. At the monochromator and analyzer only those neutrons are transmitted, which fulfill the respective Bragg conditions. Neutrons scattered in the sample can gain or lose energy or be simply diffracted (with no change in slope). Since the time of arrival at the detector can be calculated for each setting of the spectrometer, no filters are needed.

b) More than one incident energy can be used to fill in more of the time between pulses to obtain useful information over a wider range of momentum transfer. This is shown in Fig. 5 for the case of a (powder) diffractometer where several orders of two monochromator crystals with different d-spacings (C002 and Si220 at $2\theta_M = 130°$) are used. The figure is semi-quantitative for 60 Hz, 1 ms using the pulse shape given in Fig. 9 for the 230 μs case. In a time resolving mode the (position sensitive) detector will record diffraction patterns corresponding to the various wavelengths arriving at different times. In the example shown in Fig. 5, six packets between 1 and 3.5 Å are used.

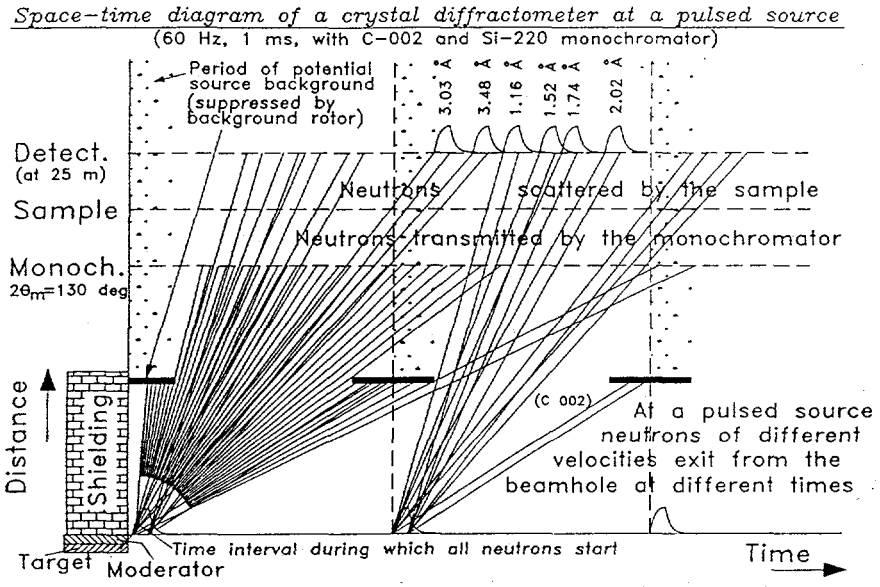

Fig. 5: Example of the use of higher order monochromator reflections to measure diffraction patterns with different incident wavelengths in one period of a long pulse source. While the source is on, the fast neutrons are blocked by a background rotor in the beam. In this example, the background rotor also blocks the C002 reflex, which would otherwise interfere with the Si220 reflex of the following pulse. Of course, reflex-blocking choppers can also be installed elsewhere in the incident flight path. This technique has been called "multiplexing".

It should be noted that, like on a CW source, the resolution in this type of experiment is independent of the pulse length of the source. In contrast to a CW source, however, no filters against higher orders of the monochromator need to be used, which results in an estimated added intensity gain of 1.2 to 1.4.

As usual, if a different dynamic range is covered, the effective gain from using more incident wavelength packets is difficult to quantify. Assuming that about 80% of the data recorded with the setup used in Fig. 5 are useful (for each packet one obtains the typical resolution function of the crystal spectrometer) and taking into account that there are no intensity losses from filters and that wavelength-dependent effects can be sorted out immediately in the regions where the coverage of d-spacings overlaps, it is probably fair to say that the gain over a crystal

diffractometer on a CW-source is given by the number of usable wave packets, i.e. of the order of 6 to 10 in the baseline case.

This technique has been called "multiplexing". More sophisticated variants have been proposed which allow to fill the time frame more efficiently and with much narrower wavelength bands to suit special purposes (see e.g. [2], [3]). To a certain extent such techniques may also be applicable in triple axis spectroscopy. The effective degree of multiplexing G_M, i.e. the number of wavelength packets that can at most be stacked between two pulses is determined by the time t_{int}, out to which one must collect data for a given wavelength to avoid excessive packet overlap. Integrating eq. (1) up to an upper limit t_{int}, one finds that the fraction of neutrons not accounted for in a pulse by counting to t_{int} only is

$$K = \frac{\tau}{t_p}\left(\exp\left\{\frac{t_p}{\tau}\right\} - 1\right) \cdot \exp\left\{-\frac{t_p}{\tau} \cdot x\right\} \tag{2}$$

with $x = \frac{t_{int}}{t_p}$. Fig. 6 shows this fraction as a function of x for various values of $\frac{\tau}{t_p}$. The effective maximum gain from multiplexing therefore becomes $G_M \leq \frac{T}{t_{int}}$ and depends on the amount of packet overlap that can be tolerated.

Direct time-of-flight techniques

In direct time of flight techniques a chopper is used to define the pulse width of the beam and one or more further choppers or a crystal monochromator define one single wavelength incident on the sample. In this case the chopper can be phased to the peak of the pulse to take full advantage of the peak to average flux ratio. Since the repetition rate of the source may be not matched to the required interval of data taking, the gain over an optimized instrument on a steady state source is

$$G_{TOF} = \frac{\hat{\phi}}{\bar{\phi}} \cdot \frac{\nu_{act}}{\nu_{opt}} \cdot f_{pul} = \frac{T}{t_p} \cdot \left(1 - \exp\left(-\frac{t_p}{\tau}\right)\right) \cdot \frac{\nu_{act}}{\nu_{opt}} \cdot f_{pul} \tag{3}$$

with ν_{opt} and ν_{act} being the optimum and the actual $\left(= \frac{1}{T}\right)$ repetition rates respectively and f_{pul} is the fraction of pulses actually used if $\nu_{act} > \nu_{opt}$.

If it is possible to reduce the pulse length in favor of a higher repetition rate, as long as $f_{pul} = 1$, this results in a more than proportionate gain. The quantity $G_{TOF} \cdot \nu_{opt}$ is shown in Fig. 7, together with the actual repetition rate and the situation for a short pulse source ($\Delta t_s = 40$ µs) with coupled moderators. The baseline case corresponds to the 1 ms, 60 Hz point. Going e.g. to a 0.5 ms 120 Hz regime would benefit direct TOF instruments by an extra factor of 1.6.

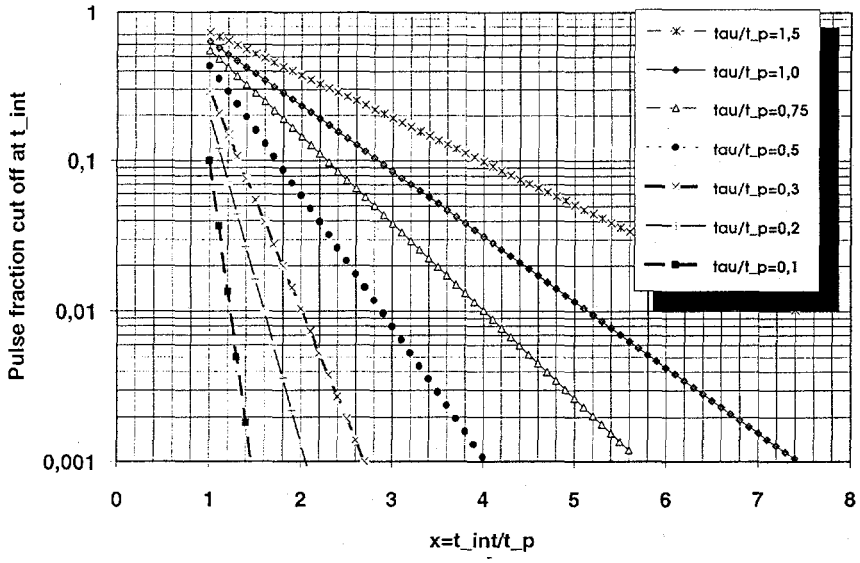

Fig. 6: Fraction of the pulse intensity not recorded by counting only up to a time t_{int} on a long pulse source, given as a function of the ratio of t_{int} to the proton pulse duration t_p for various ratios of the decay constant τ to t_p. $x = 1$ corresponds to counting from the beginning of the pulse to the point, where the peak flux is reached only. For $\tau/t_p = 0.1$ 90% of the flux is recorded, whereas for $\tau/t_p = 1$ more than 60% of the pulse intensity is lost in this case.

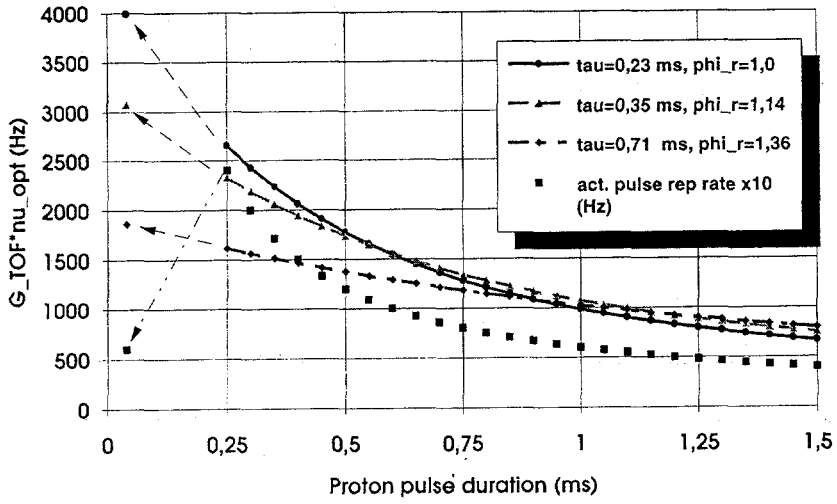

Fig. 7: Product of the gain factor of the peak-to-average flux for a standard time of flight spectrometer and the optimum repetition rate of this spectrometer at a CW-source as a function of the proton pulse duration (at constant average proton current). The required actual repetition rate at a linac designed for 1 MW at 60 Hz and 1 ms pulse length is given by the solid squares. To obtain the real gain factor, the figure corresponding to a given decay constant and selected pulse duration must be divided by the optimum repetition rate ν_{opt}. For example, for $\nu_{opt} = 240$ Hz, a 1 ms (60 Hz) pulse results in a gain of about 1000:240 = 4.2 at 1 ms and of 1600:240 = 6.7 for 0.5 ms, 120 Hz at $\tau = 0.23$ or 0.35 ms. Pulse shapes used for this calculation are those of Fig. 9 for an H_2-moderator with different reflectors.

Inverted time-of-flight techniques

The seemingly most attractive way to use the time structure of a pulsed source is to allow the different neutrons energies to spread out in time and to pick consecutive energy bands by selecting time bins at a given distance from the source. This technique is often referred to as "time of flight monochromatization", which is somewhat misleading because no monochromatic beam is actually produced. Obviously, in order to obtain reasonable wavelength resolution at a distance L from the sample, relatively short pulse widths Δt are required because, if L is taken in m, t in ms and λ in Å,

$$\Delta\lambda \approx 4 \cdot \Delta t / L \tag{4}$$

This is why up to a factor of 20 in average flux is sacrificed on short pulses sources to keep the neutron pulse short by poisoning and decoupling. On a long pulse source it is necessary to use a chopper at a distance L_c from the moderator. Since, as can be seen in Fig. 8, such a chopper has a bandwidth limiting effect, one would try to place it as close as possible to the source. (At present, a distance of 4 m is considered to be safe in terms of radiation effects, but 2 m should be feasible).

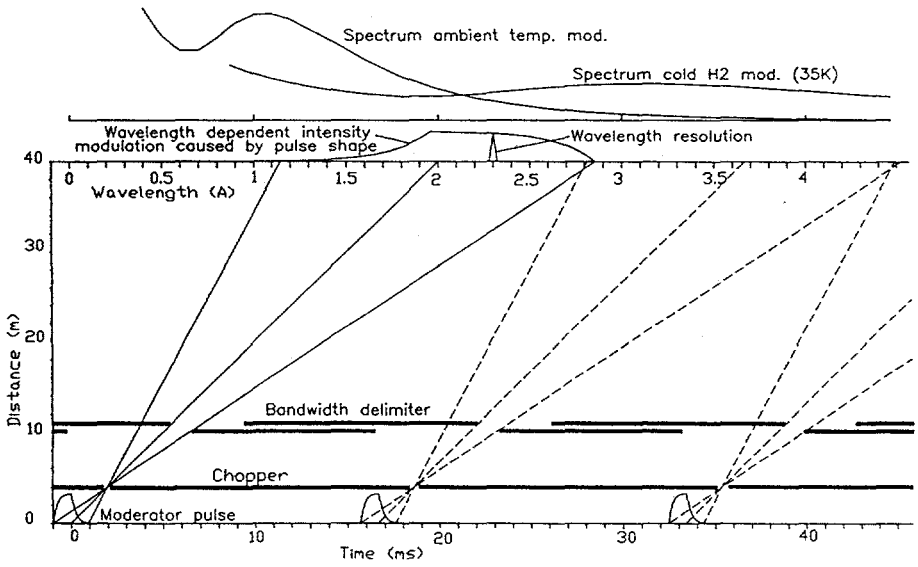

Fig. 8: The space-time diagram for a pulsed neutron source with 1 ms pulse length and a chopper at 4 m from the moderator phased to transmit a wavelength band around 2.3 A. The resulting wavelength scale at a distance of 40 m is given at the top, together with the corresponding spectral distributions of an ambient temperature (300 K) and a cold (35 K) moderator. Due to the "pinhole" effect of the chopper, the time distribution of the moderator pulse is transformed into a wavelength-dependent intensity modulation, which limits the useful band width and requires a bandwidth delimiter to suppress the low intensity part.

As is obvious from Fig. 8, a chopper with a short opening time acts as a pinhole for the time distribution of the neutron pulse which, due to the spreading of wavelength in time, transforms itself into an intensity modulation at the position of the sample. Even if those wavelengths which are severely damped because they come form the trailing edge of the moderator pulse are cut off by a band width delimiter one is still far from utilizing the full peak flux over the whole time at thermal neutron energies. Adjusting the flight path such, that the whole time frame is filled will improve the wavelength resolution (if useful), but will not result in a better source utilization in terms of a wider wavelength band. This would require a chopper closer in to the moderator. With a 40 m flight path and a chopper at 4 m from the moderator a more or less complete filling of the frame and hence a good utilization of the time between two pulses near the peak flux level of the respective wavelength can only be achieved for nominal wavelengths of 5 Å or more in the baseline case. The effective nominal utilization factor can be derived from Fig. 6 by tracing the "cut off" back to the moderator pulse and thus determining t_{int}/t_p. For example, cutting off at the peak as shown in Fig. 8 would result in a loss of 30 % for a decay constant of 300 μs and of 55% for a decay constant of 750 μs at 1 ms proton pulse. How high this penalty really is and how it can be minimized for a given instrument by placing it at a proper distance and selecting an appropriate wavelength band, must be determined for each case separately. On top of the variation due to the pinhole effect, the intensity will also vary as a function of the wavelength due to the spectral distribution at the moderator as indicated in the upper part of Fig. 8, depending on how wide a band is used and where in the spectrum it is located. Since the necessary data taking time will most likely be determined by the relevant resolution element(s) with the lowest intensity and very often a significant fraction of the data will be taken in "uninteresting" areas of the Q-ω-space, it is not possible to assess in a general way, how beneficial this method actually is. It also requires the samples to be placed in the direct beam which may result in difficulties to correct for the sample dependent background and in general impedes multiple use of a neutron guide, which is easily possible with crystal monochromatization.

Correlation techniques: It is possible to improve significantly the resolution of a long pulse source when used in inverted time of flight by superimposing a sequence of short pulses of variable length on the long pulses and correlate the time of detection of a neutron to the possible times of start at the correlation chopper, also taking into account the possible periods of start of the moderator. Relative to the same technique on a CW-source this will not result in an intensity gain, but will substantially reduce the background of "unsuccessful" correlations because of the extra boundary condition for the source pulse. A correlation chopper does not introduce the "pinhole effect" discussed above.

Considerations relating to source optimization; further steps

The data given in Figs. 1 through 3 were obtained by applying a long proton pulse to a well studied target-moderator-reflector concept for a SPSS, but eliminating the poison and decouplers and varying the reflector size to maximize the time average flux. This is certainly a valid first approach to provide experimentalists with some baseline data they can refer to when evaluating the performance potential for a given instrument concept. It goes without saying that, based on these evaluations, a selection of "promising" instruments will have to be made and the question will have to be asked, how these instruments can, on average, be served best by adjusting the

parameters of the source. Clearly this is a very involved task due to the wide range of parameters that can be varied on the instrument side as well as on the source and will require several iterations.

Pulse repetition rate versus pulse length

A linac, while limited in average beam power and pulse current by design, will in general offer some flexibility to trade pulse duration against repetition rate. As shown in chapter 2.2, higher repetition rates and shorter pulses are certainly an advantage for direct time of flight techniques which can usually run at 200 Hz or even more. (For example, a direct TOF-spectrometer which can use 240 Hz would benefit a factor 4.2 from the 60 Hz, 1 ms pulse and a factor of 6.7 from running at 0.5 ms, 120 Hz relative to a CW-source of the same time average flux). For these instruments it is important to maximize the product of peak flux and repetition rate. The shape of the pulse and potential long tails are of no concern.

For multiplexing techniques, on the other hand, the pulse shape matters because it determines the possible degree of multiplexing. In this case it is important to optimize a "fast" reflector system for pulse intensity. A non-moderating reflector and an intensity-optimized moderator will therefore be preferable to a reflector which enhances the average intensity by contributing a long time constant. Increasing the repetition rate and shortening the pulse may help to bring the instruments closer to the moderator and to reduce guide losses, in particular at thermal energies, but in general the maximum possible degree of multiplexing will be mainly affected by the ratio of the decay constant to the proton pulse duration (Fig. 6).

For inverted time of flight techniques the effect of the pulse shape must be controlled by bandwidth delimiters (Fig. 8). In order to obtain a good utilization of the pulse-to-average flux ratio, a fast buildup of the pulse flux is desirable. The question of the preferred repetition rate is closely connected to the wavelength band one wants to use. A shorter proton pulse will result in a more limited wavelength band, unless choppers very close to the moderators can be used. In view of the fact, however, that not all of a scan involving a large wavelength band will yield data which relate to the problem under investigation, it may be an advantage to scan over a smaller band more often and vary the chopper phase for a second scan in cases where necessary.

In any case, the question, whether a certain research task can be performed best on a LPSS by inverted time of flight, direct time-of-flight or a multiplexing instrument will need very careful examination taking into account what fraction of the data recorded actually contributes to the solution of the problem.

Pulse shape versus average flux

According to eq. (1) and, as can be clearly seen in Fig. 2, the buildup, as well as the decay of the pulse are affected by the long time decay constant. In fact, eq. (1) can only be used for "qualified estimates". For detailed considerations the full time response as given e.g. in Fig. 1 and Fig. 2 must be taken into account by Monte Carlo calculations. This response - and, as the most important measure of it, the long time decay constant - can be affected by the size of the reflector as in Fig. 1, but a more important option seems to be the choice of the moderator geometry and

the reflector material. For example, Fig. 9 gives pulse shapes calculated from eq. (1) for the decay constants and relative average fluxes measured for three different reflector configurations and a liquid H_2 source [4]: a large D_2O-reflector, a large graphite reflector with an H_2O premoderator and a lead reflector with an H_2O premoderator. It is clearly seen that, while the time average fluxes differ by as much as 36%, there is only a 5% difference in the peak fluxes and the "fast" lead reflector gives a much more favorable pulse shape than the "high average flux" D_2O-reflector. The D_2O-reflector falls behind even more, if the pulse is shortened to 0.5 ms.

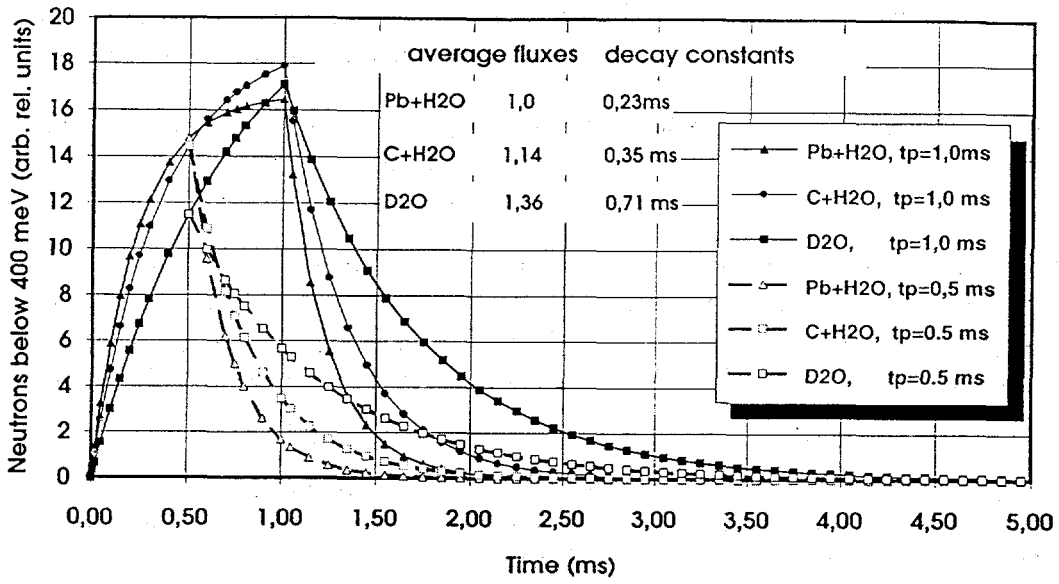

Fig. 9: Pulse shapes calculated with eq (1) for the measured average fluxes and decay constants for a cold H_2 moderator with different premoderator reflector configurations [5] for a 1 ms proton pulse. Also shown are the pulse shapes that would result from simply terminating the proton pulse at 0.5 ms to double the repetition rate at the same average power.

The present paper is not meant to, and could by no means, treat these problems exhaustively. This is a widely open and still poorly explored field. The important message is that, while useful for a first round, the figures of merit evaluated for different instruments on the basis of the "facts sheets" used at the workshop should not be mistaken for a final result. They should rather be considered as a lower limit. In this sense even the comparison to a CW-source of the same time average flux is questionable. As it happened for short pulsed sources, the continuing interaction of scientific users, instrument designers and source designers will allow to make best use of any given boundary conditions, such as time average beam power and maximum current of the linac.

The temptation and the difficulty of intercomparison: CW and short pulse sources

Although this is likely to be an irrelevant exercise, because it assumes that the option to choose a different source concept really exists under any given set of boundary conditions (such as available assets or funds, for example), the performance comparison to alternative source

concepts will probably always be made. The exercise is even more problematic, since very often some arbitrarily chosen, optimized but unproven, design is picked for the "alternative option" (such as a 1 MW SPSS, for example).

As far as the comparison to a CW-source is concerned, the situation may still be relatively transparent as long as one restricts the comparison to instruments which could also run there, such as standard time of flight and crystal spectrometers. But even here, the best figure one can come up with is the time average flux that would be required to obtain the same performance. As soon as one starts to quote thermal reactor power one already implies a certain reactor design or a scaling law of flux with power, which clearly does not exist, in particular not in the field of cold neutrons, where the source performance is largely dominated by heat removal problems.

It is a fact that the use of presently feasible long pulsed sources can be expected to lead to performance levels for a number of instruments which could not be achieved by any research reactor using present day technology. This alone makes it worth trying.

With regards to short pulse sources the situation is even more problematic. The SPSS has certain features which make it unique, such as the 1/v dependence of the pulse width in the slowing-down regime. The opportunity to use high incident neutron energies at excellent resolution alone makes it worth to have an SPSS. There is no way a reactor or an LPSS could compete in this field.

The temptation of comparison will be particularly high for inverted time of flight instruments which are the concept of choice on an SPSS also for thermal and cold neutrons. There is, however, little chance for a fair and significant result because

a) Realistically one should compare to what has been realized in the past and can be verified (i.e. ISIS) rather than to what one might hope to have in the future.

b) Such comparison will involve the use of coupled moderators on the SPSS. Depending on the other source characteristics, the distinction to the LPSS may then come only from the shape of the neutron pulse.

c) The technical effort to build an SPSS of the same average power cannot be easily compared to the one required for an LPSS but will certainly be significantly higher.

d) The main problem arises when, as is often the case, intensity at a given Q, ω point is traded for the number of points measured simultaneously or for a larger dynamic range. The value of this tradeoff can only be judged for a specific scientific problem.

For example, if one were to build a SPSS with coupled moderators (i.e. the same moderator-reflector system as used on the LPSS) from the baseline linac, this would imply adding a compressor ring which could transform the 1 ms pulses into 1 μs pulses. Apart from the need to accelerate H^- in the linac, which is slightly more demanding than accelerating protons, the main change would be the introduction of a chopper in the low energy end in order to prepare the beam in such a way that, after stacking several hundred beam bunches in the ring, there would still be part of the ring free of beam in order to allow activation of the extraction kicker without

losses. According to the current ESS-study [5], this implies a 60% duty factor in the linac pulse. Since the macro-duty cycle of the linac is normally a design feature, this results in a corresponding reduction of average beam current. At the same time, the pulse shape would change from the one given in Fig. 2 to the one shown in Fig. 1. Assuming a decay constant of 400 μs, the resulting moderator pulses are compared to one another in Fig. 10. For inverted time of flight instruments, where a chopper needs to be used to obtain the necessary resolution, the pinhole-effect discussed before (Fig. 8) leads to the wavelength dependent intensity modulation as shown. In the SPSS-case with coupled moderators, the modulation is obviously much more severe than in the LPSS case and the useful wavelength band is narrower. Clearly, it is not obvious that the SPSS would be of any advantage over the LPSS in this case. Of course, on the SPSS the pulse width can be affected by poisoning and decoupling, thus eventually avoiding the need for a chopper. This, however, is of direct consequence on the average flux and makes a comparison of the two sources even more difficult.

In summary, since different optimization criteria apply for CW-sources, SPSS and LPSS, an advantage for one instrument may turn out to be a disadvantage for the other. On an SPSS with coupled moderators the pulse shape can only be affected through its trailing edge. The large dynamic range obtained by using a broader wavelength band will be of little use, if the measuring time is determined by the low intensity tail and unnecessarily good counting statistics are obtained at the high intensity end.

Many more details could be discussed in this context, but the bottom line is that each type of source has its own merits and problems. It is the task of the scientists and engineers to make the best use of the respective potential and select a method to obtain a scientific result, which is best matched to the source available. The opportunity to take advantage of the time structure of an LPSS is there and it should be used!

Conclusions

The present workshop was a first attempt to assess the possibilities offered by a long pulse source of a given set of baseline parameters. Several promising instrument concepts have been identified. Other opportunities, especially those further off the beaten track have not yet been dealt with. At the end of an initial selection process one will have to ask the question, how the types of instruments with the highest performance potential can be served best and to what extent the resulting requirements to the source can be fulfilled within the given boundary conditions. This process is far from being completed at the present stage and in this sense, performance estimates that were produced during the workshop should be considered as lower limits. More work remains to be done!

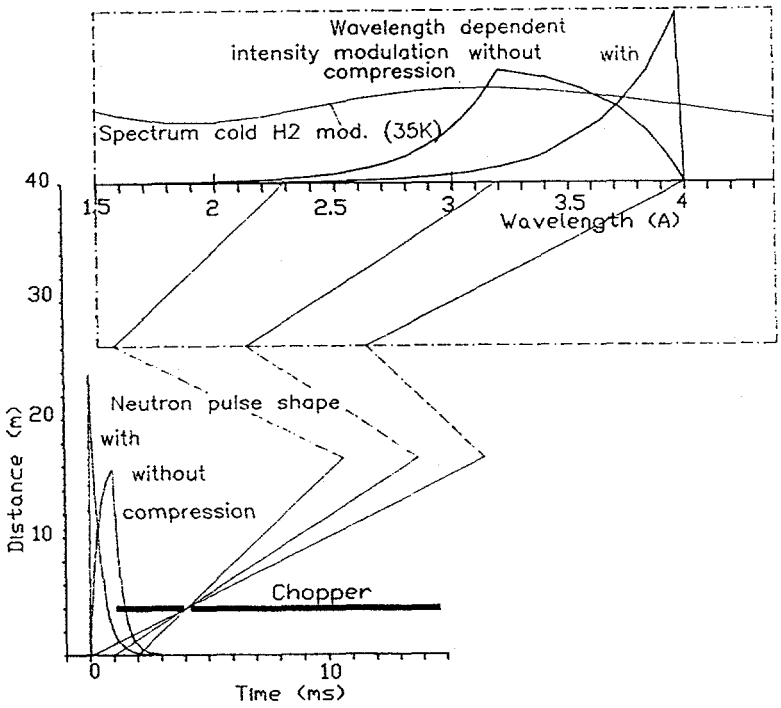

Fig. 10: Moderator pulses resulting from a LPSS and a SPSS with the same coupled moderator of 400 μs decay constant. The integral over the SPSS-pulse is 60% of that over the LPSS-pulse due to the need for chopping the linac beam. After passing through a chopper, the two pulses result in a wavelength dependent intensity as shown. (Chopper set for 4 Å nominal wavelength and located at 4 m from the moderator).

References

[1] G.J. Russell, E.J. Pitcher and P.D. Ferguson, data presented at the workshop

[2] R. Scherm, B. Alefeld "Instruments for High Flux Sources with Time Structure of Neutron Flux" paper IAEA-CN-46/80 in "Neutron Scattering in the 'Ninties", IAEA conference proceedings, Vienna, (1985) p. 247-259

[3] H. Rauch, "Novel beam bunching methods by perfect crystals and electromagnetic means" paper IAEA-CN46/40 in "Neutron Scattering in the 'Ninties", IAEA conference proceedings, Vienna, (1985) p. 35-52

[4] G.S. Bauer, H. Conrad, W. Fischer, K. Grünhagen and H. Spitzer "Leakage flux, life-time and spectra of cold neutrons from H_2-moderators with various reflectors" Proceedings of the Eighth Meeting of the International Collaboration on Advanced Neutron Sources, report RAL-85-110 (1985) p. 344-354

[5] H. Lengeler "Proposals for Spallation Sources in Europe", paper presented at EPAC-94

NEUTRONIC PERFORMANCE OF A BENCHMARK 1-MW LPSS

G. J. Russell, E. J. Pitcher, and P. D. Ferguson

Los Alamos National Laboratory, Los Alamos, New Mexico

A 1-MW LPSS Computational Model

We used split-target/flux-trap-moderator geometry in our 1-MW LPSS computational benchmark performance calculations because the simulation models were readily available. Also, this target/moderator arrangement is a proven LANSCE design and a good neutronic performer. The model has four moderator viewed surfaces, each with a 13×13 cm field-of-view. Our 1-MW benchmark computational model is depicted in Fig. 1.

For our scoping neutronic-performance calculations, we attempted to get as much engineering realism into the target-system mockup as possible. In our present model, we account for target/reflector dilution by cooling; the D_2O coolant fractions are adequate for 1 MW of 800-MeV protons (1.25 mA). We have incorporated a proton beam entry window and target canisters into the model, as well as (partial) moderator and vacuum canisters. The model does not account for target and moderator cooling lines and baffles, entire moderator canisters, and structural material in the reflector.

Neutronic Performance

To estimate the neutronic performance of a reference 1-MW LPSS, we used several indicators. The performance estimators were: a) moderator source brightness; b) moderator pulse shapes; and c) unperturbed thermal neutron flux. The data given here assume a 1-MW (1.25 mA at 800 MeV), 1-ms-long proton pulse at 60 Hz. We used a moderator size of 5×13×13 cm for our reference liquid H_2 (50% ortho / 50% para) cold source, and 4×13×13 cm for our reference ambient-temperature H_2O moderator. We also compared the calculated time-averaged moderator brightness of a 1-MW LPSS cold source relative to the calculated moderator brightness of the ILL cold sources.

To illustrate the degree of agreement expected between calculated and measured reactor source performance, we show calculated and measured source brightness of the ILL horizontal liquid D_2 cold source in Fig. 2 [1]. Above about 1.5 Å, the calculated performance is consistently below the measured value, so the calculated results are conservative. The calculated and measured neutron spectra from the LANSCE liquid H_2 moderator are shown in Fig. 3 [2]. Note that at low energies (long wavelengths) the calculated data significantly under-predict the measured results. We are presently trying to understand this discrepancy in detail. The ratio of calculated-to-measured data for both the ILL and LANSCE cold sources are depicted in Fig. 4. From about 1.5 to 6 Å, the calculated-to-measured ratios agree to about 20%. The severe underprediction of the calculated LANSCE data above about 6 Å is clearly evident. Calculated source brightnesses for the ILL horizontal and vertical liquid D_2 sources are compared to the calculated source brightness of our 1-MW LPSS benchmark geometry in Fig. 5. Below about 6 Å, the 1-MW cold source brightness is equivalent to one quartet of the ILL cold source brightness. Again, the drop in the calculated liquid H_2 source brightness above about 6 Å is evident.

The calculated neutron energy-spectrum from the 1-MW LPSS benchmark for a (5×13×13 cm) liquid H_2 moderator is depicted in Fig. 6. The wavelength-dependent pulse structure is shown on a semilog plot in Fig. 7; the pulse shapes are convoluted with a 1-msec proton pulse. The same data are shown for a 4×13×13 cm H_2O moderator in Figs. 8-10.

The effects of a composite reflector of Be/Ni (cooled with D_2O) are shown in Fig. 11 for an instantaneous proton pulse. The beryllium is a slow-neutron/moderating-reflector, whereas the nickel is a fast-neutron/reflector-shield. Note that the all-beryllium reflector gives the highest integrated and "peak" neutron intensities, but with a relatively long decay constant which puts "tails" on the pulses. The addition of nickel reduces the decay constant, but with an overall penalty in time-averaged brightness. For a beryllium reflector size of 60 cm diameter and 60 cm height, the "peak" neutron intensity is lower by about 13% while the integrated intensity drops by about 34% compared to a 150×150 cm Be reflector. For a composite Be/Ni reflector, the choice of the reflector composition is a compromise between high time-averaged brightness and peak intensity, and short decay times.

We are continuing to study ways of improving the neutronic performance of a LPSS by looking at various target/premoderator/moderator/reflector combinations. We are also constructing other target/moderator geometries to study the effects of target/moderator coupling.

References

[1] P. Ageron, NIM, **A284**, 197 (1978).

[2] T. O. Brun, et al., "LAHET Code System/CINDER'90 Validation Calculations and Comparison With Experimental Data," in Proceedings of the Twelfth Meeting of the International Collaboration on Advanced Neutron Sources, 24-28 May 1993, Rutherford Appleton Laboratory report 94-025, The Cosener's House, Abingdon, Oxfordshire, U.K.

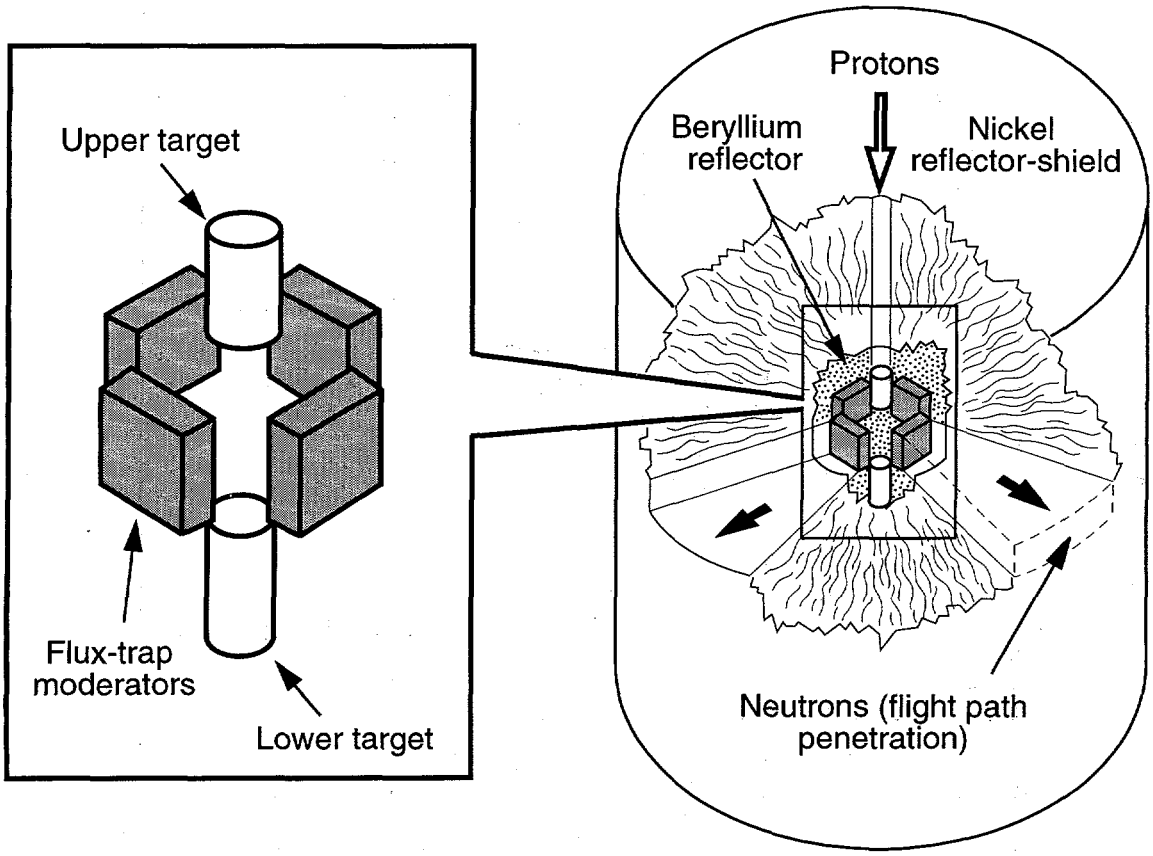

Fig. 1. Split-target/flux-trap moderator benchmark geometry for a 1-MW LPSS.

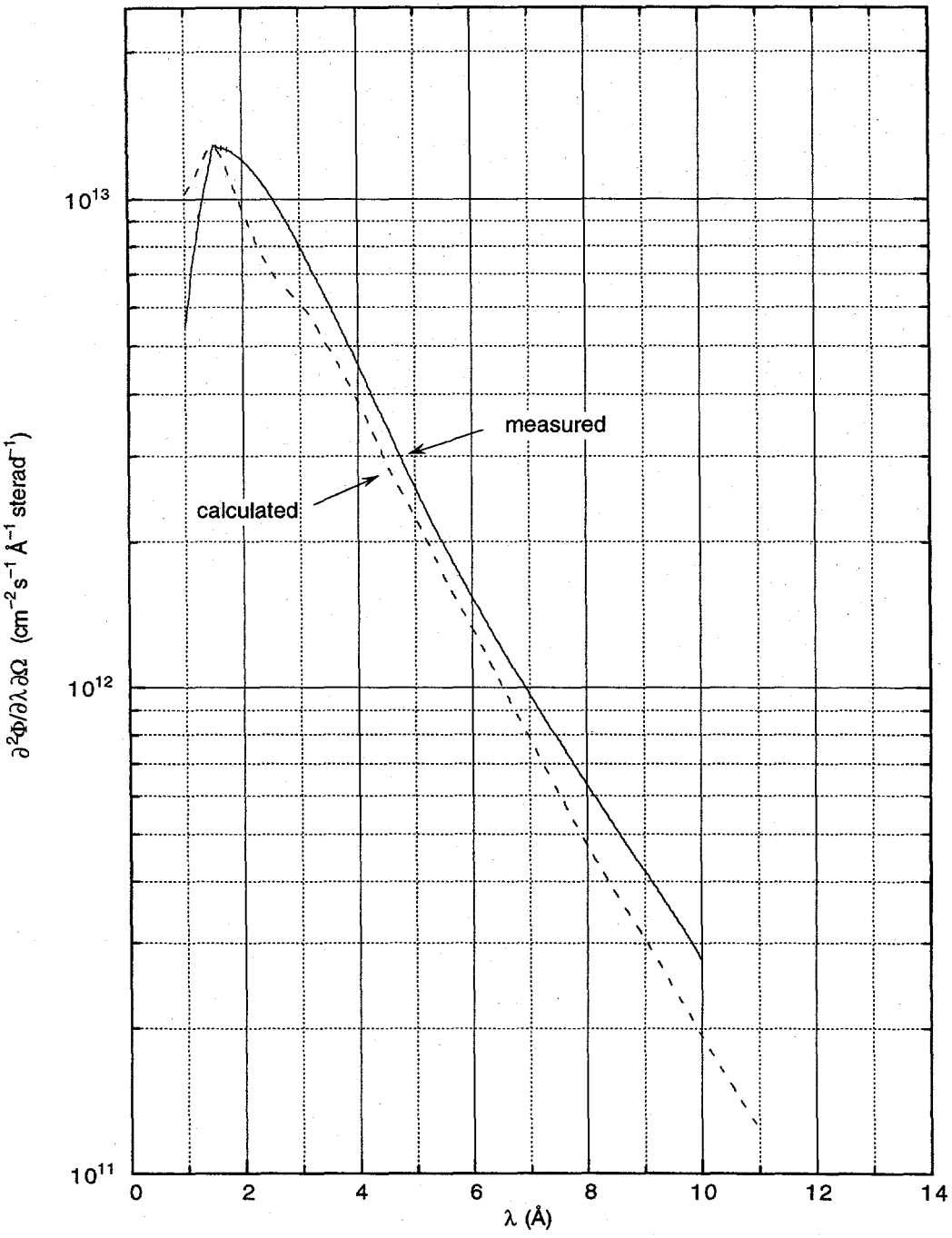

Fig. 2. Comparison of calculated and measured source brightness for the ILL horizontal liquid D_2 moderator.

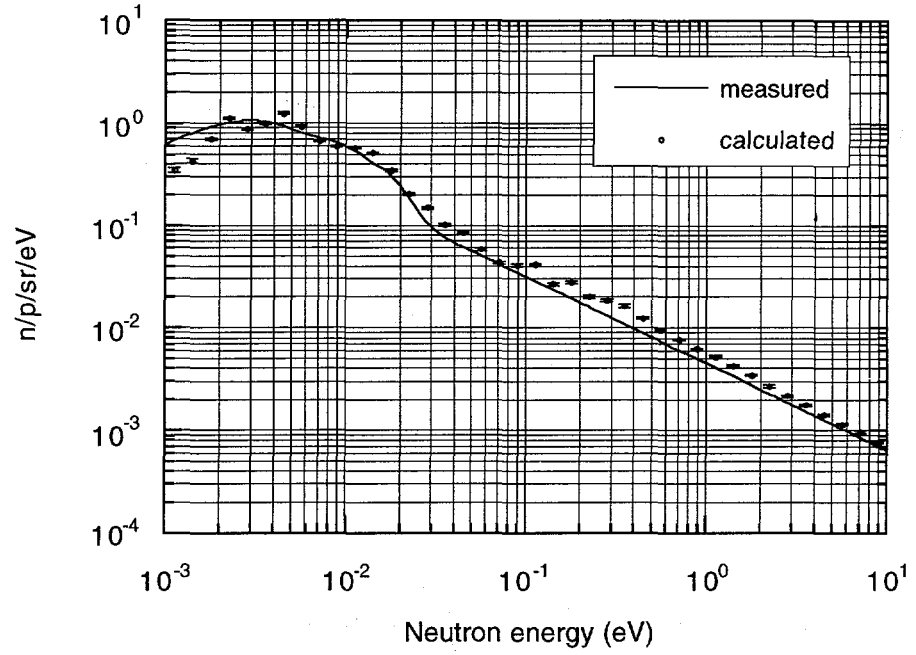

Fig. 3. *Comparison between calculated and measured source brightnesses for the LANSCE as-built liquid H_2 moderator.*

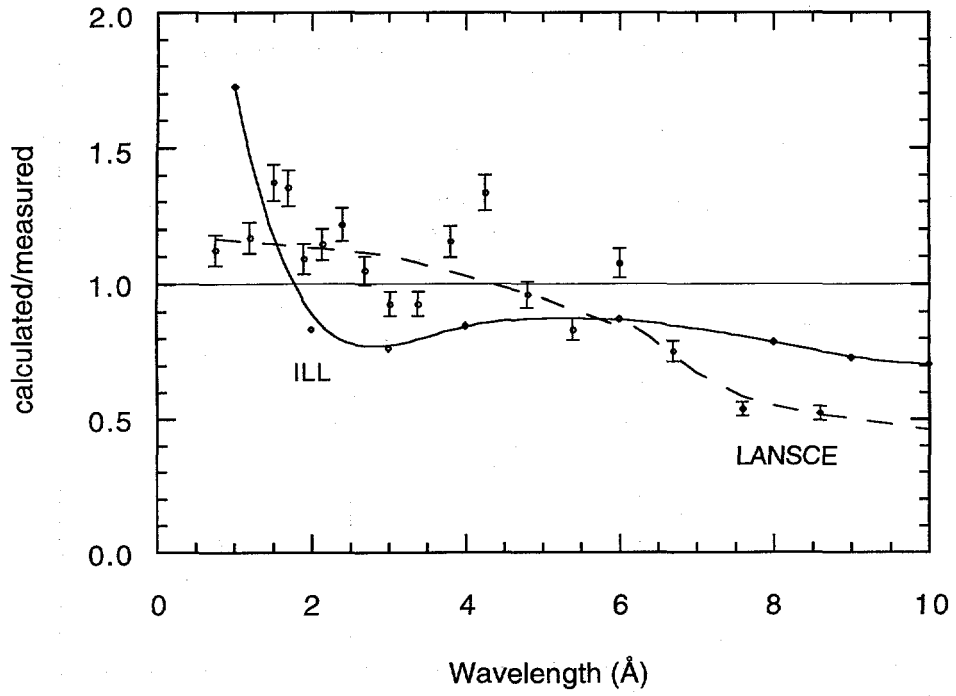

Fig. 4. *Ratio of calculated-to-measured cold source brightness for the ILL horizontal liquid D_2 source, and the LANSCE liquid H_2 source.*

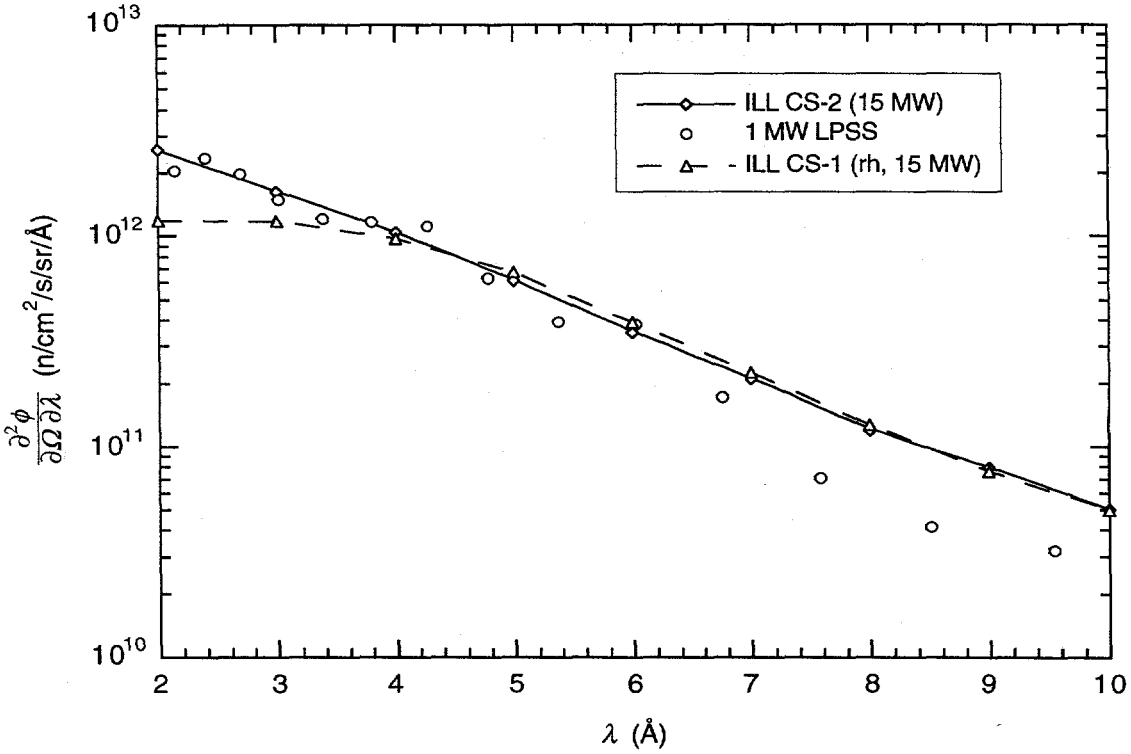

Fig. 5. Time-averaged brightness as a function of wavelength from a 5×13×13 cm³ coupled liquid hydrogen moderator for the 1-MW benchmark geometry compared with the brightness of the two cold sources at the ILL. The brightness of the ILL sources have been divided by 4.

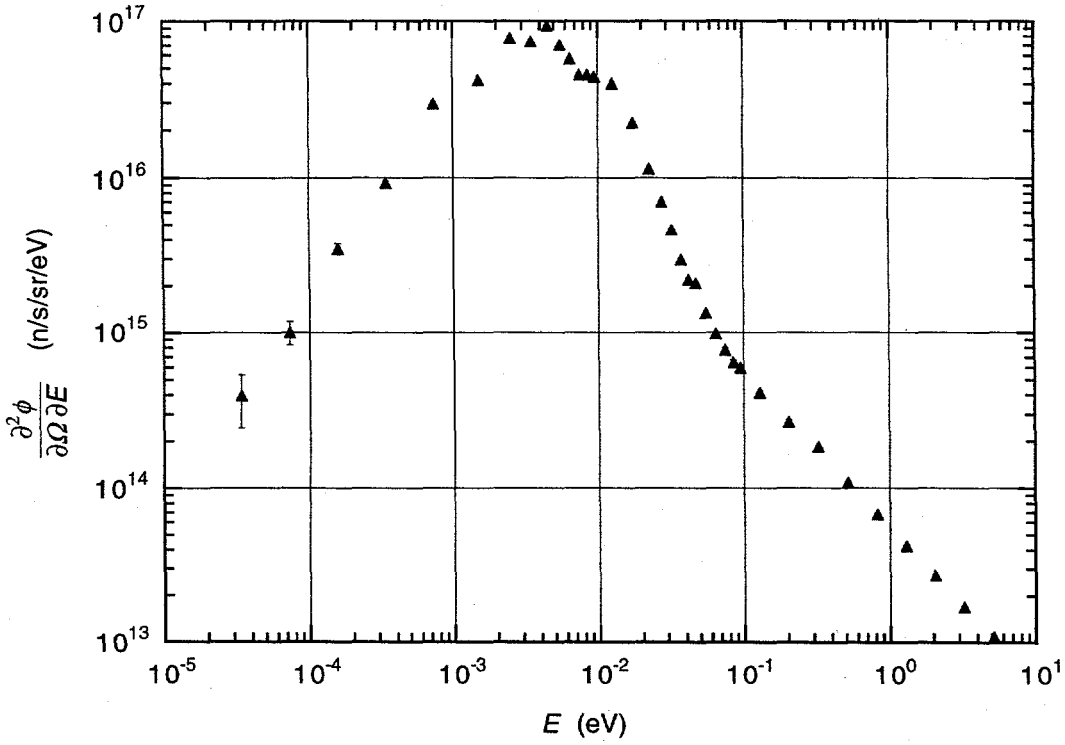

Fig. 6. Benchmark liquid hydrogen energy-spectrum.

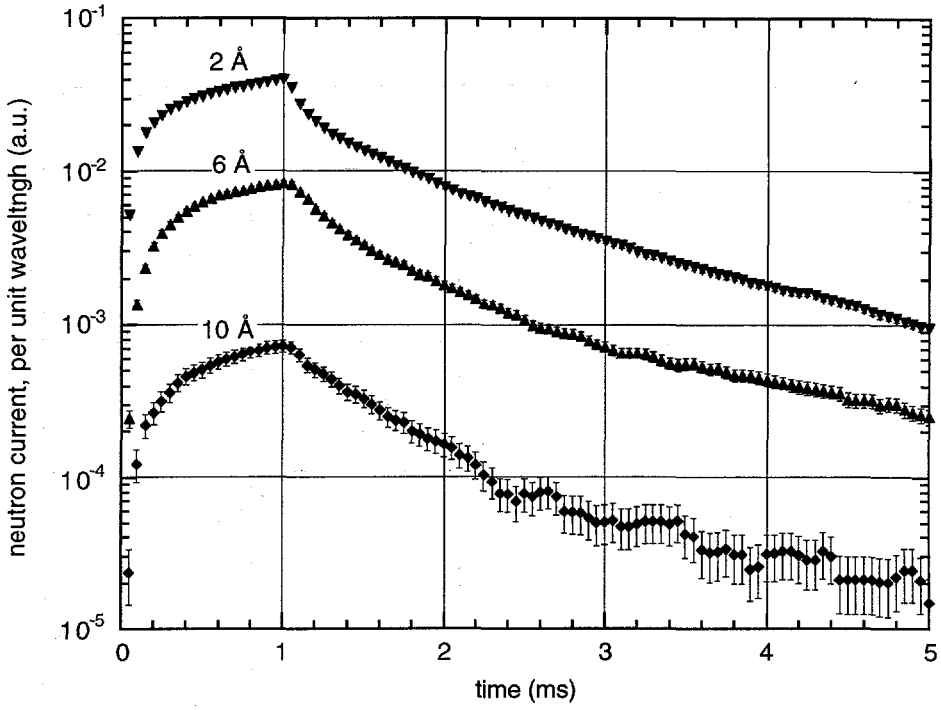

Fig. 7. Pulse shapes from a 5×13×13 cm³ coupled liquid hydrogen moderator for the 1-MW LPSS geometry, for a 1-ms proton pulse. These pulse shapes are obtained by convoluting the neutron pulse structure as shown in fig. 5 with a 1-ms proton pulse. The data are summed over 0.25-Å bins about the specified wavelengths. The inner Be reflector size is 150 cm.

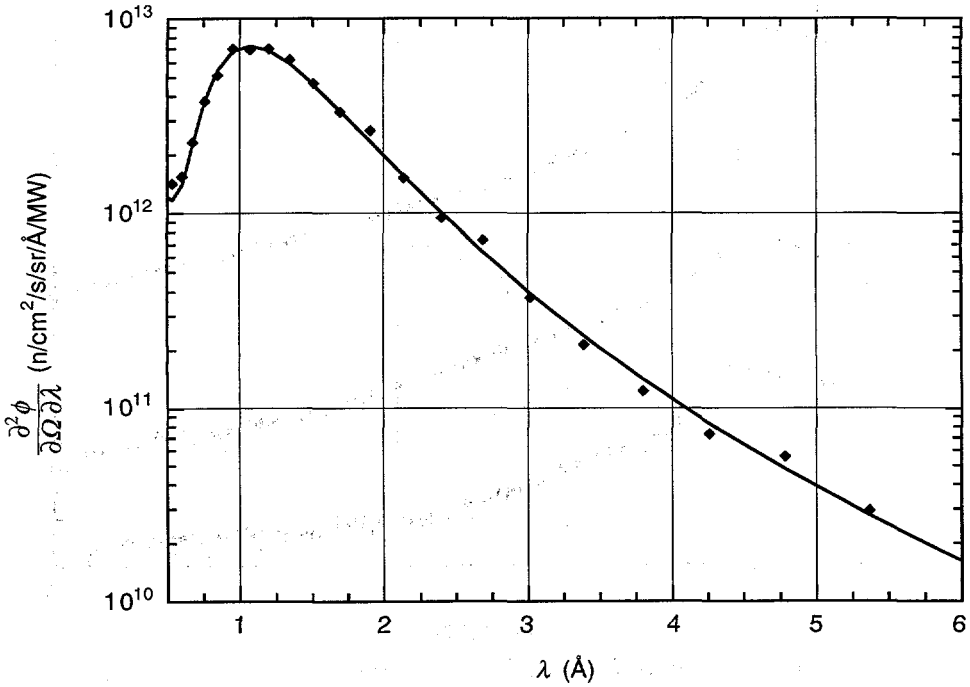

Fig. 8. Time-averaged brightness as a function of wavelength from a 4×13×13 cm³ coupled light water moderator for the 1-MW benchmark geometry.

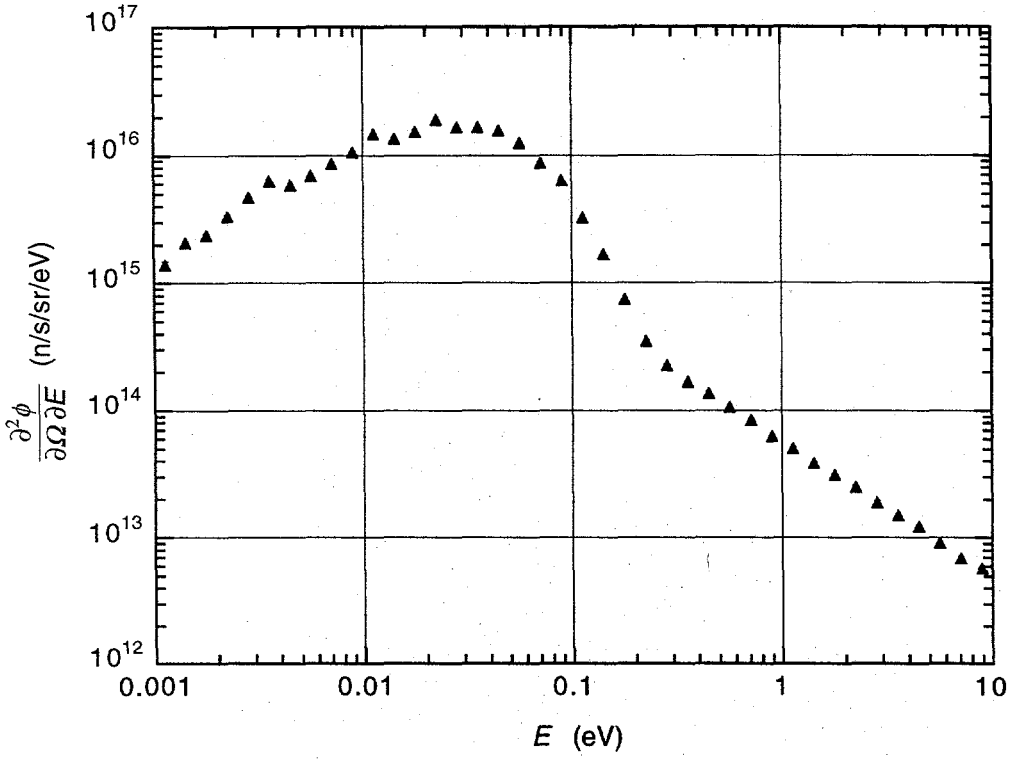

Fig. 9. Benchmark water energy spectrum.

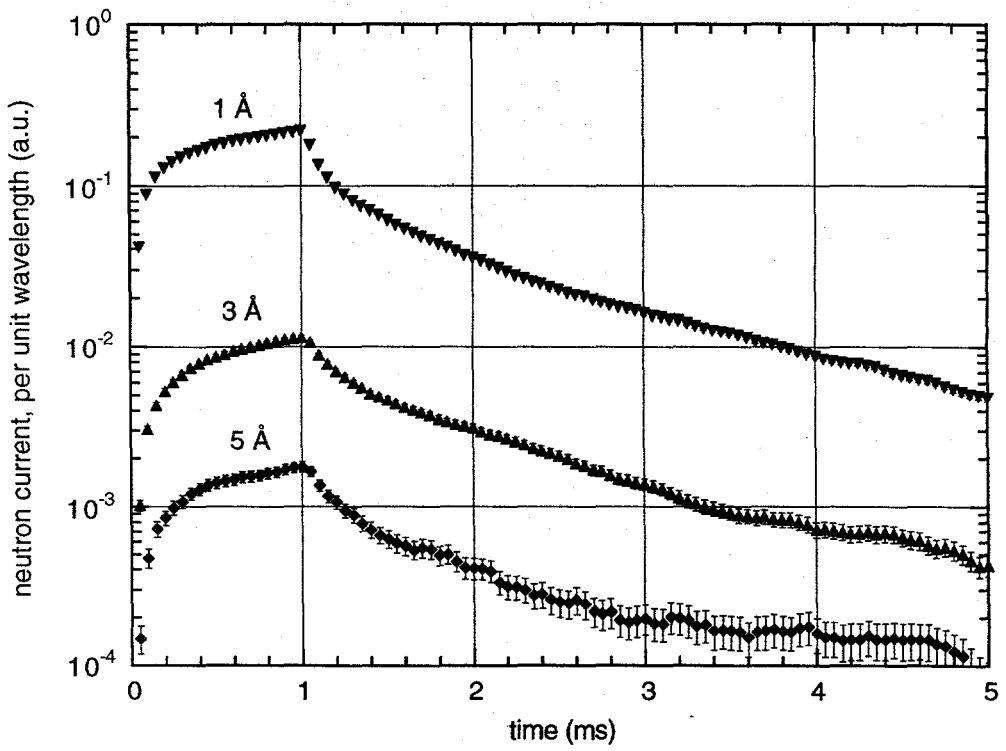

Fig. 10. Pulse shapes from a 4×13×13 cm³ coupled light water moderator for the 1-MW LPSS geometry, for a 1-ms proton pulse. Other parameters are the same as those given in fig. 7.

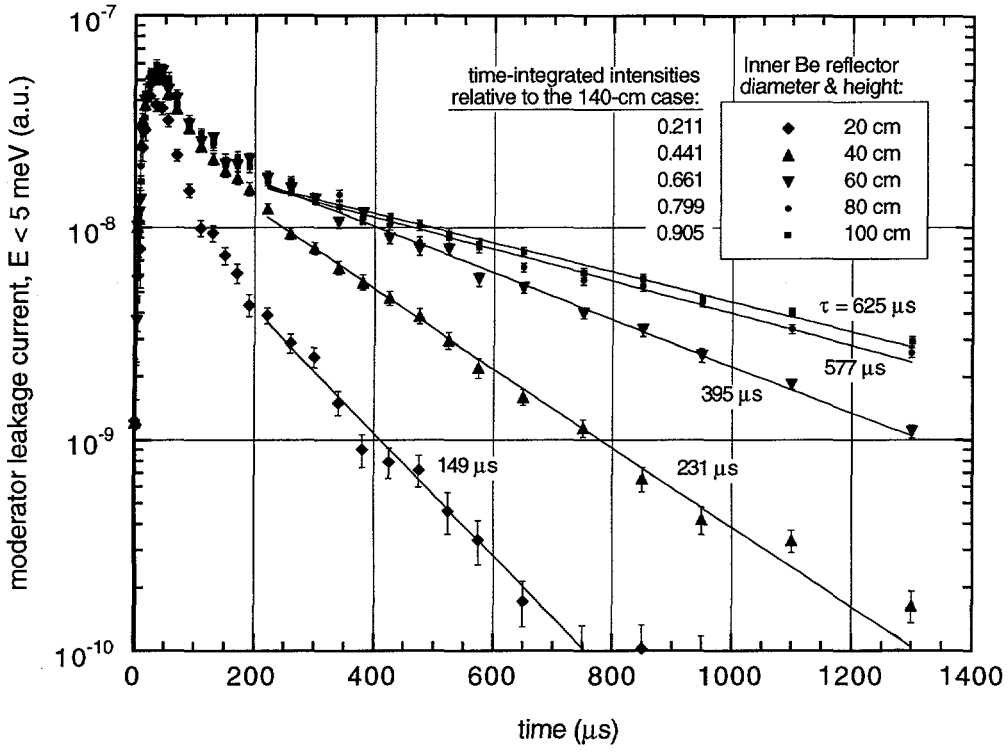

Fig. 11. Pulse shapes for an instantaneous proton pulse for various inner Be reflector sizes.

MONTE CARLO SIMULATION OF NEUTRON SCATTERING INSTRUMENTS

P. A. Seeger

Sumner Associates and LANSCE

Abstract

A library of Monte Carlo subroutines has been developed for the purpose of design of neutron scattering instruments. Using small-angle scattering as an example, the philosophy and structure of the library are described and the programs are used to compare instruments at continuous wave (CW) and long-pulse spallation source (LPSS) neutron facilities. The Monte Carlo results give a count-rate gain of a factor between 2 and 4 from using time-of-flight analysis. This is comparable to scaling arguments based on the ratio of wavelength bandwidth to resolution width.

Statement of the Problem

We want to know how an instrument copied from D11 at the Institut Laue-Langevin (ILL) reactor would perform on a long-pulse spallation source (LPSS). We choose to compare at a specific configuration of D11, namely 10.5 m collimation length and 10.5 m sample-to-detector distance, for a total instrument length of 21 m as shown in fig. 1. Instead of simulating the losses of the guides and velocity selector at D11, we use the measured flux at the sample [1], doubled to represent improvement seen in initial tests of the new velocity selector "Costanze" [2]. The wavelength distribution is assumed to be triangular with 12% FWHM. To make the collimation identical for the two cases, we restricted the view of the LPSS moderator down to be the same as the D11 guide exit, 30 x 50 mm^2, and we fixed the sample diameter at 10 mm. The same detector is also assumed for both cases.

The wavelength bandwidth of an LPSS instrument is limited by the pulse repetition rate and the total moderator-to-detector distance; wavelength resolution on the other hand is achieved by measuring the time of flight (TOF) of each neutron from the moderator to the detector. Higher total neutron flux on sample is available because the bandwidth does not need to be limited by the resolution; a simple measure of TOF Gain is the ratio of the bandwidth to the resolution width. (More precisely, it is the integrated flux on sample over the full bandwidth divided by the integrated flux over one resolution width.) The maximum achievable bandwidth is inversely proportional to the instrument length and to the pulse repetition rate. For 21 m and 60 Hz, it is 3.1 Å. From this we can estimate the "ideal" TOF Gain for this simulation as a function of neutron wavelength as

$$G = 3\ \text{Å} / (0.12\ \lambda)\ .$$

Thus for 10-Å neutrons we can expect a gain of nearly 2.5, and at 6 Å a gain of about 4. We have used a FWHM of 12% because that is typical of present day small-angle scattering measurements. The TOF method has the potential of improved resolution without sacrifice of count rate; if better resolution is useful, then the TOF gain factor will be correspondingly larger, up to a value of about 15 set by the duty cycle of the source.

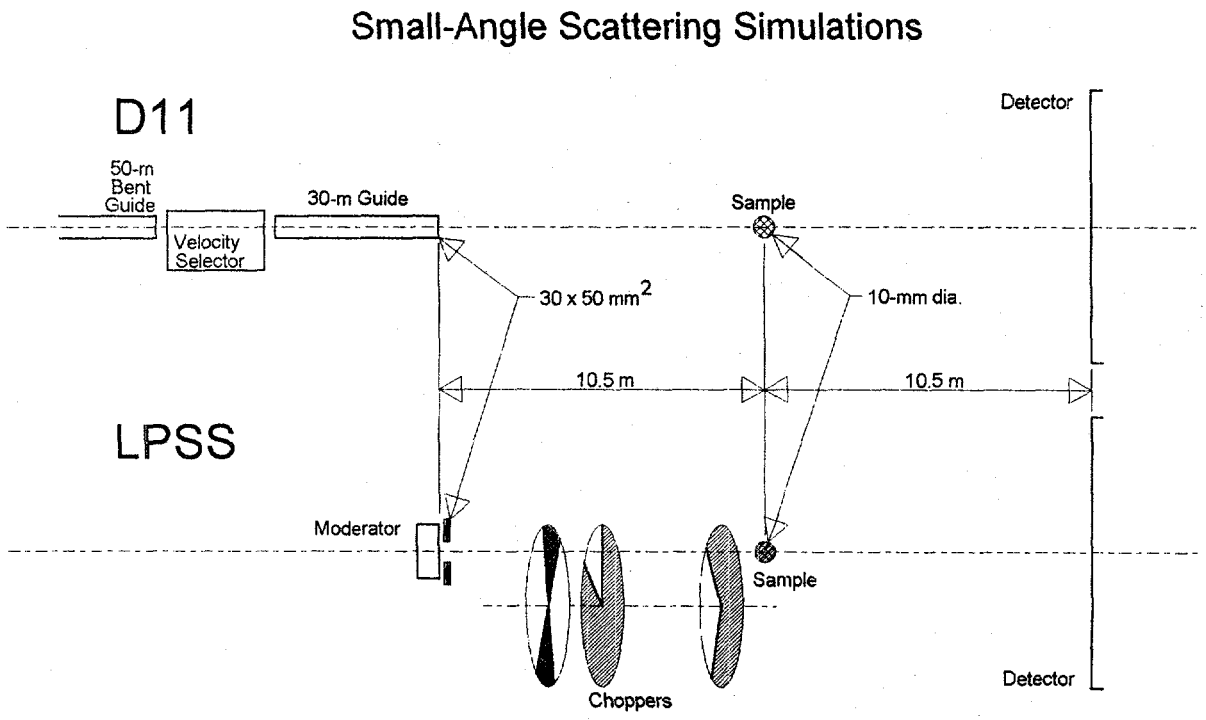

Fig. 1. Geometry of the test case for comparing small-angle neutron scattering at a CW source vs. an LPSS. Identical collimation, sample, and detectors are used to assure identical geometric contributions to the resolution.

This "ideal" estimate of the TOF Gain must be reduced in "real life" because choppers (of finite speed) must be used to guarantee that no neutrons from different pulses can reach the detector while it is counting the frame of interest. Several "real-life" questions must be addressed:

- What factors affect the $\Delta\lambda$ bandwidth?
- Is the TOF resolution really as good as CW?
- Does the full bandwidth contribute useful information?
- What is the dynamic range in Q?

To find the answers to these questions we must include the effects of the neutron pulse shape and the choppers, as well as the geometry of the collimation and detector. Monte Carlo techniques are very useful in studying these effects.

Monte Carlo Library MCLIB

Monte Carlo is a method to integrate over a large number of variables. Random numbers are used to select a value for each variable, and the integrand is evaluated. The process is repeated a large number of times and the resulting values are averaged. For a neutron transport problem, we first select a neutron from the source distribution, and project it through the instrument using either deterministic or probabilistic algorithms to describe its interaction whenever it hits something, and then (if it hits the detector) tally it in a histogram representing where and when it

was detected. This is intended to simulate the process of running an actual experiment (but it is *much* slower).

The present MCLIB library has been derived from codes written by Mike Johnson at the Rutherford Laboratory [3]. Significant additions and revisions were made by this author in 1984, and the entire code was rewritten in a structured form in 1994. Whenever the code has been applied to new problems, additions have been made. Thus significant contributions to the present library have been made by Richard Heenan (Rutherford-Appleton Laboratory), and specifically for the LPSS by Glenn Olah, Bob VonDreele, Greg Smith, and Luke Daemen (LANSCE). Mike Fitzsimmons and Joyce Goldstone have contributed greatly to the debugging process.

The geometry of a system is described by surfaces and regions. A *surface* is defined by a general 3-dimensional quadratic equation of the form

$$Ax^2 + Bx + Cy^2 + Dy + Ez^2 + Fz + G + Pxy + Qyz + Rzx = 0$$

with 10 coefficients, plus a roughness parameter. The geometric shape of each *region* is defined by its relationship to each surface: the region is said to be on the positive (negative) side of a surface if the quadratic expression for the surface evaluates to a positive (negative) value for all points within the region, and the entry for that surface in the region structure is therefore made positive (negative). Information about what is contained within a region is stored by assigning a predefined type number (*e.g.*, 31 for a scattering sample of hard spheres) to the region, along with however many parameters are needed. Future development of the library should be accomplished by defining new region types and implementing the corresponding algorithms for how a neutron interacts in such regions. A complete description of the library will be given in ref. [4].

Features of MCLIB which are different from other Monte Carlo libraries include

- Simplified transmission through materials. Rather than compute microscopic interaction in a simple (amorphous unpolarized) region, attenuation of the transmitted neutron is calculated.
- Optics at surfaces. When a neutron reaches a surface, the (complex) index of refraction is computed to decide whether the neutron will reflect or refract.
- Time-dependent devices. There are region types to describe moving devices such as choppers or a gravity focuser (a moving aperture to correct for gravitational droop).
- Scattering functions. Each kind of scattering sample is a region type. The scattering algorithm may be deterministic (reflectometry), probabilistic (hard-sphere scatterer), or a combination (Bragg reflection into a Debye-Scherrer cone).

Results of Monte Carlo Simulations

Since we will be combining and comparing distributions of different shapes, it is essential that we define "resolution" in proper statistical terms as the root-mean-square (rms or standard deviation, σ) of a distribution, rather than trying to represent it as full-width-half-maximum. For instance, for a square distribution such as the proton pulse width or a detector pixel, σ(square) =

FWHM/$\sqrt{12}$; for a triangular distribution such as the velocity selector, σ(triangle) = FWHM/$\sqrt{6}$; and for an exponential such as the long-time response of the moderator, σ(exponential) = τ = FWHM/ln(2). The σ values may always be combined quadratically to calculate the σ of a convolution, or it may be computed from the second moment of the result. After many effects are combined, the resulting distribution will approach a Gaussian, so that the standard deviation may be converted back to FWHM using σ(Gaussian) = FWHM/$\sqrt{(8 \ln(2))}$ = FWHM/2.355.

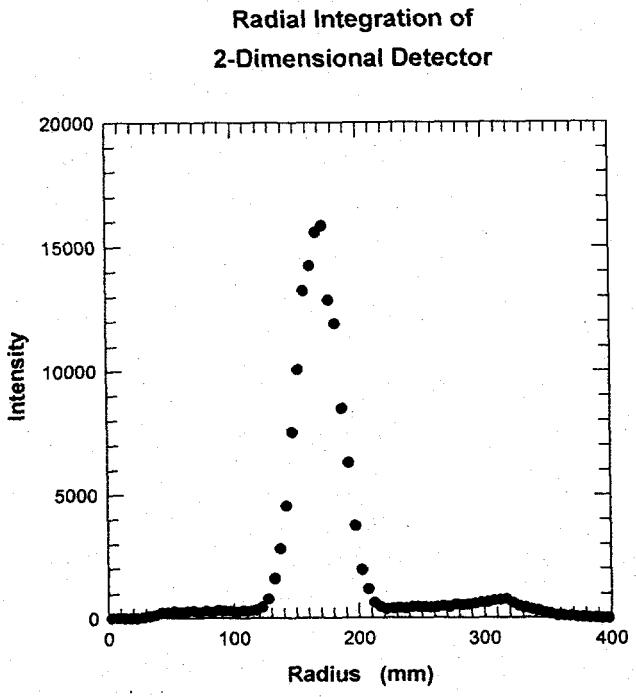

Fig. 2. Simulated response of D11 (at ILL) for a hypothetical scattering sample which scatters every neutron at the same value of Q (Q = 0.01 Å^{-1}). The shape of the peak is the overall resolution of the instrument, including both geometric and wavelength contributions. Double scattering can also be seen.

Figure 2 illustrates the raw data result of the simulation of D11 (*cf.* fig. 1), for the velocity selector centered at 10-Å, scattering at a fixed value of Q = 0.010 Å^{-1}, integrated in rings on a 640-mm square detector with 5x5 mm^2 pixels and rms encoding precision 3.4x3.4 mm^2. The peak is at 170 mm radius, and double scattering gives a second peak just off the edge of the detector, but visible in the corners. When converted to Q, the result reproduces the input value with high accuracy and precision. The instrumental resolution is the root-mean-square (rms) of the distribution, σ = 10.7%. This test simulation must now be compared to the LPSS case.

The moderator spectrum and also the time distribution of neutron emission (which is a function of neutron wavelength) are important when simulating a spallation source. We have used the spectrum for the coupled H_2 moderator, with Be reflector decoupled at a radius of 60 cm, as presented by Gary Russell [5]. The time dependence from the output of the MCNP computation has been fitted to a 6-parameter algorithm. We now try to answer the "real life" questions asked above.

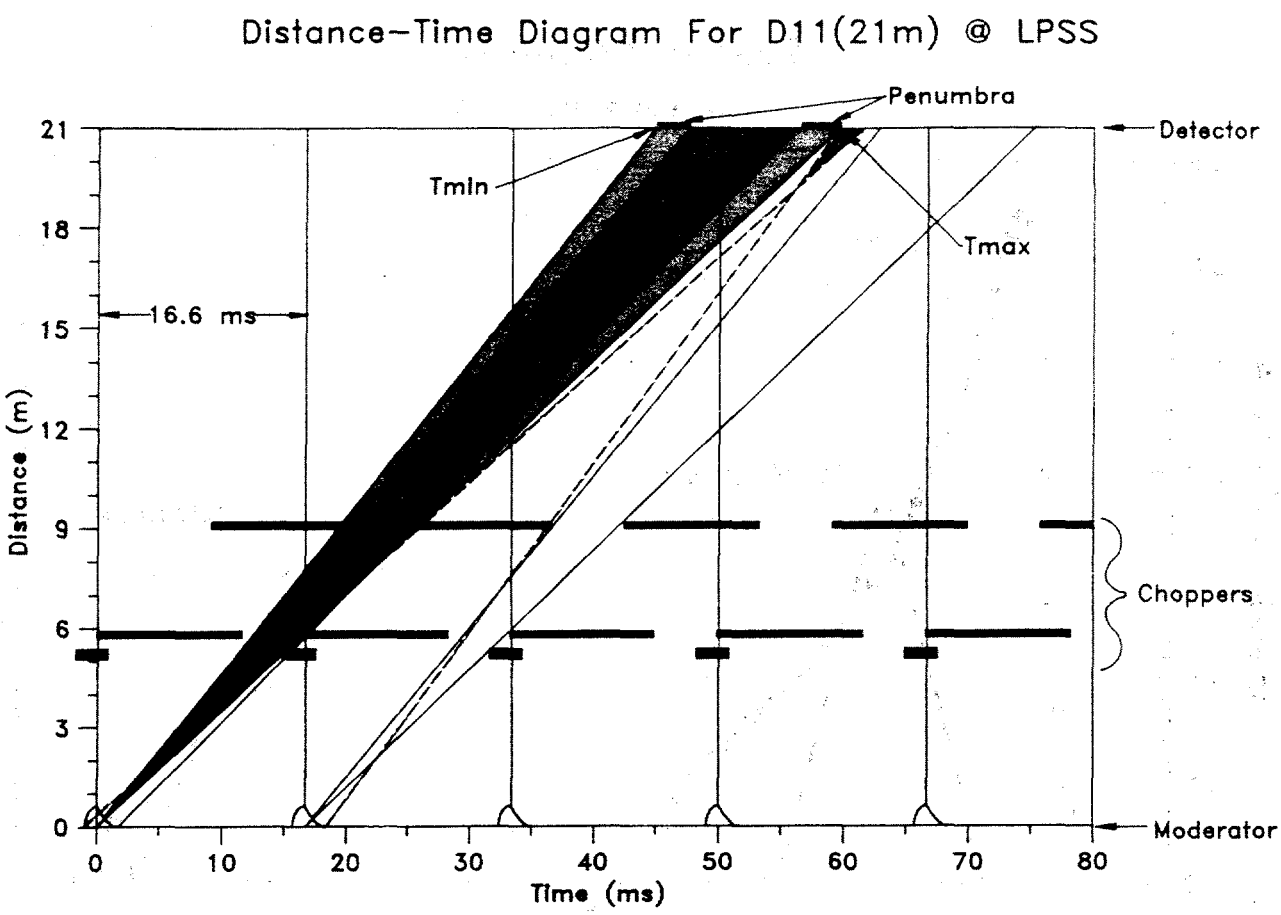

Fig. 3. Chopper phasing diagram. The functions of the three choppers are defined in the text. Slopes of the lines are equal to neutron velocity, which is inversely proportional to wavelength. With the phases drawn here, neutrons of wavelengths 8.5 to 11.5 Å are being counted in the detector.

What factors affect the $\Delta\lambda$ bandwidth?

As indicated in fig. 1 and in the distance-time diagram in fig. 3, there are three choppers in the LPSS simulation. The first, placed at 5.2 m from the moderator, is a massive "T_0" chopper to reduce room background for the duration of the proton pulse. The second chopper ("frame overlap", at 5.8 m) assures that fast neutrons from the following pulse cannot reach the detector. The actual "frame definition" chopper has been placed at 9.2 m (based on an optimization study by Glenn Olah). Its phase is adjusted to be half closed for the maximum wavelength to be recorded for neutrons emitted at t = 0; this defines T_{max}. We have arbitrarily chosen that the chopper must not begin to open again until the tail of the following pulse has decayed to 1/1000 (*i.e.*, 4.6 times the decay time constant). Finally, the T_{min} of the following pulse is defined by the delay after T_{max} after which we can guarantee that the frame definition chopper is fully closed (including rms phase jitter of 20 μs). As shown in fig. 3, there is a large penumbra associated with the finite velocity and the phase jitter of the choppers, and the bandwidth is limited by the overlap between closing for one pulse and opening for the next. These effects are seen quantitatively in fig. 4, which shows two Monte Carlo results for neutron spectra passed by the choppers when set for bands centered at 6 Å and 10 Å respectively.

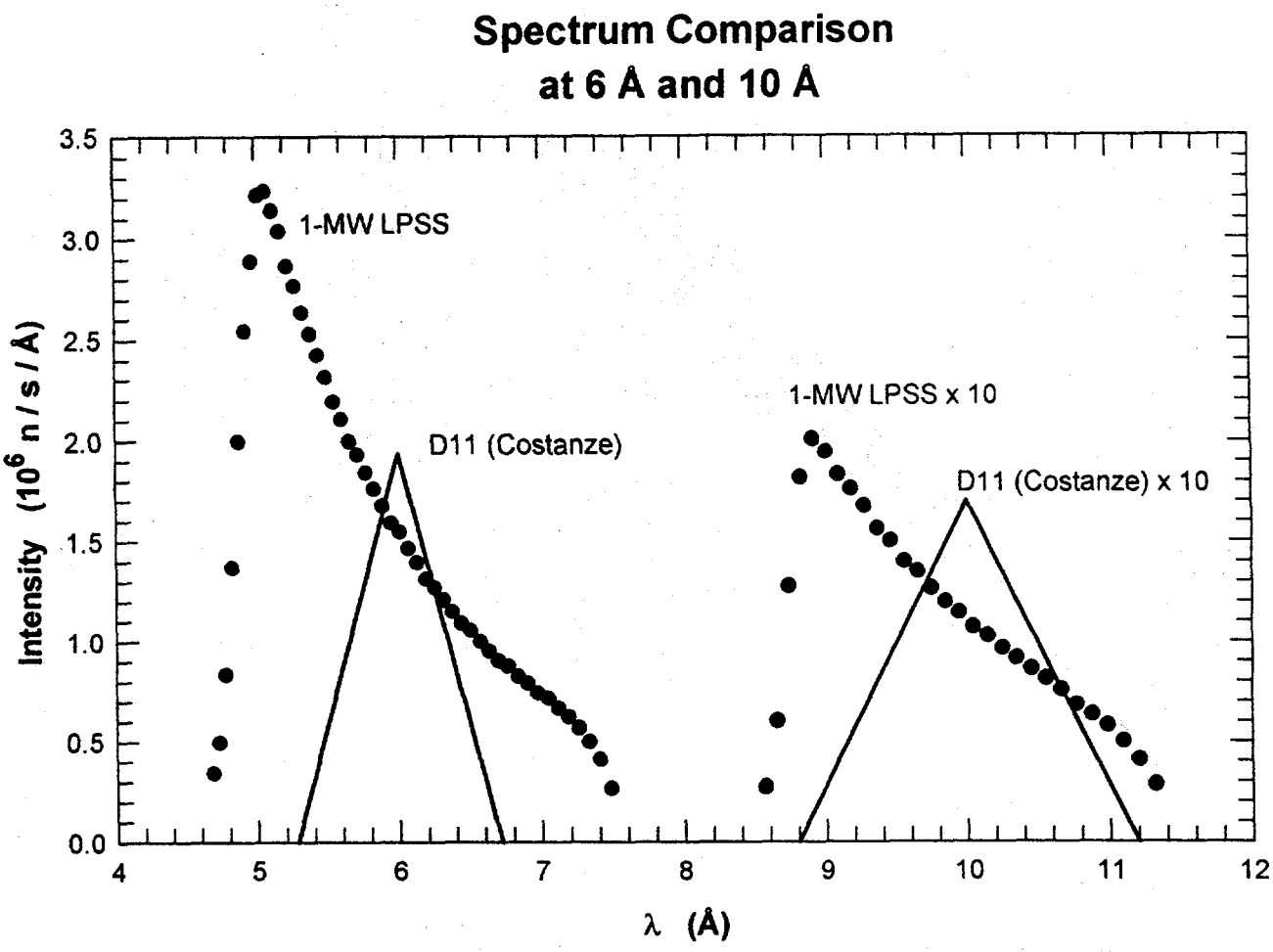

Fig. 4. Neutron spectra passed by the chopper system at two different phase settings, compared to the assumed triangular distribution of the "Costanze" velocity selector.

Is the TOF resolution really as good as CW?

The most significant time-of-emission parameter for the relatively long wavelength neutrons used here is the exponential decay of the Maxwellian component, which is 375 μs. This exponential dominates the time resolution; when it is convoluted with the 1 ms wide proton pulse, the resulting time resolution is 473 μs, corresponding to 0.09 Å at a flight path of 21 m. This is better than the 4.9% (rms) resolution of the Costanze velocity selector at any wavelength longer than 2 Å. In the LPSS simulation near 10 Å, data were tallied in 29 nominal wavelength slices depending on time of arrival at the detector. Thus we acquired 29 data sets similar to fig. 2; fig. 5 presents these on a 2-dimensional plot. For each longer wavelength, the scattered peak is further out on the detector. If the rows are added without first making the wavelength correction, resolution is degraded; a 12% velocity selector corresponds to adding up the center 12 rows. TOF gives us the power to make wavelength-dependent corrections, and to convert each slice to a function of Q before combining, and thus to retain the full resolution. Even with the relatively long pulses of an LPSS, TOF resolution is inherently better than a velocity selector designed to pass a significant number of neutrons.

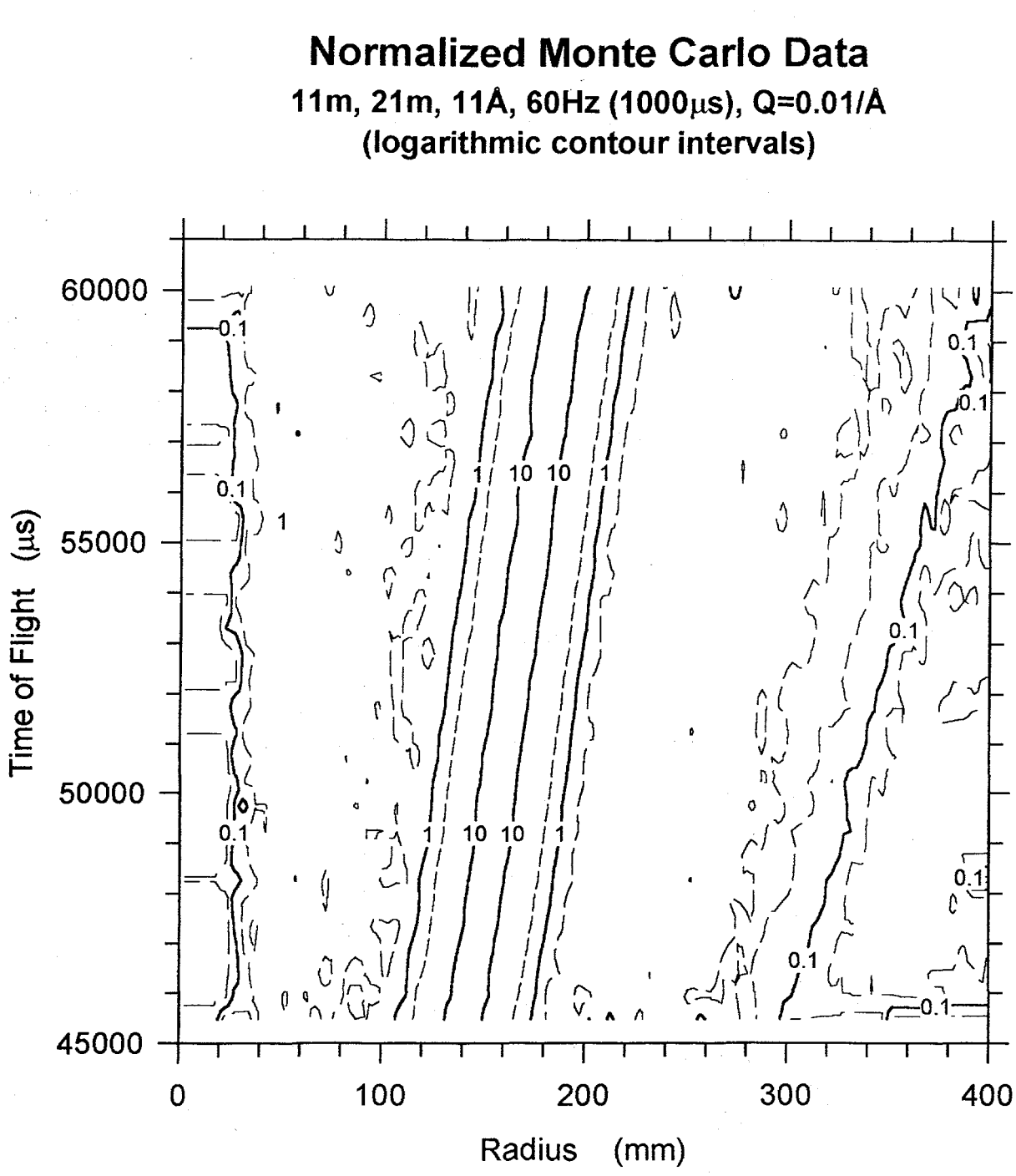

Fig. 5. Radially integrated data for the 1-MW LPSS simulation. A horizontal slice would correspond to a single wavelength, and would be similar to fig. 2. The 29 independent wavelength slices are converted to a Q scale before summing, virtually eliminating the wavelength contribution to the resolution.

Does the full bandwidth contribute useful information?

For the case shown in fig. 5, the answer is "yes". For the case near 6 Å, however, a good deal of the count rate comes from neutrons nearer to 5 Å wavelength. The peak for those slices is at 5/6 of the radial position on the detector, and the relative error due to detector geometry increases by 6/5. To keep resolution equal to that of D11, the first 12 or so (of 48) time slices would be omitted from the final data analysis. This is indicated in Table 1 in the row labeled "Equal Resolution." Since all of the data are recorded during the experiment, the user may decide during data reduction to sacrifice resolution for higher count rate; this gives the "Maximum Count Rate" row in Table 1, corresponding to a 15% resolution degradation. The table shows what fraction of our original estimate of "Ideal" TOF Gain is realized in a relatively realistic simulation of D11.

Table 1: Time-Of-Flight Gain Factor

3-Å Bandwidth *vs.*

12% Velocity Selector

	λ = 6 Å	λ = 10 Å
"Ideal" TOF Gain	**4.2**	**2.5**
"Real Life" Equal Resolution	**2.7**	**2.2**
"Real Life" Maximum Count Rate	**3.8**	**2.2**

What is the dynamic range in Q?

From fig. 4 we see that useful data may be obtained at wavelengths both longer and shorter than the nominal band center. The effect is limited by the pulse repetition rate, however, and is not very significant at 60 Hz. As is also the case with D11 at a CW, most experiments would require two instrument settings; at an LPSS this involves changing wavelength bands by changing the phasing of the choppers. Another option would be to have the phase of the frame overlap and frame definition choppers continuously varying (*e.g.*, by running at 59.9 Hz instead of 60 Hz), so that every 10 seconds or so the complete Q range would be collected. This could be helpful in measuring kinetics of systems on time scales of minutes or shorter.

Table 2: Calculated Ratios of D11 Monte Carlo Benchmark

at Q = 0.01 Å^{-1}

1-MW LPSS / ILL

	λ = 6 Å	λ = 10 Å
Count Rate: high resolution (total)	**2.8** (4.0)	**1.4**
Q_{min}	**0.80**	**0.88**
Q Resolution: at reduced rate (full count rate)	**0.95** (1.10)	**0.93**
Q_{max}	**1.3**	**1.2**

Conclusions

Table 2 compares the simulated experimental results for the cases illustrated in fig. 1, a D11-type instrument at the ILL reactor and at a 1-MW LPSS (60-Hz, 1-ms proton pulses), using 6-Å and 10-Å neutrons, respectively. The LPSS exceeds the CW source in all four performance measures: count rate is higher; minimum Q is lower; resolution is better; and dynamic range is wider. The latter three of these are not terribly significant, and are readily understood from the use of TOF instead of a velocity selector. We must ask, however, why the count rate is significantly *higher* than ILL, when we expect our time-average flux to be only a quarter of that of the 60-MW reactor. In fig. 4 we see that our estimated flux at 10 Å is 63% of the peak for Costanze (based on a preliminary measurement), or a factor of about 2.5 higher than anticipated.

We believe there are three probable loss terms in the flux observed at D11. D11 is not on the CS-2 cold source, but on a less efficient source. There are about 80 meters of guide between the source and D11, and a typical loss is 1% per meter would reduce the transmission to about 45%. The transmission of the velocity selector may be between 80% and 90%. These factors may easily account for a factor of 2.5 decrease of the D11 flux from the ideal CW source. We await clarification from ILL, as well as the results of more precise measurements of the Costanze flux.

We believe the scaling rules work. Furthermore, we state that a D11-type instrument at a 1-MW LPSS would outperform the existing D11 for any experiment which requires a Q_{min} greater than or equal to that provided by the 21-m configuration. Note that we have used the D11 collimation

apertures and constant sample size throughout these simulations. Optimization studies begun by Glenn Olah show that some additional gains (of the order 20–30% in count rate, and even larger improvements in resolution) are possible beyond those shown in Table 2, by using a circular collimator entrance aperture and using asymmetric flight paths. Even larger gains will be possible if larger sample sizes and multi-aperture collimators are used, because we can view a moderator area much larger than the D11 guide size. We also note that these results depend strongly on the pulse rate; at 30 Hz instead of 60 Hz, for example, we would have twice the TOF Gain and would be equivalent to four times D11 instead of double.

References.

[1] P. Lindner, R. P. May, and P. A. Timmins, "Upgrading of the SANS instrument D11 at the ILL," Physica **B180** (1992) 967.

[2] P. Lindner, e-mail communication, March 19, 1995.

[3] M. W. Johnson and C. Stephanou, "MCLIB: A Library of Monte Carlo Subroutines for Neutron Scattering Problems," Rutherford Laboratory report RL-78-090.

[4] P. A. Seeger, "The MCLIB Library: Monte Carlo Simulation of Neutron Scattering Instruments," Proceedings of ICANS-XIII, Paul Scherrer Institut, Villigen, Switzerland, Oct. 11–14, 1995 (in preparation).

[5] G. J. Russell, "The Calculated Performance of a Benchmark Target/Moderator System for an LPSS," Instrumentation for a Long-Pulse Spallation Source Workshop, Lawrence Berkeley Laboratory, Berkeley, CA, April 18–21, 1995 (these proceedings).

PERFORMANCE OF A REFLECTOMETER AT CONTINUOUS WAVE AND PULSED NEUTRON SOURCES

M.R. Fitzsimmons

Manuel Lujan, Jr. Neutron Scattering Center, Los Alamos National Laboratory,
Los Alamos, New Mexico 87545

Introduction

The Monte-Carlo simulations presented here involve simulations of reflectivity measurements of one sample using a reflectometer of traditional geometry at different neutron sources. The same reflectometer was used in all simulations. Only the characteristics of the neutron source, and the technique used to measure neutron wavelength were changed. In the case of the CW simulation, a monochromating crystal was used to select a nearly monochromatic beam (MB) from the neutron spectrum. In the simulations of the pulse sources, the time needed to traverse a fixed distance was measured, from which neutron wavelength is deduced.

A "reflectometer of traditional geometry" is an instrument which uses a pair of slits of height h and width w separated by a distance L_S to define an incident beam that is highly collimated in the reflection plane. Since studies of liquid surfaces are not to be excluded, the reflection plane is taken to lie in the vertical plane, so h is small and w is large. An example of such a reflectometer is shown in Fig. 1.

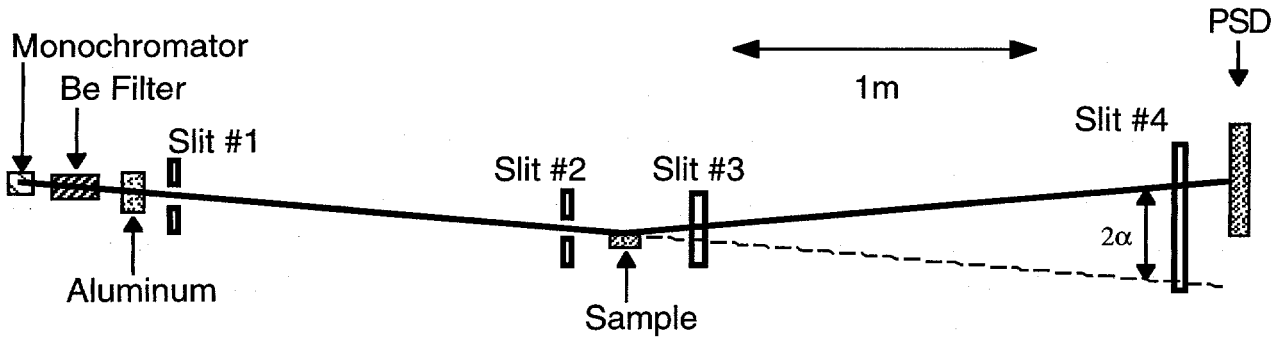

Fig. 1 *A reflectometer of traditional geometry is depicted. The reflectometer is configured with a monochromator and Be filter, which together produce a monochromatic neutron beam (MB) that is used in the MB simulation. The monochromator and Be filter are removed for the TOF simulations.*

The procedure for collecting a reflectivity profile involves adjustment of the slits in the vertical plane so that neutrons passed through the slits and intersected at an angle of α_i a sample resting in the horizontal plane. The sample was lowered as α_i increased so the footprint of the beam remained centered on the sample. The widths of the slits were equal (40 mm) and were not changed during the experiment. The vertical dimensions of the slits were also equal, but were adjusted to be proportional to the magnitude of the scattering vector, $Q=4\pi\sin(\alpha_i)/\lambda$, and equaled 1 mm when $Q=0.1\text{Å}^{-1}$. By changing the heights of the slits in this manner, the geometrical contribution, $d\alpha/\alpha_i$, to the resolution, $\delta Q/Q$ was kept constant with Q, since the other component

of $\delta Q/Q$, the spread in wavelength, $\delta\lambda/\lambda_0$, is always constant. Since the acceptance of the neutron beam by the slits varies as $\phi=(hw)^2/L_S^2$, the intensity of the neutron beam reaching the sample increased with Q^2. This increase partly negated the loss of signal owing to the decrease of the sample reflectivity which varied as approximately Q^{-4}.

The intensity of the radiation reflected by the sample was recorded in a position sensitive detector (PSD). The variation of the detector efficiency with neutron wavelength was included in the Monte Carlo simulation. After data collection, a new value of α_i was chosen, and if necessary, the process was repeated until the reflectivity profile was measured.

Details of the MB Simulation

The monochromated (MB) technique utilized a graphite crystal to select a nearly monochromatic beam from a coupled l-H_2 moderator providing a distribution of neutrons with different wavelengths. The trajectories of neutrons emanating from the moderator were chosen to be the same as that at the end of a Ni neutron guide for λ_0=4.1Å neutrons, or 0.8° (FWHM). The mosaic spread of the monochromator in the diffraction plane of the crystal was 1.4° (FWHM). The divergence of neutrons from the moderator, and the acceptance of the horizontal slits (in the diffraction plane of the monochromator) determine the wavelength spread of the incident beam to be $\delta\lambda/\lambda_0$=2% (FWHM). The projection of the monochromator onto the moderator equaled the size of the moderator, which was taken to be 13 cm by 13 cm. The reflectivity of the monochromator was 80%. The contamination of the neutron beam from harmonics of λ_0 was removed by a 150 cm-thick l-N_2 cooled Be filter.

Details of the TOF Simulations

The simulations of the TOF technique used the same reflectometer geometry; however, in lieu of a crystal monochromator and Be filter, the time of flight from the moderator to the detector was measured from which neutron wavelength was calculated. The TOF studies involved simulations of the performance of the reflectometer at long and short-pulse spallation sources. The operating parameters of each source are given by the repetition or pulse frequency, $f=1/\Delta T$, proton pulse width, δt, and composite time constant, τ.

In the TOF experiment, the contribution to the resolution corresponding to $\delta\lambda/\lambda_0$ is the temporal resolution, $\delta t/t$, where δt is the uncertainty in the starting time of the neutron, t_0, and t is the neutron time-of-flight. For this study, δt was chosen to be the FWHM of the top-hat function which represents the shape of the proton pulse. The change in the intensity of the neutron pulse with time, or the shape of the neutron pulse, can be thought of as the convolution of a top-hat function, representing a proton pulse of width with a damped exponential function with composite time constant τ. In all cases the power integrated under the top-hat function, or proton pulse, was constant. The integrated intensity under the neutron pulse; however, is strongly dependent on τ, so longer time constants produce brighter sources. The time-averaged brightness of the source where τ = 375 μs (LPSS-2, 4 and 5) is the same as that of the CW source. The FWHM of the neutron pulses very nearly equaled the proton pulse width, δt, for all the sources.

While the operating characteristics of the SPSS studied here are not the same as those proposed by the ESS, the FWHM of the neutron pulse from both are nearly identical (about 300 μs).

Since the geometrical configuration of the reflectometer was unchanged from the MB experiment, the geometrical contribution to $\delta Q/Q$ was also unchanged. Therefore, in order to achieve as good resolution as that used in the MB simulation, $\delta t/t \leq 2\%$ in the TOF simulation. Using this relation, the time-of-flight must be greater than or equal to $\delta t/0.02$, or $t \geq t_{min} = \delta t/0.02$. The length of the instrument, L [m]— the length of the neutron guide plus the 4m long reflectometer, was determined by the shortest wavelength neutron desired and t_{min} [s], i.e. $L = 3956 t_{min}/\lambda_{min}$. The maximum wavelength was $3956 t_{max}/L$, where $t_{max} = t_{min} + \Delta T$, and the bandwidth was $\Delta\lambda = \lambda_{max} - \lambda_{min}$ [Å]. For the simulation of the reflectometer viewing the LPSS, λmin was chosen so that λmin and λmax straddled the wavelength used in the MB simulation. The operating parameters of the instruments investigated in the simulations are shown below.

Table 1: Operating Parameters of the Different Sources and Characteristics of the Instruments

Source	f [Hz}	δt [ms]	τ [us]	B •10^{16} n/st/m^2/s	L [m]	λ_{min} [Å]	Δλ [Å]	F	t_{min} [ms]
CW	steady	-	-	5.5	4	4.1	=δλ	-	n/a
LPSS-1	60	1	230	3.9	60	3.38	0.94	3	51
LPSS-2	60	1	375	5.5	60	3.38	0.94	3	51
LPSS-3	60	1	490	6.7	60	3.38	0.94	3	51
LPSS-4	120	0.5	375	5.5	30	3.41	0.95	3	26
LPSS-5	120	0.735	375	3.9	36	3.76	0.62	4	34
SPSS	10	0.3	230	3.9	30	1.96	11.3	1	15

The TOF instruments vary in length from 30 to 60m. Only the last 4m of each instrument is the same for all the simulations. Since the penumbra of the slits in the horizontal plane is generally larger than the width of the moderator at these distances, some intensity from the moderator can be retained by transporting the neutrons to the reflectometer along a neutron guide. The attenuation of the neutron beam by a neutron guide coated with Ni^{58} was included in the Monte Carlo simulations for the TOF technique. No guide was used in the MB simulation. In practice, however, reflectometers at CW sources also view the source through a neutron guide, so the loss of performance due to the guide should also be included (but was not) in the performance of the MB simulation. The additional loss is probably similar to that identified for the 30m long SPSS instrument.

The TOF instruments also used up to three choppers to condition the neutron beam. The first is called the t_0 chopper and was placed at 5m. The purpose of the t_0 chopper is to stop most high energy neutrons and γ-radiation from reaching the experimental area. The second chopper is the frame overlap chopper and is used to intercept most of the very slow neutrons generated during earlier pulses. The frame overlap chopper was located 6m from the moderator. The third chopper is called the frame definition chopper and, as its name implies, serves to define which frame, F, neutrons are detected relative to their creation at t_0. The position of the frame

definition chopper (between the frame overlap chopper and the reflectometer) was chosen to select neutrons with wavelengths between λ_{min} and λ_{max}. The frame definition chopper was not needed for the simulation of the reflectometer at the SPSS, since the SPSS instrument used neutrons produced in the first frame only. The wavelength of a neutron was calculated from its velocity, which was measured by noting the time when the neutron arrived at the detector after traveling the length of the instrument.

Simulations of the Reflectivity Profiles

The sample used in the Monte Carlo simulations for which the reflectivity profile is desired, was taken to be a 600Å thick film of d-polystyrene (d-PS) on a Si substrate. The roughness of both interfaces was 5Å (FWHM). The selection of such a relatively simple sample tended to favor the simulation of the MB technique over the TOF technique, since information over a very broad region of Q was not needed in order to fit a simple model. By favoring the MB technique, the intensity gains realized when employing the TOF technique over the MB technique are believed to be conservative estimates.

The reflectivity profile [•'s in Fig. 2(a)] was measured using the MB technique from Q=0.009 to $0.106Å^{-1}$ by taking equal steps in α_i of 0.02°. For $Q>0.02Å^{-1}$, the counting time was increased with Q^2 as shown in Fig. 2(b). This increase combined with the increase of the acceptance of the slits yielded an exposure that varied as Q^4 and largely negated the Q^{-4} decay of the reflectivity profile. The result was a reflectivity curve whose fringe maxima had equal statistical precision [Fig. 2(b)]. The resolution in Q, $\delta Q/Q$ of each measurement is shown in Fig. 2(c). The presence of small peaks in Fig. 2(c) coincident with fringe minima in Fig. 2(a) is an indication that the real resolution of the instrument was better than that given by the vertical heights of the slits; rather, the geometrical contribution to the resolution should have been determined by the size of a detector element on the PSD.

Whereas the MB simulation required 100 separate measurements to sample the Q-range from 0.008 to $0.106Å^{-1}$ [because $\Delta\lambda$ ($=\delta\lambda$) was so small], a dozen or so separate measurements (one such measurement is called a macro-measurement— within one macro-measurement there are many more micro-measurements) were needed in LPSS simulations and only two for the SPSS simulation. The reflectivity profile from the simulation of the LPSS-2 source is shown in Fig. 3(a). The profiles produced by the other LPSS and SPSS simulations were generally similar to that shown in Fig. 3. The solid and dashed lines in Fig. 3(a) are used to distinguish different macro-measurements. These measurements were made by changing α_i, rather than changing the portion of the spectrum sampled by $\Delta\lambda$. The vertical dimensions of the slits were changed to be the same as those used in the MB simulation for the same values of α_i. The statistical precision and exposure time are shown in Fig. 3(b), and the resolution in Fig. 3(c). The statistical precision and resolution of the measurements from the LPSS-2 simulation are comparable to those of the MB simulation.

Gain Factors

The performance of an instrument will be measured relative to the time needed to collect the data shown in Fig. 2 for the MB simulation. The overall intensity gain, $G_{\prod}$, was calculated from the ratio of the collection times. The collection times (see Table 2) are those times needed such that

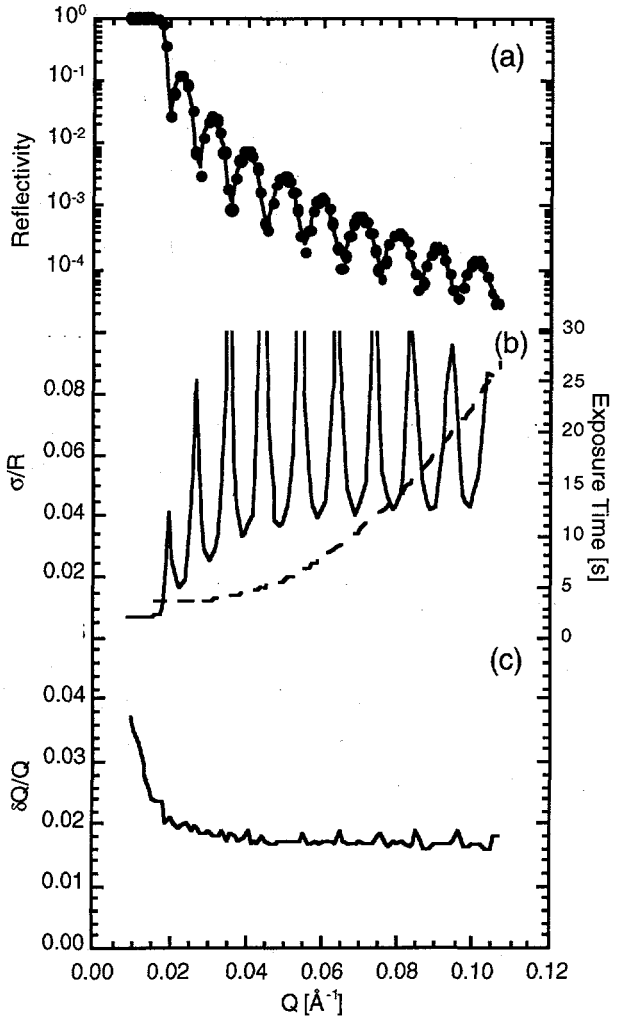

Fig. 2 (a) Data [•] simulated using the MB technique. 100 data points are shown. The curve is the reflectivity profile of a simple model. (b) The rms standard deviation divided by reflectivity for the simulated data plotted with the measurement time per point. (c) The rms resolution, δQ/Q, per point.

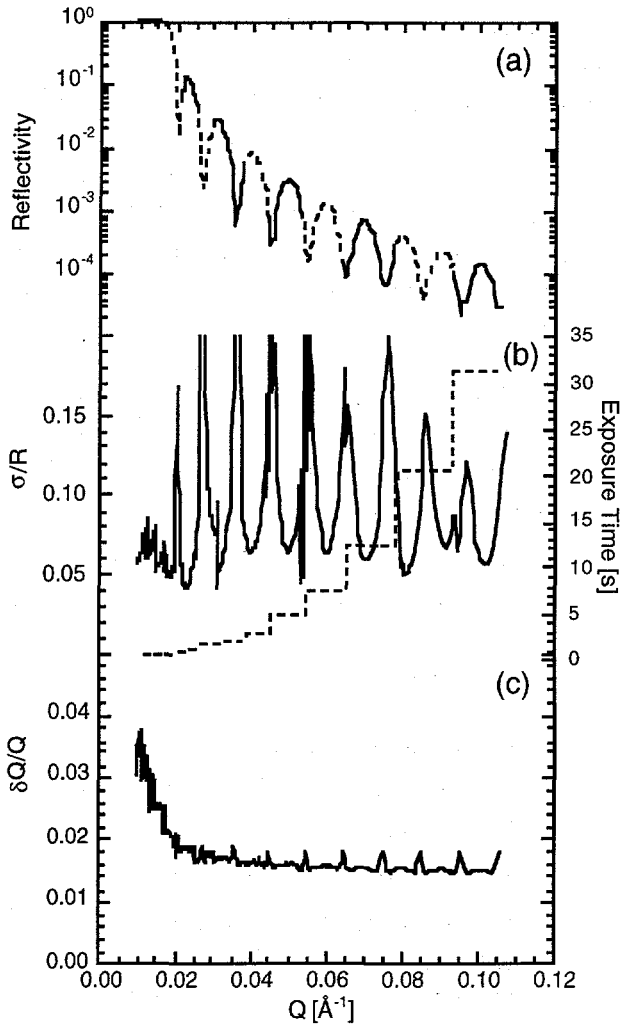

Fig. 3 (a) Data simulated using the TOF-technique. The profile is a concatenation of 13 separate macro-measurements shown as alternating solid and dashed lines. There are about 33 smaller micro-measurements within each macro-measurement. (b) The rms standard deviation divided by the reflectivity. The dashed curve shows the time needed for each macro-measurement. (c) The rms resolution, δQ/Q, for the measurements.

when a model is refined to the simulated data, the parameters of the model, i.e. the scattering length density of the d-PS film, its thickness and the roughness of the air-film and film-substrate interfaces, were equally precise for all simulations.

The overall gain is a product of several factors, ΠG_j. which represent sources of gains and losses for the different techniques. Often the individual values can be computed by hand or measured in the Monte Carlo simulation, since the simulation records sources of neutron losses.

The most important of the individual factors is the time-of-flight gain, G_{TOF}, which is also the most difficult to quantify, particularly in the case of the SPSS simulation. The naive approach is to equate G_{TOF} to $\Delta T/\delta t$, or preferably $\Delta\lambda/\delta\lambda$; however, this approach neglects some effects, for example time-dependent shadowing of the detector by the choppers. While the naive approach might be applicable to a small bandwidth instrument like that at an LPSS, the approach is perhaps inappropriate for a large bandwidth instrument like that at a SPSS. One purpose of this study is to determine when the naive calculation yields the correct answer. This can be easily accomplished here, since G_{TOF} can be calculated from the simulations by inverting the relation for G_{Π}.

The difference in the collection times of the simulations in addition to the TOF gain can be attributed to other "instrumental" factors. For example, the reflectivity of the monochromator was 80%, so the gain of the TOF technique, which did not use a monochromator, over the MB technique is $G_M=1/0.8 = 1.25$. Other factors include:

- Acceptance of the monochromator, G_A.
- Acceptance of the slits, G_ϕ. The intensity per unit energy of the neutron beam on the sample is the product of the brightness and acceptance of the slits, ϕ, (or sample, whichever was smaller). The MB technique has a degree of flexibility in that the sizes of the slits can be changed for each Q-measurement. The TOF technique using an LPSS has a similar ability to adjust the slits but only between macro-measurements. The TOF technique using a SPSS does not have this degree of flexibility.
- Transmission of the Be filter, G_{Be}.
- Transmission of the neutron guide, G_G.
- Variation of the spectrum, G_λ. The large-Q region is measured using the peak of the spectrum and measurements of this region invariably take the longest time; therefore, G_λ for the LPSS and SPSS simulations is nearly unity.
- Source brightness, G_B.
- TOF gain, G_{TOF}. A rough estimate of the TOF gain, G_{TOF}, is given by $\Delta T/\delta t \approx \Delta\lambda/\delta\lambda$, which is unity for the CW instrument, and about 8-12 for the various LPSS instruments listed in Table 2. For the SPSS, G_{TOF} is between 50 and 333 depending upon λ. The values of $\Delta T/\delta t$ are tabulated in Table 2. The values of G_{TOF} were deduced from the Monte Carlo simulation such that $G_{\Pi} = \prod G_i$. The TOF gain represents the number of measurements taken collectively at a pulse-source in the same time that would have been needed to take just one MB measurement at a CW source.

Table 2: Collection Time and Gain Factors

Source	T [s]	G_{Π}	G_M	G_A	G_ϕ	G_{Be}	G_G	G_λ	G_B	G_{TOF}	$\Delta T/\delta t$
CW	994	1	-	-	-	-	1	1	1	-	1
LPSS-1	115	8.6	1.25	1	0.94	1.08	0.7	0.97	0.7	14	17
LPSS-2	90	11	1.25	1	0.94	1.08	0.7	0.97	1	13	17
LPSS-3	63	15.8	1.25	1	0.94	1.08	0.7	0.97	1.23	15	17
LPSS-4	95	10.5	1.25	1	0.94	1.08	0.8	0.97	1	11	17
LPSS-5	126	7.9	1.25	1	1.03	1.08	0.8	1	1	7	11
SPSS	24	41.4	1.25	1	0.25	1.08	0.8	1	0.7	219	333

Conclusions

Simulations of a traditional reflectometer viewing CW, long-pulse and short-pulse neutron sources can produce equally accurate reflectivity profiles. Equally precise profiles can be obtained using any of the techniques studied here simply by collecting data for a long enough period of time.

All simulations of the TOF technique at a pulse source showed significantly reduced collection times compared to the MB simulation at a CW source, even when the collection times for the TOF techniques were increased so that the reflectivity profiles from all simulations were equally precise. The reflectometer viewing the LPSS-1, -2, -3 or -4 sources would out-perform (collection time was reduced) the same reflectometer at a CW source with the same time-averaged brightness by a factor of between 11 and 13. The SPSS instrument would out-perform the same instrument at a CW source of equal time-averaged brightness by a factor of more than 58.

The gains predicted for the reflectometers at pulse sources come primarily from the gain when TOF is used to measure neutron wavelength rather than monochromating the neutron beam. For the LPSS instruments, the TOF gain is given by the ratio of bandwidth to resolution in wavelength, $\Delta\lambda/\delta\lambda$, where $\delta\lambda \approx 0.02\langle\lambda\rangle$, which yield values between 13 and 15 for a pulse source with a 6% duty factor. Alternatively, the TOF gain for the LPSS instrument is between 80 and 90% of $\Delta T/\delta t$.

For the SPSS instrument, neither of these relations are very satisfactory. The TOF gain for this instrument is about two-thirds of that predicted by the relation $G_{TOF} = \Delta T/\delta t$. The failure of the relation for the SPSS is due in part to the choice of δt made here— the proton pulse width. For a short-pulse source with $\delta t = 0.3$ ms and $t = 300$ μs, the moderator time constant is a much larger fraction of the proton pulse width than is the case for the long-pulse sources; therefore, the neutron pulse width for the short-pulse source is correspondingly larger than δt.

The performance of the SPSS simulation, while impressive, is perhaps not as impressive as might have expected based on its time of flight gain, particularly in terms of delivering count-rate at Q_{max}. The performance of the SPSS simulation was hindered primarily for two reasons: First, the desire to use the peak of the neutron spectrum, and the requirement to achieve $\delta t/t$ no worse than 2%, dictated the choice of a relatively long flight path. Even though the repetition frequency was only 10 Hz for the SPSS, the relatively long flight path limited the bandwidth of the instrument and so reduced the time-of-flight gain. Secondly, and perhaps more importantly, the angle of incidence used in the SPSS simulation was only half that of the MB and LPSS simulations, so the acceptance of the neutron beam in the SPSS simulation was reduced by one fourth. The angle of incidence can be increased by using longer wavelength neutrons but only at the expense of using a portion of the neutron spectrum where there are fewer neutrons. Alternatively, an approach where slits are not employed in measuring specular scattering might result in an additional gain of four for the TOF technique at the SPSS, since G_ϕ would become unity for this source.

Acknowledgments

I wish to thank P.A. Seeger for providing and maintaining the Monte Carlo simulation code with which this study was possible. I also acknowledge valuable discussions with L. Daemen, R. P. Hjelm, C. F. Majkrzak, E. Pitcher, R. Pynn, S. Satija and G. S. Smith. This work was supported by the U.S. Department of Energy, BES-DMS, under Contract No. W-7405-Eng-36.

MONTE CARLO SIMULATION OF THE SPEAR REFLECTOMETER AT LANSCE

Gregory S. Smith

Manuel Lujan, Jr. Neutron Scattering Center
Los Alamos National Laboratory, Los Alamos, New Mexico, 87545

Introduction

The Monte Carlo instrument simulation code, MCLIB[1,2], contains elements to represent several components found in neutron spectrometers including slits, choppers, detectors, sources and various samples. Using these elements to represent the components of a neutron scattering instrument, one can simulate, for example, an inelastic spectrometer, a small angle scattering machine, or a reflectometer. In order to benchmark the code, we chose to compare simulated data from the MCLIB code with an actual experiment performed on the SPEAR reflectometer at LANSCE. This was done by first fitting an actual SPEAR data set to obtain the model scattering-length-density profile, $\beta(z)$, for the sample and the substrate. Then these parameters were used as input values for the sample scattering function. A simplified model of SPEAR was chosen which contained all of the essential components of the instrument. A code containing the MCLIB subroutines was then written to simulate this simplified instrument. The resulting data was then fit and compared to the actual data set in terms of the statistics, resolution and accuracy.

Experimental

The data chosen for modeling was from a simple system of a single deuterated-(poly)styrene (d-PS) layer spun coated from a solvent onto a 75 mm diameter polished silicon wafer [3]. The reflectivity was measured on the SPEAR reflectometer for 11.7 μamp-hours (i.e. a proton beam current of 70 μamps for 10 minutes). The angle of incidence was chosen to be ~1 degree and the wavelength range was 1-16 Å. The detector used was a linear position sensitive detector and the data was reduced using the standard constant Q_z binning scheme used for all SPEAR data reduction[4]. The data was fit using a standard iterative method [5] over a Q_z range where the statistics were adequate not to introduce a background term into the fit. A simple model was chosen consisting of a single layer of d-PS on silicon with the allowance for rough surfaces at the polymer-silicon and polymer-air interfaces each having the same rms roughness. The value of β for the substrate was fixed to the theoretical value for silicon since the thick d-PS layer makes the fit insensitive to the scattering length density of the substrate. The data and the fit are shown in Figure 1. The data is plotted as (Reflectivity*$Q_z^{4)}$ versus Q_z. The best fit parameters for this system were film thickness = 1437Å, $\beta_{film} = 6.17 \times 10^{-6}$ Å^{-2}, and $\sigma_{roughness} = 9.45$ Å. These parameters were then used in all subsequent MCLIB simulations.

The *Surface Profile Analysis Reflectometer (SPEAR)* views the liquid hydrogen moderator. The moderated neutrons are collimated into two beams inclined downwards at angles of 1.5° and 1.0° to the horizontal and converge at a common sample position, which is 8.73 m from the moderator. A specially designed shutter allows the beams to be operated either independently or simultaneously. The vertical resolution of each beam ($\Delta\Theta/\Theta$) is ±5% for horizontal surfaces and

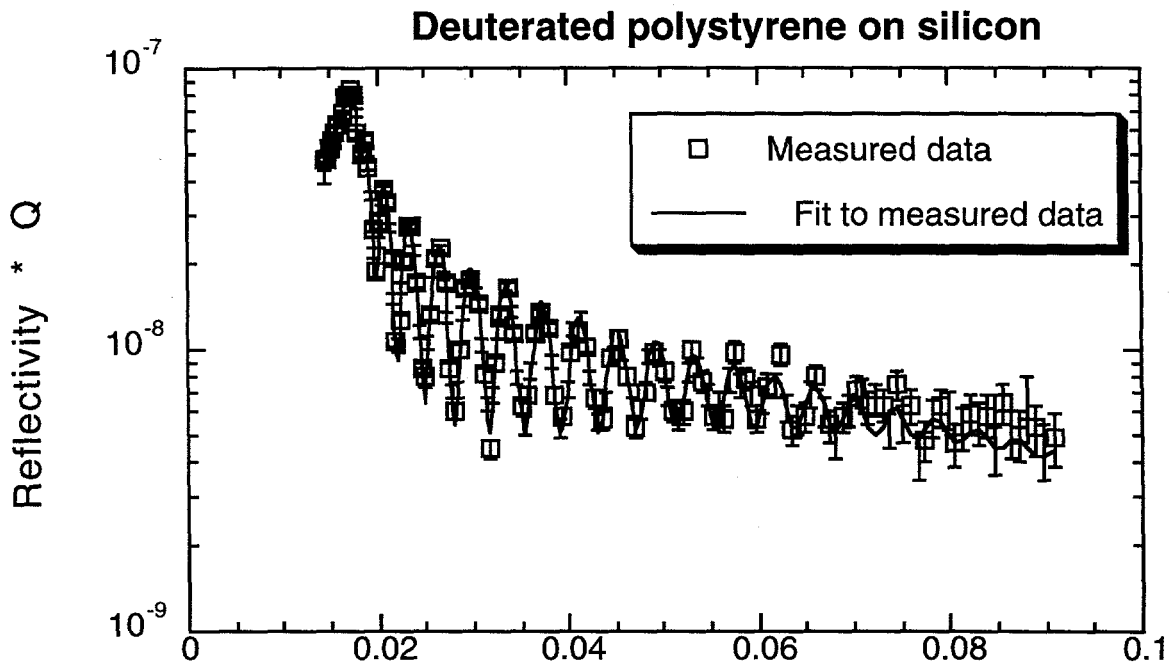

Fig. 1. Measured data on the polystyrene on silicon system using a single layer model.

the horizontal resolution ($\Delta\Theta$) is $\pm 0.125°$. The minimum reflectivity obtainable on this instrument is 10^{-7}. The t-zero chopper located just outside the bulk shield interrupts the beam during the initial flash of high-energy neutrons and gamma rays and significantly reduces the background that limits reflectivity measurements. At the midpoint of the beam line is the frame-overlap chopper, which defines the wavelength band (1 to 16 Å or 16 to 32 Å) to be used and suppresses frame-overlap background problems. A 2-m section of the beam line before the sample allows for further tailoring of the incident beam by slits or polarizers. In this section there is a set of three frame overlap mirrors (nickel coated silicon wafers 1 mm thick) set to reflect neutrons with wavelengths greater that 32Å from the beam. A goniometer at the sample position allows solid samples to be tilted in order to change the angle of incidence of the beam relative to the reflecting surface. For samples that must be isolated from external sources of vibration, an EVIS vibration isolation system (Newport Corporation) supports the sample and actively dampens vibrations transmitted through the floor or air. The detector system currently used is an Ordela model 1202N linear position-sensitive detector with 2-mm resolution.

Modeling

We have simplified the SPEAR instrument to minimize the computational time while keeping all of the functionality. We first produced the simplified schematic diagram of SPEAR shown in Figure 2. A single beam is defined by two sets of opaque slits. This beam has the same divergence ($\Delta\theta/\theta$=+/-5%) and incident angle (1.5° with respect to the horizontal) as the upper beam on the actual SPEAR instrument. The beam defined by these slits converges vertically at the sample position and horizontally at the detector (at 8.73 m and 12.4 m from the moderator,

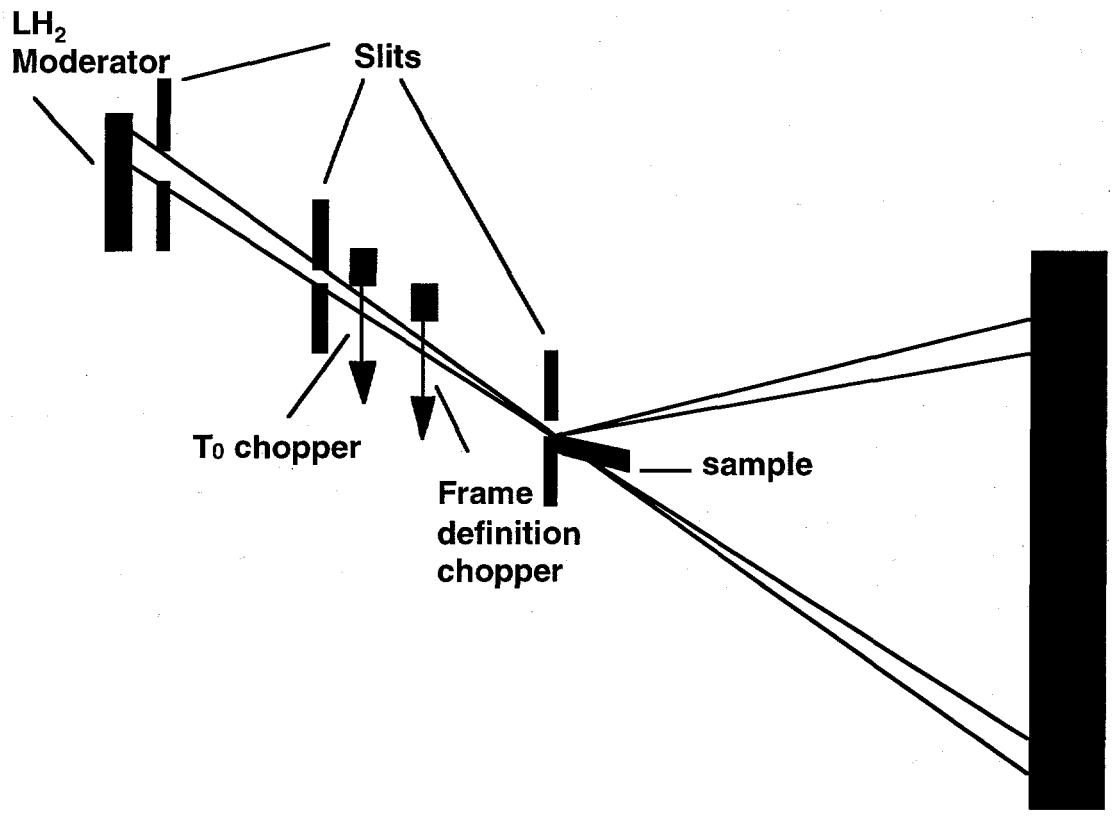

Fig. 2. Components for SPEAR mockup.

respectively) . A T_0 chopper lies just beyond the second slit and a frame overlap chopper is placed at one half of the moderator to detector distance. A third guard slit was placed immediately in front of the sample. This slit was set to limit the sampled phase space to shorten the computation time, but not to change the illumination of the sample determined by the collimation slits. It also prevents neutrons from entering the substrate through the front edge of the sample. The sample was defined by its geometric size to be the same as the measured sample (75 mm diameter) and it was set at a 1.0° incident angle . A kernel for the reflectivity of a sample was calculated based on an iterative approach [5]. The detector element chosen was a linear position sensitive ^{3}He detector. The incident beam spectrum used was one previously measured for the SPEAR liquid hydrogen moderator using a low sensitivity ^{3}He monitor type detector. This incident beam spectrum was normalized according to the number of μamp-hours on target during the measurement and the sampled phase space. An aluminum absorber was placed in the beam path to account for the beam loss due to the mirrors, and windows. An additional region consisting of a thin layer of ^{3}He was added to produce a simulated direct beam spectrum equivalent to the one measured with the SPEAR linear PSD. This was done to account for the difference in efficiencies between the low efficiency detector used to measure the spectrum and the Ordela detector.

After the key components of SPEAR were identified, this simplified geometry was programmed into the MCLIB simulation package [1,2]. Using the identified subset of the instrumental elements on SPEAR (Figure 2) ensured that the instrumental resolution was the same as for the test sample measured on SPEAR. The fitting parameters obtained for the test sample were used as the sample parameters in the reflectivity simulation kernel. The input number of neutrons was

chosen such that the number of μamp-hours of beam on target were the same as those obtained from measurements on the test sample. The resulting data set was reduced in the same manner as an actual SPEAR data set using the constant Q_z binning to produce a plot similar to Figure 1. The simulated data set was analyzed using the same parametrized model which fit the test sample data. The resolution used in the simulation was determined from the simulated SPEAR instrument. The fitting parameters are listed in Table I.

TABLE I

	Measured test data	Simulated data
$\beta_{silicon}$ (fixed)	2.153 X 10^{-6} Å^{-2}	2.153 X 10^{-6} Å^{-2}
$\beta_{polymer\ layer}$ (X 10^{6} Å^{-2})	6.17 +/- .01	6.22 +/- .01
thickness polymer layer	1437 +/- 10 Å	1437 + /- 2 Å
interlayer roughness, σ	9.5 +/- .4 Å	10.1 +/- .5 Å

Results and Discussion

As a figure of merit, we chose to compare the simulated data to the actual data in three areas. First, we compared the statistical error bars on the data points in each case. This allows us to verify that the normalization of the incident flux as well as the flux at the sample are correctly simulated. Second, we compare the resolution of the two data sets. The comparison of the counting statistics above is only valid if the data were measured for comparable resolution elements. Finally, we compare that the accuracy of the results are consistent between the actual and simulated data sets.

Figure 3 is a plot of the ratio of the gaussian resolutions and a plot of the ratio of the statistical gaussian resolutions both plotted versus Q_z. This plot shows that the resolution determined for the simulated instrument is nearly identical with that of SPEAR over this range of Q_z values. In addition, the mean of the ratio of the statistical error's is nearly one. The oscillations in this plot are due to a slight shift in the fringe positions between the two sets of data. Finally, as we look at Table I, we see that the fitting parameters for the simulated data are consistent with those of the actual measurements . Since the fitting parameters are so close to one another, the slight shift between the data sets which gives rise to the oscillations seen in Figure 3 is seen to be insignificant.

Conclusions

The conclusion from this study is that we can adequately simulate the behavior of a well characterized instrument with the Monte Carlo technique. In this particular case, we have shown that a simplified version of the instrument serves to produce a very good simulation of the actual instrument. This gives us confidence in using these calculations to examine the effects of

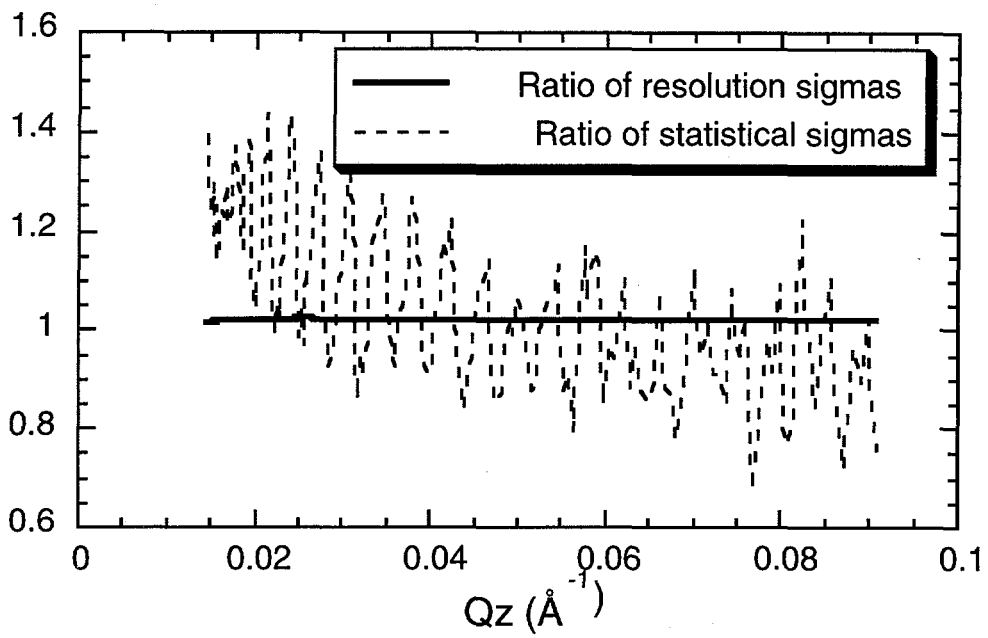

Fig. 3. *The solid line is the ratio of the standard deviation for the resolution of the actual data to the simulated data set. The dashed line is the ratio of the statistical standard deviations of the actual data to the σ's for the simulated data.*

changes to an instrument ranging from the addition of a single device to building an entirely new instrument. In addition, the option of changing the input energy spectrum allows one to compare instrument designs on different neutron sources.

References

[1] P. A. Seeger, "Monte Carlo Calculations for the Optimization of the Beam Optics of the LOQ Spectrometer," report to Rutherford Appleton Laboratory, 28 April, 1994.

[2] P.A Seeger, G.S. Smith, M. Fitzsimmons, G. A. Olah, L Daemon, R.P. Hjelm, Jr., various contributions, Instrumentation for a Long -Pulse Spallation Source Workshop, Lawrence Berkeley Laboratory, Berkeley, CA, April 18-21, 1995.

[3] Supplied by Tom Russell, IBM, Almaden Research Center.

[4] W. A. Hamilton, J.B. Hayter, and G.S. Smith, "Neutron Reflectometry as Optical Imaging," J. Neutron Res., 2 (1), 1(1994).

[5] T.P. Russell, " X-ray and Neutron Reflectivity for the Investigation of Polymers," Matls. Sci. Reps. **5**, 171 (1990).